POLITECNICO DI MILANO

Scuola di Ingegneria Industriale e dell'Informazione

Tesi di Laurea Magistrale in Ingenieria Biomedica

Assessment of spatial heterogeneity of ventricular repolarization in patients with atrial fibrillation

Relatori:

Prof. Luca T. Mainardi

Prof. Valentina Corino

Candidati:	Matr.
Francisco Javier Saiz Vivó	876892

Anno accademico 2017/2018

Francisco Javier Saiz Vivó, 2018

Assessment of spatial heterogeneity of ventricular repolarization in patients with atrial fibrillation.

Date: April 19th, 2018

This Master thesis has been developed within the Dipartimento di Elettronica, Informazione e Bioingegneria (DEIB) from Politecnico di Milano.

CONTENTS

LIST OF FIGURES

LIST OF TABLES

Chapter 1. SUMMARY

Introduction

Atrial Fibrillation (AF) is the most common sustained arrhythmia encountered in clinical practice. The progressive aging of the general population is associated with an inevitable rising in incidence of this particular rhythm disorder which in 2005 alone was responsible for 193,300 deaths, up from 29,000 in 1990 [1][2]. In providing proper treatment, the clinician must establish the pattern of arrhythmia, determine associated symptoms, and asses for underlying comorbidities in order to define short- and long-term management strategies.

Although there is no common agreement today on the best AF classification, current clinical guidelines advocate differentiating between paroxysmal, persistent and permanent AF [9].

1. Paroxysmal AF: AF with spontaneous interruption generally within 7 days but mostly in 24-48 h,
2. Persistent: AF that does not interrupt spontaneously but with therapeutic interventions (pharmacological or electrical), and
3. Permanent or chronic AF: AF in which interruption attempts have not been made or, if made, have not been successful.

One of the objectives of this thesis is to try to discriminate between the 3 types of AF.

The spatial dispersion of ventricular repolarization is responsible for the genesis of the T-wave on the ECG therefore, based on van Oosterom's take on Dominant T-wave formalism (DTW) and its derivatives, a novel method to quantify the dispersion of myocytes' repolarization times, rooted on a biophysical model of the ECG called the

$\mathcal{V}\text{-}index$ was derived. The $\mathcal{V}\text{-}index$ is an electrocardiogram (ECG)-based estimator of the standard deviation of ventricular myocytes' repolarization times, s_ϑ.

Specifically, the $\mathcal{V}\text{-}index$ computes s_ϑ through the ratio of the standard deviations of the lead factors measured across successive beats according to the following formula:

$$\mathcal{V}_i = \frac{std[w_2(i)]}{std[w_1(i)]} \approx s_\vartheta \quad (1\text{-}1)$$

where $w_1(i)$ and $w_2(i)$ are the lead factors which are derived from:

$$\Psi \approx w_1 T_d + w_2 \dot{T}_d \quad (1\text{-}2)$$

where $\Psi_{L\times N}$ is a matrix containing N ECG samples recorded from L leads, w_1 and w_2 are 2 sets of L x 1 vectors of leads factors, $\mathrm{T_d}$ is a 1 x N vector obtained after sampling $\dot{\mathrm{D}}(\mathrm{t})$ and $\dot{\mathrm{T}}_\mathrm{d}$ its derivative.

The objective of this thesis is the assessment of spatial heterogeneity of ventricular repolarization in patients with atrial fibrillation, which includes:

- Simulation: use physiological T-waves to study the differences that arise in the $\mathcal{V}\text{-}index$ in 3 cases:
    - Theoretical case
    - Sinus Rhythm condition
    - Atrial Fibrillation condition

  The AF condition was achieved by adding simulated f-waves to the physiological T-waves using the method described in [34].
- Study of Swiss AF database: compute and compare the $\mathcal{V}\text{-}indexes$ of 2013 patients in paroxysmal and persistent SR and Paroxysmal, Persistent and permanent AF, in the 3 main $\mathcal{V}\text{-}index$ computation methodologies.

Materials

For this thesis, Swiss Atrial Fibrillation (Swiss-AF) cohort carried out a study of 2400 patients across 13 sites in Switzerland. Out of the ECG signals of the 2400 patients, 2013 had signals clear enough to conduct the computation of the $\mathcal{V}\text{-}index$, out of which 902 patients present paroxysmal, 608 persistent and 503 permanent AF. Eligible patients had to be ≥65 years old and had to have one of the 3 AF patterns studied.

Main exclusion criteria included inability to provide informed consent, the presence of exclusively nonsustained episodes of secondary form of AF (e.g. after cardiac surgery or severe sepsis) or any acute illness within the last 4 week. The latter group of patients were eligible for enrolment after stabilization of their acute episode.

Methods

The methodology of this thesis is divided in two distinct stages: AF simulation and Study of Swiss-AF database.

AF simulation's main processes are add AF, calculate w1 and w2 and calculate the V index of the theoretical values and the experimental values with and without f waves.

Swiss-AF database's main processes include Elimination of f-waves if necessary for AF patients, and then for all the patients: a Pre-processing stage which includes filtering and Baseline Alignment, the T wave detection stage which includes the use of Pan Tompkins algorithm to determine the position of the QRS, Rough Beat Alignment, T-Wave Delineation, Beat Re-Alignment and cross correlation to identify the good leads. Finally, as in the AF simulation, the stages of w_1 and w_2 and $\mathcal{V}\text{-}index$ calculation.

AF simulation

The AF simulation started with T-waves from the 12 Standard Leads and theoretical w_1, w_2 and $\mathcal{V}\text{-}index$ values for seven patients were used.

An example of the T-waves provided for one of the patients are shown in Fig. 1-1.

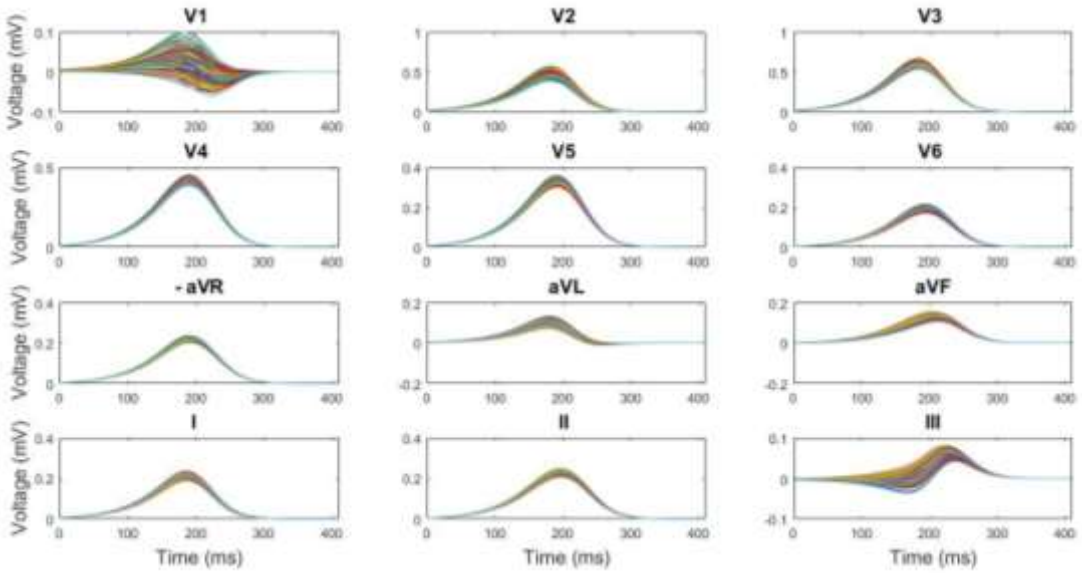

Fig. 1-1 T-waves for 12 Standard Leads.

To see the effect the f-waves had in the computation of the $\mathcal{V}\text{-}index$, fibrillatory waves were simulated and added to the T-waves following the steps described in [34]. Fig. 1-2 shows the T-waves with the added f-waves.

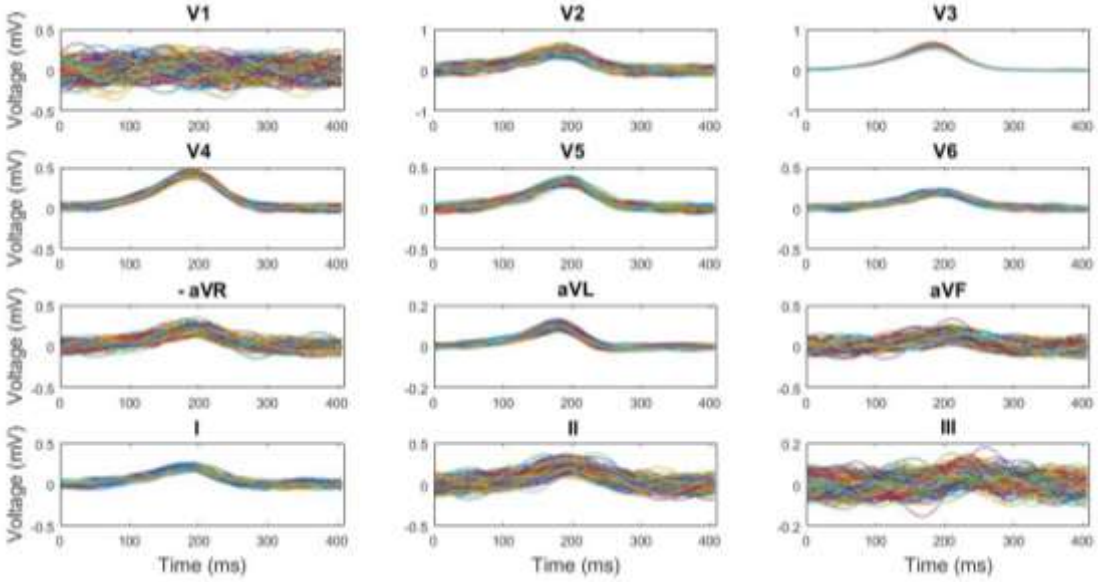

Fig. 1-2 T-waves for 12 Standard Leads with f-waves.

For the experimental values both with and without f-waves, w_1 and w_2 must be calculated in order to calculate the $\mathcal{V}\text{-}index$. To do so, this thesis describes 3 different methods hereinafter Method 1, Method 2 and Method 3.

- Method 1: estimate the dominant T-wave (DTW) of each beat.
- Method 2: estimating a single DWT, shared across beats.
- Method 3: Sinusoidal functions to estimate the dominant T-wave.

Study of Swiss AF database

The main part of this thesis was the study of the Swiss-AF database, which divided the patients into 5 groups: AF (Paroxysmal, Persistent and Permanent) and SR (Paroxysmal and Persistent) in order to later do some comparisons between the $\mathcal{V}\text{-}index$ results obtained from each of the subgroups.

The processes followed in this stage include Elimination of f-waves in AF patients if necessary and then in all the patients: Pre-processing, T-wave detection, w_1 and w_2 calculation and $\mathcal{V}\text{-}index$ calculation. The processes w_1 and w_2 calculation and $\mathcal{V}\text{-}index$ calculation are analogous to the processes described in the AF Simulation stage.

In order to determine the necessity of eliminating the f-waves of the AF patients before computing the $\mathcal{V}\text{-}index$, the study of Swiss-AF database was divided into 2 sub-stages:

- Comparison between AF patients with and without f-waves
- Comparison between AF and SR patients.

The AF patients of the second comparison will or will not have f-waves depending on the results obtained in the first comparison.

Elimination of f-waves

The method consisted on the pre-processing of the signal, T-wave detection, Atrial Fibrillation Reduction, Beat Averaging, Estimation of QRST Cancellation Parameters, QRST Cancellation and f-waves elimination.

T-wave detection

The T-wave detection was done by computing the maximum derivative and calculate a Reference Line, which is a straight line that passes through the point of maximum

derivative and has a gradient equal to a fourth of the maximum derivative. The end of the T-wave is then determined by the point of the T-wave which has the maximum distance from the Reference Line.

Results

This section will describe the most relevant results obtained in the stages of this thesis: Simulation and Swiss-AF study.

Simulation:

The simulation was done in order to determine if it was necessary to eliminate the f-waves from the AF patients before calculating the $\mathcal{V}$-$index$. Seven sets of T-waves were analysed and the theoretical $\mathcal{V}$-$index$ values were compared against the $\mathcal{V}$-$index$ of the T-waves with and without simulated f-waves. Fig. 1-3 and Table 1-1 show the results obtained for Simulation Frequency 5 Hz.

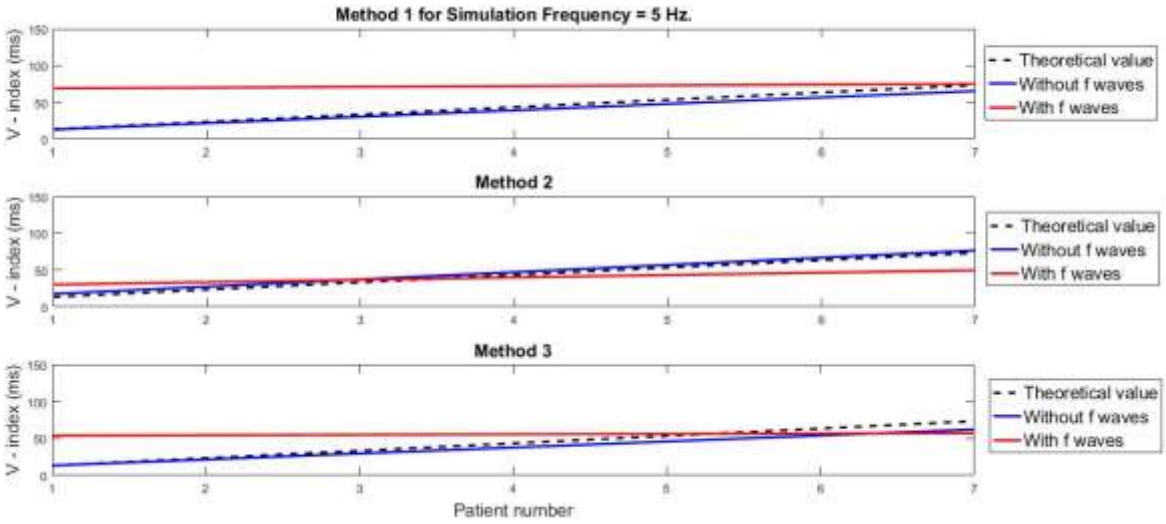

Fig. 1-3 AF Simulation Comparisons for simulation frequency = 5Hz.

Table 1-1 Mean Absolute Percentage Error between theoretical V-index values and V-index values for T-waves with and without f-waves for Simulation Frequency 5 Hz.

Simulation Frequency (Hz)	Method	Theoretical vs Signal without f waves MAPE (%)	Theoretical vs Signal with f waves MAPE (%)
5	1	9.03	116.72
	2	11.73	50.15
	3	11.60	81.18

The Mean Absolute Percentage Error (MAPE) for Theoretical vs Signal without f-waves are considerably lower than for Theoretical vs Signal with f-waves. The assumption that the f-waves affect the computation of the $\mathcal{V}\text{-}index$ is therefore proven and justifies the decision to make a previous Swiss-AF study in order to confirm the effect of f-waves in the computation of the V index in real ECG signals.

Swiss-AF Study

SR patients and AF patients without f-waves

The results obtained in the comparisons for SR patients and AF patients without f-waves are going to be presented.

Out of the 879 AF patients and 1134 SR patients, 772 AF and 1092 SR patients gave usable $\mathcal{V}\text{-}index$ results. The 772 AF patients include 135 with Paroxysmal, 217 with Persistent and 420 with Permanent fibrillatory episodes and the 1092 SR patients include 747 with Paroxysmal and 345 with Permanent episodes.

A comparison between SR patients and AF patients without f-waves was made for Paroxysmal and Persistent episodes. As an example, Fig. 1-4 shows the box plot obtained in the comparison of Paroxysmal episodes:

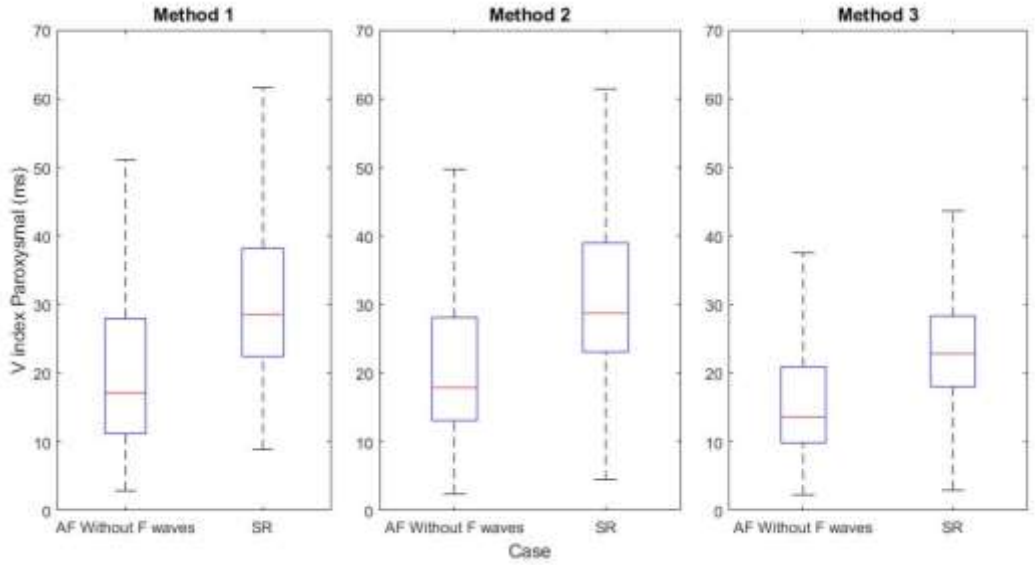

Fig. 1-4 Comparison between Paroxysmal patients in AF without f-waves and SR conditions

And Table 1-2 summarises the results:

Table 1-2 Median and Standard Deviation for the V-index values of the comparison and the Increase in Median between the values of the patients in AF without f-waves and SR conditions.

Episode	Method	$\mathcal{V}$-index		Δ Median
		AF without f-waves (ms)	SR (ms)	(%)
Paroxysmal	1	17.16 ± 18.56	28.57 ± 16.34	66.52
	2	17.90 ± 20.34	28.75 ± 14.84	60.59
	3	13.60 ± 10.51	22.86 ± 9.38	68.06

Both Fig. 1-4 and Table 1-2 show that there is an increase in the median of the $\mathcal{V}$-$index$ for patients during SR than for patients during AF without f-waves. This may be due to the fact that during fibrillation the ventricular myocytes' repolarization times decreases.

As one of the objectives was to be able to discriminate between Persistent and Permanent AF episodes, Fig. 1-5 shows the comparison between Persistent and Permanent patients in AF conditions.

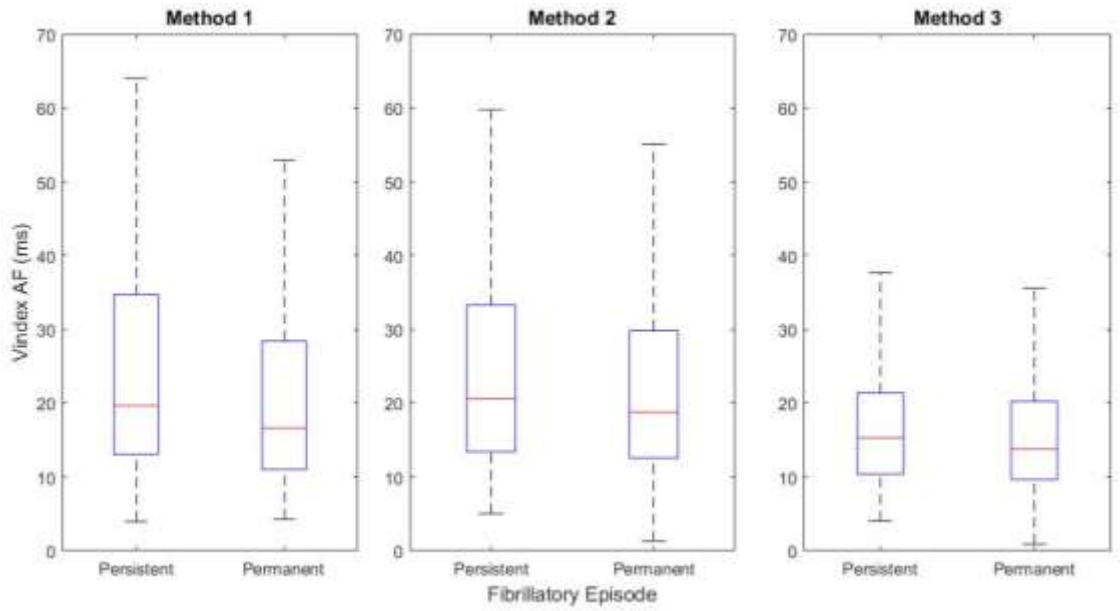

Fig. 1-5 Comparison between Persistent and Permanent patients in AF conditions.

A study was made on the statistical values of the $\mathcal{V}$-$index$ and its results are shown in Table 1-3.

Table 1-3 Median and Standard Deviation for the V-index values of the different comparisons, the Increase in Median between the values of the Persistent and Permanent patients in AF and the P value of those comparisons.

Method	$\mathcal{V}$-index		Δ Median (%)	P value ≤ 0.05
	Persistent (ms)	Permanent (ms)		
1	19.65 ± 20.31	16.62 ± 17.03	18.23	0.01
2	20.57 ± 23.71	18.76 ± 16.99	9.69	0.02
3	15.30 ± 11.16	13.77 ± 9.31	11.08	0.03

The median of the $\mathcal{V}$-$index$ for patients with Persistent episodes is higher than for patients with Permanent episodes. Furthermore, for these comparisons, the null hypothesis was rejected when the P value ≤ α, with α = 0.05. The null hypotheses were rejected in all the comparisons and were deemed statistically significant as the P values of all the comparisons were ≤ 0.05.

From these values, one could argue that it is possible to discriminate between Persistent and Permanent episodes in patients with AF.

Conclusion

The assessment of spatial heterogeneity of ventricular repolarization in patients with atrial fibrillation was the aim of this thesis. The aim was met and the results have shown that:

- the method used to estimate the lead factors w_1 and w_2 from the ECG introduce bias in the $\mathcal{V}$-index. However, throughout the comparisons, the standard deviation of the $\mathcal{V}$-index for Method 3 was the lowest. This proves that the analytical form (with 5 being the number of Taylor terms) has a more reliable estimate [36].
- there is a significant effect of the presence of f-waves when computing the $\mathcal{V}$-index and thus, the fibrillatory component should be removed from the AF signals before the computation.
- with some limitations, the methods developed for eliminating the f-waves and delineating the T-wave generally worked.
- no statistically significant results were provided when trying to discriminate paroxysmal from persistent patterns in SR patients
- in AF patients, the comparison between Persistent and Permanent patterns gave significant results as s_ϑ was higher for Persistent than for Permanent AF patients.

Chapter 2. SOMMARIO

Introduzione

La fibrillazione atriale (FA) è l'aritmia sostenuta più comune riscontrata nella pratica clinica. Il progressivo invecchiamento della popolazione generale è associato ad un inevitabile aumento dell'incidenza di questo particolare disturbo del ritmo che nel solo 2005 è stato responsabile di 193.300 decessi, contro i 29.000 nel 1990 [1] [2]. Nel fornire un trattamento adeguato, il dottore deve stabilire il modello di aritmia, determinare i sintomi associati e valutare le comorbidità sottostanti al fine di definire strategie di gestione a breve e lungo termine.

Anche se oggi non esiste un accordo comune sulla migliore classificazione FA, le attuali linee guida cliniche sostengono la differenziazione tra FA parossistica, persistente e permanente [14]:

- FA Parossistica: FA con interruzione spontanea in genere entro 7 giorni, ma per non più di 24-48 h,
- FA Persistente: FA che non si interrompe spontaneamente ma con interventi terapeutici (farmacologici o elettrici), e
- FA Permanente o cronica: FA in cui i tentativi di interruzione non sono stati effettuati o, se fatti, non hanno avuto successo.

Uno degli obiettivi di questa tesi è provare a discriminare tra i 3 tipi di FA.

La dispersione spaziale della ripolarizzazione ventricolare è quindi responsabile della genesi dell'onda T sull'ECG, sulla base dell'analisi di Van Oosterom sul formalismo dell'onda T dominante (DTW) e dei suoi derivati, un nuovo metodo per quantificare la dispersione dei tempi di ripolarizzazione dei miociti, basato su un modello biofisico

dell'ECG chiamato indice $\mathcal{V}$. L'indice $\mathcal{V}$ è uno stimatore basato sull'elettrocadiogramma (ECG) della deviazione standard dei tempi di ripolarizzazione dei miociti ventricolari, s_ϑ.

Nello specifico, l'indice $\mathcal{V}$ calcola $s_\vartheta$attraverso il rapporto delle deviazioni standard dei fattori di derivazione misurati tra battiti successivi secondo la seguente formula:

$$\mathcal{V}\text{-}index = \frac{std[w_2(i)]}{std[w_1(i)]} \approx s_\vartheta \qquad (2\text{-}1)$$

dove $w_1(i)$ e $w_2(i)$ sono i fattori principali derivati da:

$$\Psi \approx w_1 T_d + w_2 \dot{T}_d \qquad (2\text{-}2)$$

dove Ψ è una matrice [L x N] contenente N campioni di ECG registrati da lead L, w_1 e w_2 sono 2 set di vettori [L x 1] di fattori lead, T_d è un vettore [1 x N] ottenuto dal DTW e $\dot{T}_d$ la sua derivata.

L'obiettivo di questa tesi è la valutazione dell'eterogeneità spaziale della ripolarizzazione ventricolare in pazienti con fibrillazione atriale, che include:

- Simulazione: usa le onde T fisiologiche per studiare le differenze che si presentano nell'indice $\mathcal{V}$ in 3 casi:
    - Caso teorico
    - Condizione del ritmo sinusale
    - Condizione di fibrillazione atriale

    La condizione FA è stata ottenuta aggiungendo onde f simulate alle onde T fisiologiche utilizzando il metodo descritto in [34].

- Studio del database delle Swiss-AF: calcolare e confrontare gli indici $\mathcal{V}$ dei 2013 pazienti con parossistica e persistente RS e FA parossistica, persistent e permanente, nelle 3 principali metodologie di calcolo dell'indice $\mathcal{V}$.

Materiale

Per questa tesi, Swiss Atrial Fibrillation (Swiss-AF) database raccoglie tracciati ECG di uno studio su 2400 pazienti in 13 siti in Svizzera. Dei 2400 pazienti, 2013 avevano segnali ECG abbastanza puliti per condurre il calcolo dell'indice $\mathcal{V}$, di cui 902 pazienti

presentavano parossistica, 608 persistente e 503 FA permanente. I pazienti eleggibili dovevano avere ≥65 anni e dovevano avere uno dei 3 pattern FA studiati. Sono stati scelti da uno screening completo di pazienti interni ed esterni negli ospedali partecipanti e contattando i medici generici nella zona. Principali criteri di esclusione comprendevano l'incapacità di fornire il consenso informato, la presenza di episodi di forma secondaria di FA (ad esempio dopo chirurgia cardiaca o sepsi grave) o qualsiasi malattia acuta nelle ultime 4 settimane

Metodi

La metodologia di questa tesi è suddivisa in due fasi distinte: simulazione FA e studio del database Swiss-AF.

Le principali elaborazioni per la simulazione dell'FA sono l'aggiunta di FA, il calcolo di w_1 e w_2 e il calcolo dell'indice $\mathcal{V}$ dei valori teorici e dei valori sperimentali con e senza onde fibrillatorie.

Le principali elaborazioni del database di Swiss-AF includono l'eliminazione delle onde fibrillatorie (se necessario per i pazienti con fibrillazione atriale) e quindi per tutti i pazienti: una fase di pre-elaborazione che include il filtraggio e l'allineamento della linea di base, la fase di rilevamento dell'onda T che include l'uso dell'algoritmo di Pan Tompkins per determinare la posizione del QRS, l'allineamento del battito, la delineazione delle onde T, il riaggiustamento del battito e della correlazione incrociata per identificare i battiti analizzabili. Infine, come nella simulazione FA, le fasi del calcolo dell'indice w_1 e w_2 e $\mathcal{V}$.

Simulazione dell' FA

La simulazione dell'FA è iniziata con le onde T delle 12 derivazioni standard e sono stati utilizzati i valori teorici di w_1, w_2 e $\mathcal{V}$ per 7 pazienti.

Un esempio delle onde T fornite per uno dei pazienti sono mostrate in Fig. 2-1.

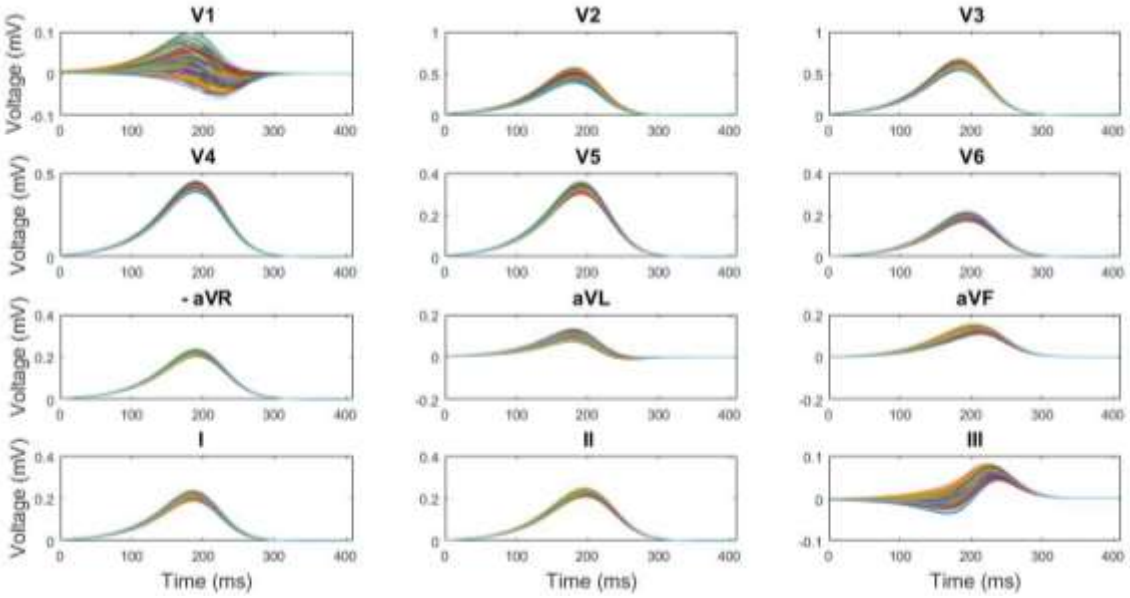

Fig. 2-1 Onde T senza onde fibrillatorie.

Per vedere l'effetto che le onde fibrillatorie avevano nel calcolo dell'indice $\mathcal{V}$, le onde fibrillatorie sono state simulate e aggiunte alle onde T seguendo i passaggi descritti in [34]. La Fig. 2-2 mostra le onde T con le onde f aggiunte.

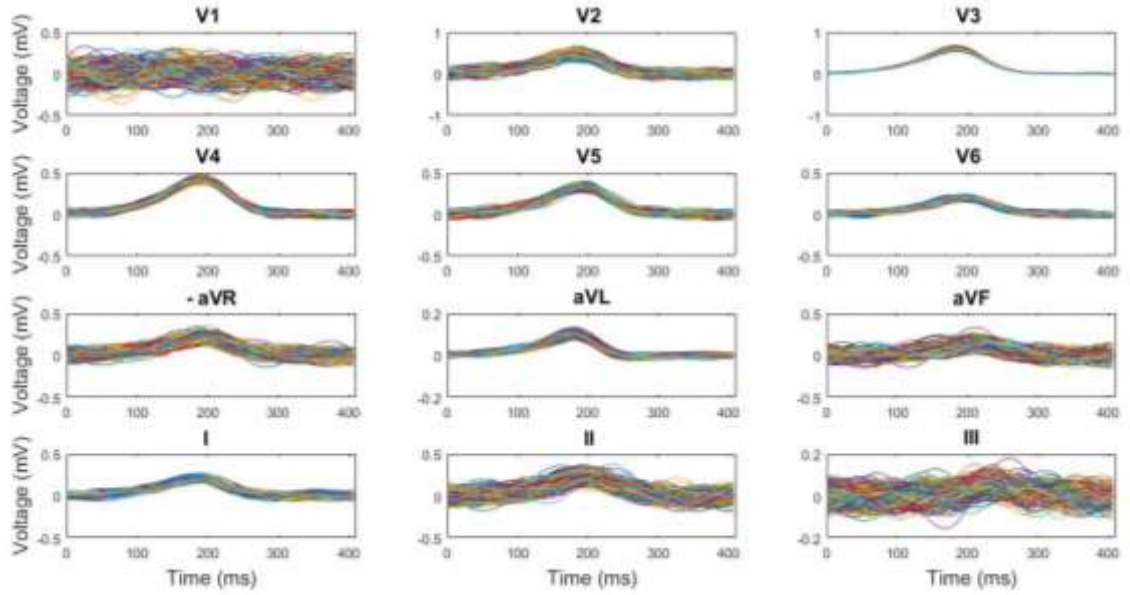

Fig. 2-2 Onde T con onde fibrillatorie.

Per i valori sperimentali con e senza onde fibrillatorie, è necessario calcolare w_1 e w_2 per calcolare l'indice $\mathcal{V}$. Con questo scopo, questa tesi descrive 3 diversi metodi in appresso Metodo 1, Metodo 2 e Metodo 3.

- Metodo 1: stima l'onda T dominante (DTW) di ogni battito.
- Metodo 2: stima di un singolo DWT, condiviso tra battiti.
- Metodo 3: funzioni sinusoidali per stimare l'onda T dominante.

Studio del database delle Swiss AF

La parte principale di questa tesi è stata lo studio della banca dati Swiss AF, che ha suddiviso i pazienti in 5 gruppi: FA (Parossistica, Persistente e Permanente) e RS (Parossistica e Persistente) per fare successivamente alcuni confronti tra i risultati dell'indice $\mathcal{V}$ ottenuto da ciascuno dei sottogruppi.

I processi seguiti in questa fase comprendono l'eliminazione delle onde fibrillatorie nei pazienti con FA, se necessario, e quindi in tutti i pazienti: pre-elaborazione, rilevamento dell'onda T, calcolo w_1 e w_2 e calcolo dell'indice $\mathcal{V}$. I processi di calcolo w_1 e w_2 e calcolo dell'indice $\mathcal{V}$ sono analoghi ai processi descritti nella fase di simulazione FA.

Al fine di determinare la necessità di eliminare le onde fibrillatorie dei pazienti con FA prima di calcolare l'indice $\mathcal{V}$, lo studio della banca dati Swiss AF è stato diviso in 2 sottofasi:

- Confronto tra pazienti con FA con e senza onde f
- Confronto tra pazienti con FA e RS.

I pazienti con FA del secondo confronto avranno oppure non avranno onde f, a seconda dei risultati ottenuti nel primo confronto.

Eliminazione delle onde fibrillatorie

Il metodo consisteva nella pre-elaborazione del segnale, il rilevamento dell'onda T, la riduzione della fibrillazione atriale, la media dei battiti, la stima dei parametri di cancellazione del QRST, l'eliminazione di QRST e l'eliminazione delle onde fibrillatorie.

Rilevazione delle onde T

Il rilevamento dell'onda T è stato eseguito calcolando la derivata massima e calcolando una linea di riferimento, che è una linea retta passasnte per il massimo e con una pendenza

uguale a un quarto della derivata massima. La fine dell'onda T viene quindi determinata dal punto dell'onda T che ha la massima distanza dalla linea di riferimento.

Risultati

Questa sezione descriverà i risultati ottenuti nelle fasi di questa tesi: simulazione e studio Swiss-AF.

Simulazione:

La simulazione è stata fatta al fine di determinare se fosse necessario eliminare le onde fibrillatorie dai pazienti FA prima del calcolo dell'indice $\mathcal{V}$. Sono stati analizzati 7 gruppi di onde T e i valori teorici dell'indice $\mathcal{V}$ sono stati confrontati con l'indice $\mathcal{V}$ delle onde T con e senza onde f simulate. La Fig. 2-3 e la Table 2-1 mostrano i risultati ottenuti per la frequenza di simulazione 5 Hz.

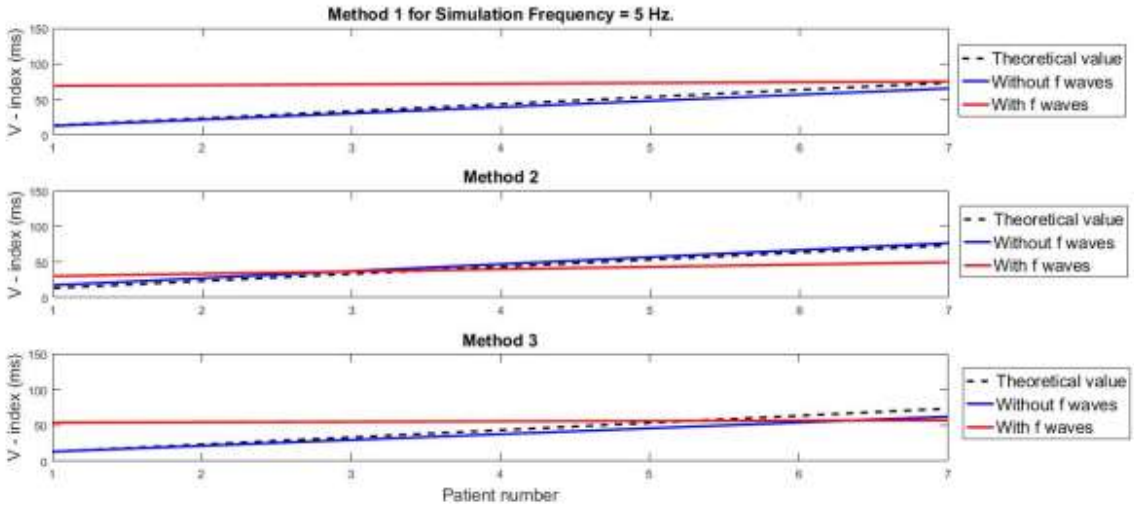

Fig. 2-3 Valori Teorici contro valori Senza Onde fibrillatorie e valori Con Onde fibrillatorie, per i tre metodi e frequenza di simulazione 5 Hz.

Table 2-1 EPAM di Segnale Teorico contro Segnale Senza Onde fibrillatorie e Con onde fibrillatorie, per i tre metodi e frequenza di simulazione 5 Hz.

Frequenza di Simulazione (Hz)	Metodi	EPAM di Segnale Teorico vs Segnale Senza Onde fibrillatorie (%)	EPAM di Segnale Teorico vs Segnale Con Onde fibrillatorie (%)
5	1	9.03	116.72
	2	11.73	50.15
	3	11.60	81.18

L'errore di percentuale assoluto medio (EPAM) per il segnale teorico confrontato con il segnale senza onde fibrillatorie è considerevolmente inferiore a quello ottenuto dal segnale con onde fibrillatorie. L'ipotesi che le onde fibrillatorie influenzino il calcolo dell'indice $\mathcal{V}$ è quindi dimostrata e giustifica la decisione di effettuare un precedente studio Swiss-AF al fine di confermare l'effetto delle onde f nel calcolo dell'indice $\mathcal{V}$ nei segnali ECG reali.

Studio Swiss-AF

Pazienti con RS e pazienti con FA senza onde fibrillatorie

Saranno presentati i risultati ottenuti nei confronti dei pazienti con RS e pazienti con FA senza onde fibrillatorie.

Dei 879 pazienti affetti da FA e di 1134 pazienti con RS, 772 pazienti con FA e 1092 RS hanno fornito risultati di indice $\mathcal{V}$ utilizzabili. I pazienti 772 FA includono: 135 con Parossistica , 217 con Persistente e 420 con episodi di fibrillazione permanente ed i pazienti 1092 RS includono: 747 con Parossistica e 345 con episodi permanenti.

Un confronto tra pazienti con RS e pazienti con fibrillazione atriale senza onde f è stato effettuato per episodi parossistici e persistenti. Le Fig. 2-4 mostrano il grafico ottenuto en il confronto per episodi parossistici:

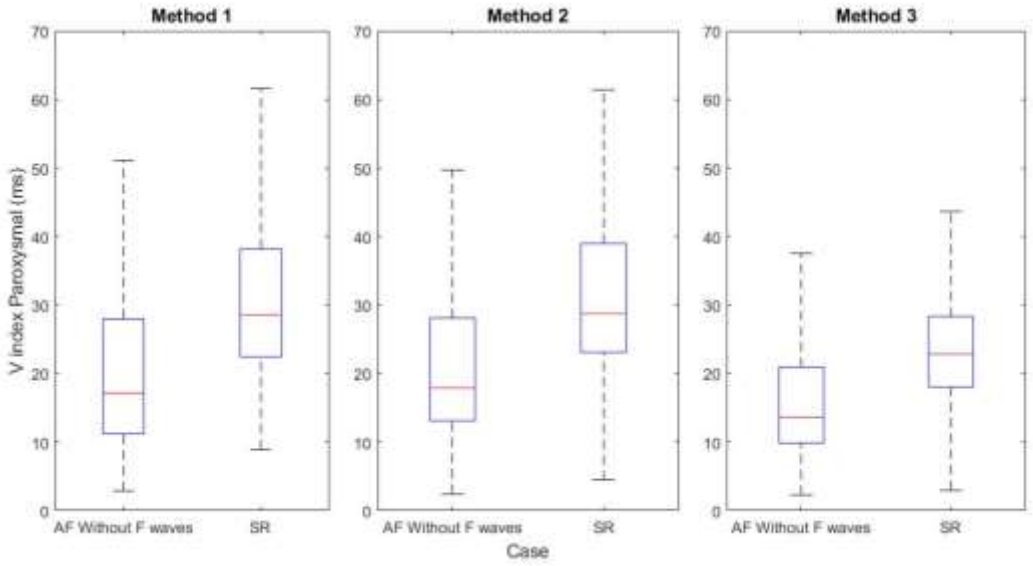

Fig. 2-4 Confronto tra Pazienti Parossistici con RS e con FA senza onde fibrillatorie.

E la Tabella 2-4 riassume i risultati:

Table 2-2 Indice V per Pazienti con RS e Pazienti con FA senza onde fibrillatorie per episodi Parossistici.

	Metodi	$\mathcal{V}$-index		Δ Mediana (%)
		FA senza onde fibrillatorie (ms)	RS (ms)	
Parossistica	1	17.16 ± 18.56	28.57 ± 16.34	66.52
	2	17.90 ± 20.34	28.75 ± 14.84	60.59
	3	13.60± 10.51	22.86 ± 9.38	68.06

Sia la Fig. 2-4 che la Table 2-2 mostrano come vi sia un aumento della mediana dell'indice $\mathcal{V}$ per i pazienti durante RS rispetto ai pazienti durante FA senza onde fibrillatorie. Questo può essere dovuto al fatto che durante la fibrillazione i tempi di ripolarizzazione dei miociti ventricolari diminuiscono.

Poiché uno degli obiettivi era quello di essere in grado di discriminare tra episodi FA Persistente e Permanente, la Fig. 2-5 mostra il confronto per i pazienti con FA Persistenti e Permanenti senza onde fibrillatorie

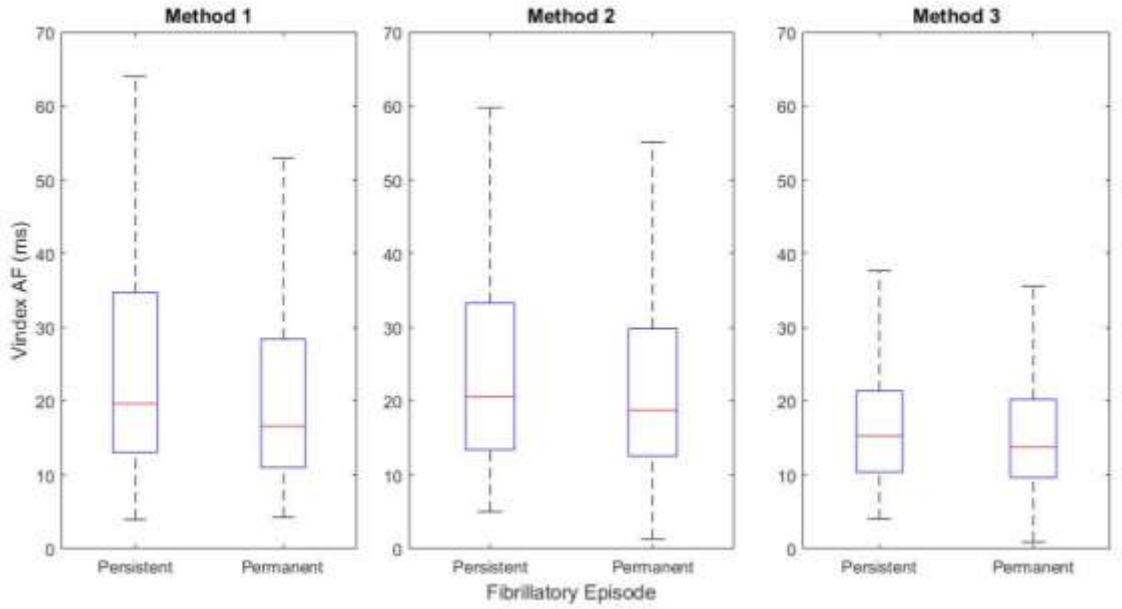

Fig. 2-5 Confronto per i pazienti con FA Persistenti e Permanenti senza onde fibrillatorie.

Uno studio è stato fatto sui valori statistici dell'indice $\mathcal{V}$ e i suoi risultati sono mostrati nella Tabella 2-7.

Table 2-3 Indice V per Pazienti con AF Persistenti e Permanente.

Metodi	$\mathcal{V}$-index		Δ Mediana (%)	p value ≤ 0.05
	Persistente (ms)	Permanente (ms)		
1	19.65 ± 20.31	16.62 ± 17.03	18.23	0.01
2	20.57 ± 23.71	18.76 ± 16.99	9.69	0.02
3	15.30± 11.16	13.77± 9.31	11.07	0.03

La mediana dell'indice $\mathcal{V}$ per i pazienti con episodi persistenti è superiore a quella dei pazienti con episodi permanenti. Inoltre, per questi confronti, l'ipotesi nulla è stata respinta quando il valore $p \leq \alpha$, con $\alpha = 0{,}05$. L'ipotesi nulla è stata respinta in tutti i confronti e sono state ritenute statisticamente significative in quanto i valori di p di tutti i confronti erano $\leq 0{,}05$.

Da questi valori, si potrebbe sostenere che è possibile discriminare tra episodi persistenti e permanenti in pazienti con fibrillazione atriale.

Conclusione

La valutazione dell'eterogeneità spaziale della ripolarizzazione ventricolare in pazienti con fibrillazione atriale era l'obiettivo di questa tesi. L'obiettivo è stato raggiunto e i risultati hanno dimostrato che:

- il metodo utilizzato per stimare i fattori principali w_1 e w_2 dall'ECG influenza la misura dell'indice $\mathcal{V}$. Tuttavia, durante i confronti, la deviazione standard dell'indice $\mathcal{V}$ per il metodo 3 era la più bassa. Ciò dimostra che la forma analitica (con 5 è il numero di termini Taylor) ha una stima più affidabile [36].
- c'è un effetto significativo della presenza di onde f quando si calcola l'indice $\mathcal{V}$ e quindi, la componente fibrillatoria deve essere rimossa dai segnali FA prima del calcolo.
- con qualche limitazione, i metodi sviluppati per eliminare le onde f e delineare l'onda T hanno generalmente funzionato.
- non sono stati forniti risultati statisticamente significativi quando si cercava di discriminare il parossistico da pattern persistenti nei pazienti con RS
- nei pazienti con fibrillazione atriale, il confronto tra i modelli persistenti e quelli permanenti ha fornito risultati significativi che dimostrano come s_ϑ sia maggiore per i pazienti persistenti che per quelli con FA permanente.

Chapter 3. INTRODUCTION

3.1 Academic Motivation

This thesis serves as the culmination of the Technologies for Electronics track of the Biomedical Engineering Laurea Magistrale done in Politecnico di Milano. For its development, I used knowledge acquired in subjects such as Biomedical Signal Processing and Medical Images, Biomedical Signal Processing Laboratory and Bioengineering of Biomedical Control Systems. I also improved my Matlab skills, and discovered what a career in research could be like as I searched for papers and learned how to properly refer the information found when writing a report.

3.2 Research Motivation

Atrial Fibrillation (AF) is the most common sustained arrhythmia encountered in clinical practice. The progressive aging of the general population is associated with an inevitable rising in incidence of this particular rhythm disorder which in 2005 alone was responsible for 193,300 deaths, up from 29,000 in 1990 [1][2]. In providing proper treatment, the clinician must establish the pattern of arrhythmia, determine associated symptoms, and asses for underlying comorbidities in order to define short- and long-term management strategies. For these reasons, the study of Atrial Fibrillation has increased over the years but there are many parts of its pathophysiology, the best way of classification and best way to diagnose that are still unknown or not fully understood.

3.3 Heart

The heart is a muscular organ, whose main function is to pump blood into the circulatory system. Within the heart, two different types of fibres are capable of generating action potentials: muscular fibres responsible for the heart´s contraction and special fibres which are used to propagate the potentials throughout the myocardium. In order to fully describe this process, we need to briefly explain the heart´s anatomy and the electric potentials

involved in a full cardiac cycle. The heart is comprised by four chambers: two atria and two ventricles which are connected by the atrioventricular valves also known as the tricuspid or right valve and the mitral or left valve. The ventricles are separated from the aorta and the pulmonary artery by the semilunar valves also known as the aortic and the pulmonary, and both ventricles are separated by the interventricular septum. The interior walls of the ventricles are called the endocardium, the middle part the myocardium and the exterior of the heart the epicardium. A double-membrane sack called the pericardium [3] also surrounds the heart. Fig. 3-1 shows a diagram of the heart.

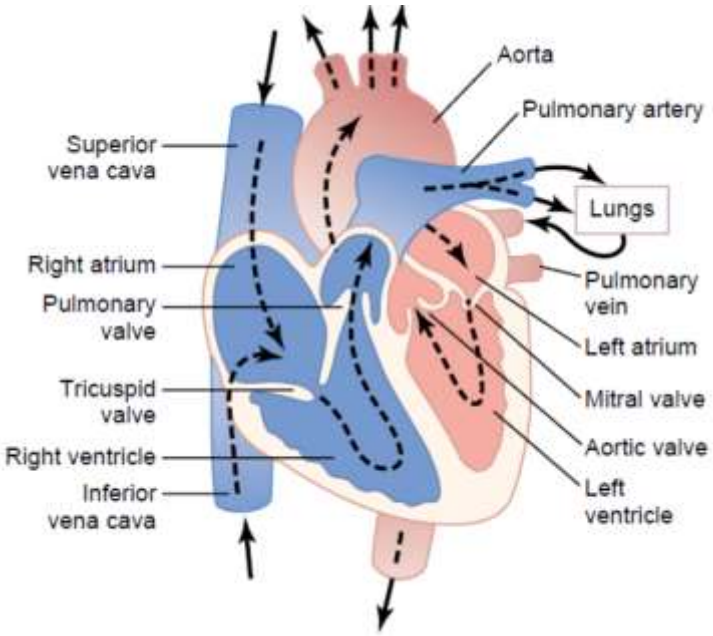

Fig. 3-1 Structure of the heart, and course of blood flow through the heart chambers and heart valves. From [3].

The heart acts as a pump which, in order to continuously provide a stream of blood, contracts itself rhythmically giving forth the cardiac cycle. To do so effectively, the muscles in the myocardium has a swirling pattern.

The heart has specialized cells in the sinoatrial (SA) node responsible for generating autonomously the electrical impulses used to contract these muscles. This property is called autorhythmicity. As mentioned before, a second system of specialized fibres is in charge of distributing this electric impulse throughout the cardiac muscle. There are three specialized pathways: anterior, middle and posterior internodal tracts between the SA node and the atrioventricular (AV) node. The passage of the impulse is delayed at the AV node before it continues to the bundle of His, which in turn divides into the right bundle branch and the left bundle branch, and finally reaches the Purkinje network. If any of

these paths were to be blocked or the electrical impulses were to be diffused randomly, it would arise different pathological heart conditions.

The heart cycle can be described in many ways, two of which are the biological and the electrical. To understand the relationship between the physical response to the electrical impulse and to the ECG, both approaches must be described. Biologically speaking, the heart cycle has two main stages (the ventricular diastole and systole) that can then be divided into sub-stages which are summarized in the following image.

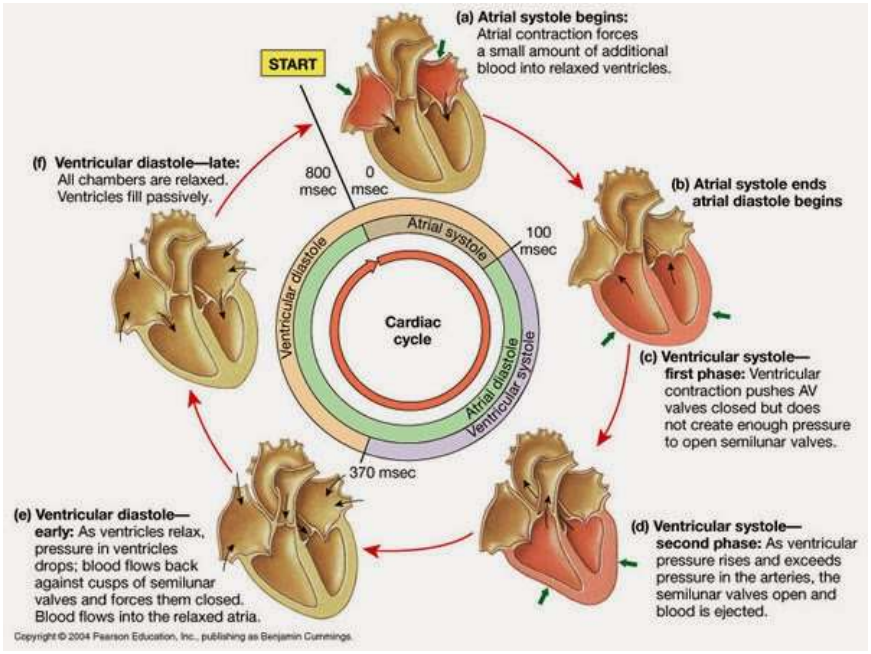

Fig. 3-2 Summary of the two main heart stages: Systole and Diastole. From [4].

Firstly, in the ventricular filling or late diastole, the atrioventricular valves open and the ventricles are filled with blood due to the pressure difference between them and the atria. When the ventricle is almost full, there is a small flow of blood directly from the veins. This process is called diastasis. The last phase of the diastole is the atrial systole, during which the atria contract so that the remaining blood inside them flows into the ventricles. This phase is responsible for filling almost one third of the ventricles. The second stage or the systole starts with the isometric ventricular contraction, which as the atrioventricular valves are closed, results in an increase of pressure. The pressure keeps building up until the aortic and pulmonary valves burst open and the ventricular ejection takes place. This phase takes 3 times longer than the contraction. Even as the pressure has decreased, blood keeps flowing due to ventricular contraction in a process called protodiastole which is said to end when the semilunar valves close. Finally, the isovolumetric relaxation takes place where all the ventricular fibres relax and as the

semilunar valves are closed the pressure drops. When it decreases enough, the atrioventricular valves reopen due to the difference in pressure and as the atria are filled with blood during the systole, the cycle starts again.

3.4 Cardiac Electrophysiology

The electrical signals are responsible for the physical activity of the heart and need to be studied to fully describe the ECG generation.

Some specialized cells that can be found in the body such as neurones and muscular cells have excitable membranes that undergo important changes in their behaviour when exposed to depolarising stimuli. This produces a cellular electrical activity called the action potential. ECG and electroencephalograms (EEG) are examples of signals that are usually measured externally. For this reason, extracellular bioelectric potential signals started being used for medical purposes.

3.5 Extracellular bioelectric potential signals

Extracellular potentials occur due to intracellular potentials i.e. the action potential. When there is an action potential, different types of currents go through the cell membrane. There are ionic currents that physically break through the cell membrane and also displacement currents that are created by the capacitive characteristic of the membrane.

These currents circulate into and out of the cells creating differences in potential that propagate throughout the body until its surface were can be detected using contact electrodes. Many have tried to find a relationship between intra and extracellular potentials and various mathematical methods have been developed.

Continuing with the previous description of the biological processes involved in the cardiac cycle, and in order to study the ECG waveforms, the different stages of the action potentials of a myocardial cell should be understood. The cellular action potentials are caused by the movement of ions between intra and extracellular regions and are dependent of the semipermeable property of the cell membrane. The diffusible ions that originate the electric activity are mainly sodium Na^{+}, potassium K^{+}, and calcium Ca^{2+}. These actions have 5 phases numbered 0 to 4. Fig. 3-3 shows the effect of the different ions on the action potential.

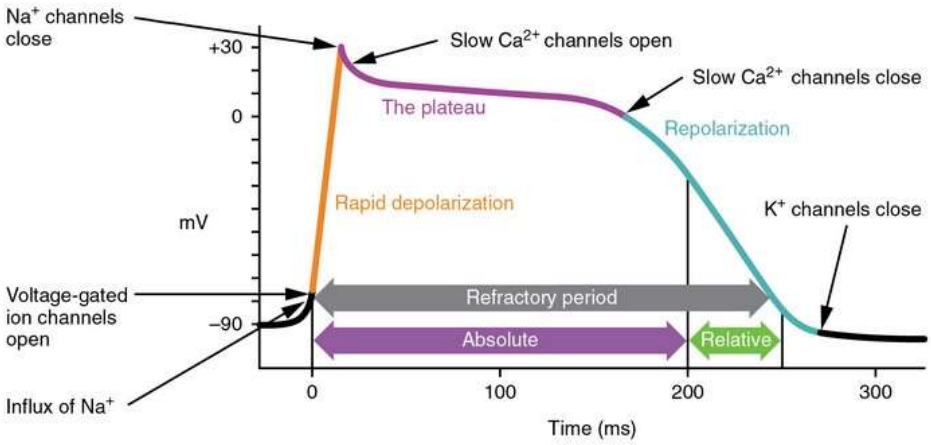

Fig. 3-3 Effect of different ions in the phases of generation of AP. Modified from [5].

Phase 0 corresponds to rapid depolarization, phases 1, 2 and 3 the repolarization and phase 4 (resting phase) the electric diastole. The repolarization consists of 3 stages, an initial stage (phase 1) that represents a brief repolarization which results on an intracellular potential of almost zero, a second stage (phase 2) of slow repolarization also known as plateau and a final stage (phase 3) called rapid repolarization where the potential returns to its baseline. Phase 4 corresponds to the resting membrane potential when the cell is not being stimulated (-85 to -95 mV).

3.6 Electrical Activity of Normal Heart

As these phases occur, the electrical activity which is generated spreads throughout the body and is registered on the body surface by the contact electrodes giving forth the ECG. The ECG generation depends on four electrophysiological processes: the formation of the electrical impulse developed in the sinoatrial node, the transmission of this impulse through the specialized fibres, the activation (depolarization) and the recuperation (repolarization) of the myocardium. Fig. 3-4 shows the typical action potentials (AP) in the principal cardiac structures and their combined effect resulting in the ECG.

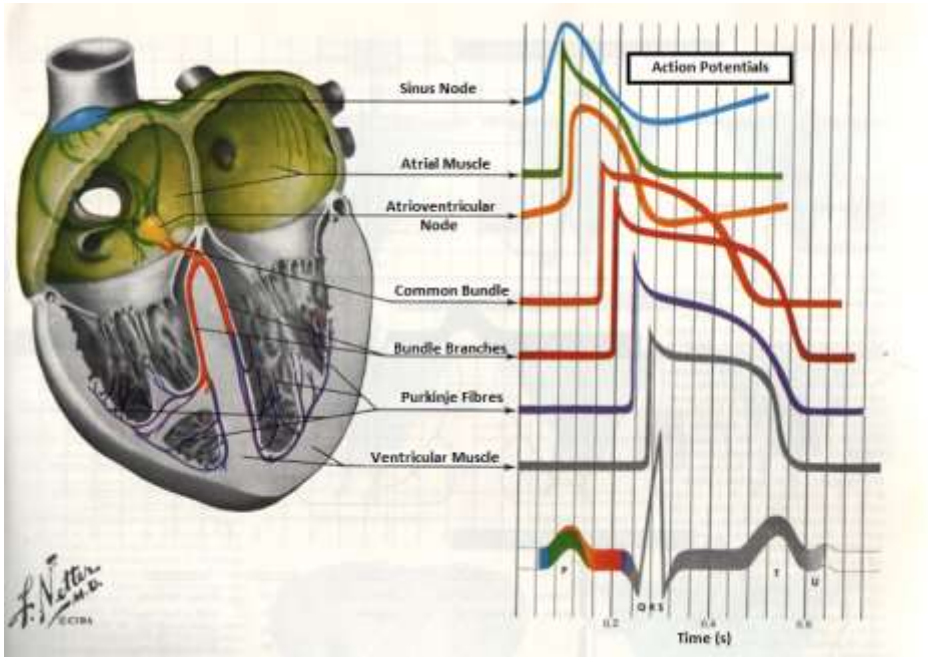

Fig. 3-4 Typical APs in the principal Cardiac Structures and their combined effect resulting in the ECG. From [6].

3.7 ECG signal

The standard ECG pulse have distinct intervals that were named by Willem Einthoven, the inventor of the first practical electrocardiogram. Fig. 3-5 shows a typical scalar electrocardiographic lead while Table 3-1 shows the usual durations of each of the intervals.

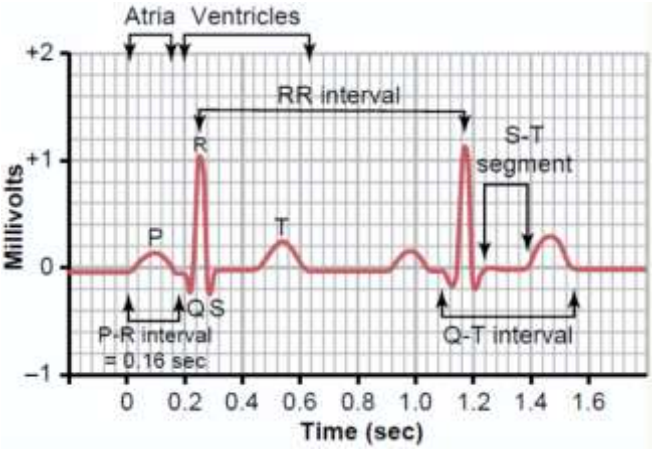

Fig. 3-5 Normal Electrocardiogram. From [3].

Table 3-1 Usual duration of ECG intervals.

P-R Interval	200 ms
Q-T Interval	310 ms
P-R Segment	100 ms
S-T Segment	140 ms
Q-R-S Complex	70 ms

The first wave that usually appears in an ECG is the P-wave, which is produced by the atrial depolarization during the atrial systole. Its low amplitude is due to the fact that the number of atrial fibres, responsible for the atrial contraction, is relatively smaller compared to the number of myocardial fibres responsible for the rest of the ECG waves.

The next three waves constitute the QRS complex. These waves are product of the contraction of the ventricular fibres. First, the Q wave which has a very low amplitude and has a negative polarity, then the R-wave which has a great amplitude and has a positive polarity and lastly, the S-wave, similar to the Q-wave but with a slightly higher amplitude. The time interval between two high amplitude R-waves (R-R Interval) is used to calculate the instantaneous heart rate.

The last wave and the focus of this thesis is the T-wave which is produced by the ventricular repolarization and is similar to the P-wave but has a higher amplitude. Between the T and the P-wave there is a horizontal line named baseline where in Sinus Rhythm (SR) there is no electrical activity due to the isoelectric phases of the cardiac cycle. These phases are the diastole and the diastasis, during which all the cells of the heart are polarized.

A very small additional wave called the U-wave is sometimes registered 40ms after the T-wave, but it has such a low amplitude that it does not appear in most ECG apparatus and although there are no certainties of it, it is believed to be due to slow repolarization of ventricular papillary muscles.

This study will assess the heterogeneity of the T-waves of atrial fibrillation (AF) patients with and without fibrillation episodes for the 12 Standard Leads.

3.8 The 12 Standard Leads

This project will focus on the study of the potentials generated by the heart. Since 1903 when Willem Einthoven registered the first ECG using a galvanometer, the ECG has become an essential tool for clinic analysis and diagnosis.

The 12 Standard leads are constituted by Einthoven's triangle, the three Augmented Leads (Goldberg Leads) which together are commonly called the six frontal leads, and the six Precordial leads, also known as the six chest leads.

The first technique for registering the ECG was developed when Einthoven studied the relationship between the location and the ECG obtained and developed an equilateral triangle where the heart constituted the centre. This triangle was called Einthoven´s triangle, and is used when determining the electrical axis of the heart as it is shown in Fig. 3-6. The potential difference between the axes of Einthoven´s triangle were called Standard Leads I, II and III which are summarized in

Table 3-2.

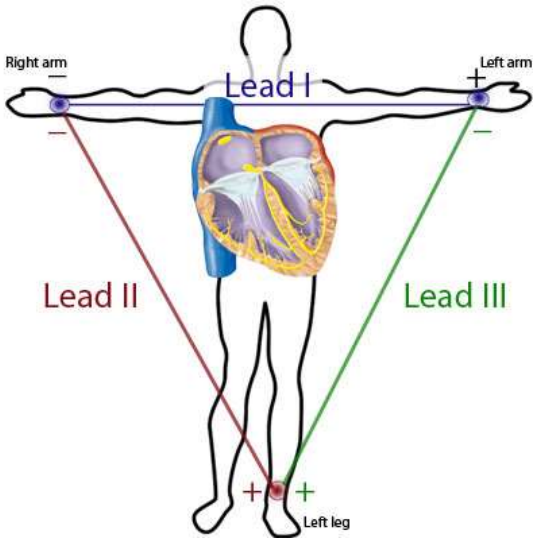

Fig. 3-6 Einthoven's Triangle. From www.medicine.mcgill.ca/physio/vlab/cardio/setup.htm.

Table 3-2 Potential difference in Leads I, II and III.

LEAD I	RIGHT ARM (-) TO LEFT ARM (+)
LEAD II	RIGHT ARM (-) TO LEFT LEG (+)
LEAD III	LEFT ARM (-) TO LEFT LEG (+)

Note that there is a clear relationship between the leads:

$$L_I + L_{III} = L_{II} \tag{3-1}$$

Measuring the ECG in the different leads results in different ECG waveforms. These differences are shown in the following image.

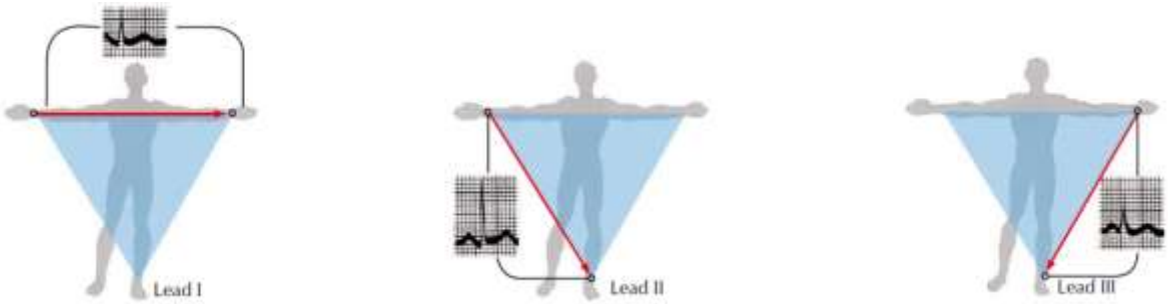

Fig. 3-7 ECG waveforms depending on the lead. From [6].

Similarly to Einthoven's triangle, the augmented unipolar leads are denoted as aVF, aVL and aVR, and describe the directions which are shifted 30◦ from the direction of Einthoven's triangle (I,II,III) as shown in Fig. 3-8.

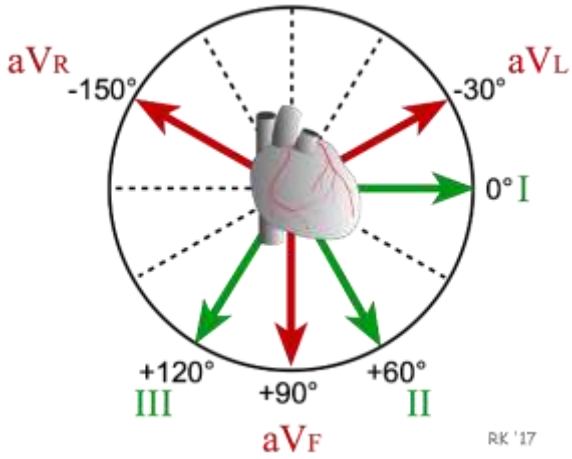

Fig. 3-8 Augmented Unipolar Leads. From http://www.cvphysiology.com/Arrhythmias/A013b.

These leads are unipolar and are calculated as the potential difference between one corner of the triangle and the average of the remaining two. They can be calculated also from leads I and II in the following way:

$$aVF = II - \frac{1}{2} * I \tag{3-2}$$

$$aVL = I - \frac{1}{2} * II \tag{3-3}$$

$$aVR = -\frac{1}{2} * (I + II) \tag{3-4}$$

As it has been shown, the six frontal leads can be numerically obtained by knowing only leads I and II.

The six precordial leads are obtained when the electrodes are placed directly on the chest as shown in Fig. 3-9. Table 3-3 describes the six unipolar standardized precordial leads.

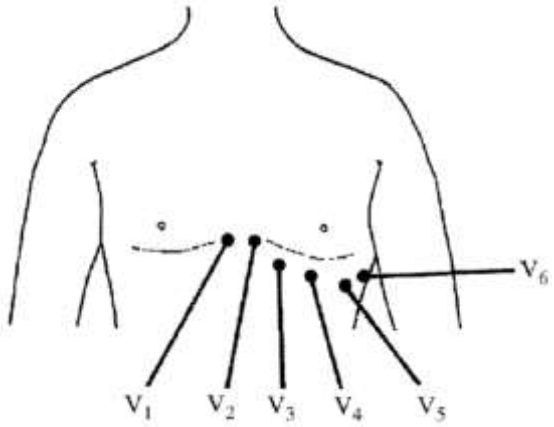

Table 3-3 Placement of intercostal leads.

V_1	4th Intercostal (right)
V_2	4th Intercostal (left)
V_3	Between V_2 and V_4
V_4	Mid-clavicular (Mid-collarbone)
V_5	5th Intercostal space (Anterior auxiliary line)
V_6	5th Intercostal space (Mid-auxiliary line)

Fig. 3-9 Placement of intercostal leads. From [7].

The six precordial leads, similarly to the three augmented leads, are unipolar, and the potential difference is calculated between the electrodes and a common point called Wilson Central Terminal (C point) as depicted in Fig. 3-10.

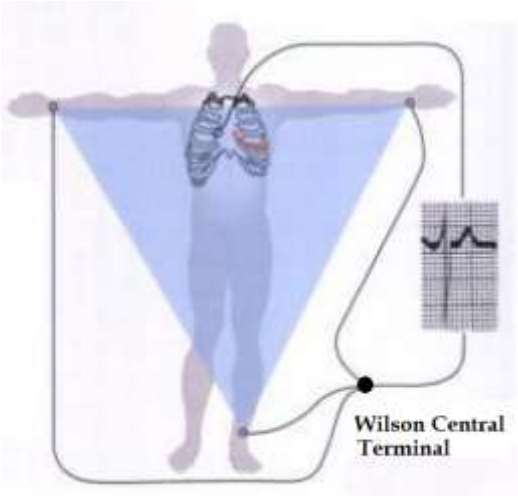

Fig. 3-10 Wilson Central Terminal. Modified from [6].

3.9 Abnormal Cardiac Conditions

According to the National Heart, Lung and Blood institute, abnormal Cardiac Conditions such as arrhythmias affect millions of people in Europe and North America. This thesis is going to focus on one type of supraventricular arrhythmia: Atrial Fibrillation (AF).

3.9.1 Atrial Fibrillation

Atrial fibrillation (AF) is characterized by chaotic and uncoordinated atrial activation and contraction that produces an irregular ventricular response as can be seen in Fig. 3-11.

Fig. 3-11 Diagram of AF. From Mayo Foundation for Medical Education and Research.

The appearance of a secondary (ectopic) pacemaker and/or areas of slow conduction may be the causes of this asynchrony. It represent a major health problem as it affects over 2 million people in Europe and roughly 2.2 million in the United States [8]. Recent studies have also shown that the prevalence of AF increases with aging and varies from 0.7%, in subjects from 55-59 years, to almost 18%, in 85-year-old patients [9]. In [10] it is stated, "The typical patient with AF is often referred to as an elder one with diabetes, left ventricular hypertrophy (LVH), and/or other electrocardiographic pathological findings, coronary heart disease (CHD) or valvular heart disease, coronary heart failure (CHF), or a history of previous stroke."

Diagnosis of AF is based on ECG rhythm studies. As the atrioventricular (AV) node is being bombarded by atrial impulses during AF, the ventricular rhythm becomes more irregular that during normal Sinus Rhythm (SR). This happens as a result of the summation and/or cancellation of waveforms in the AV node and, thus, a high level of disorganization of ventricular impulses. However, the most evident change in ECG documentation, as can be seen in Fig. 3-12 (upper ECG is an AF episode and lower ECG is SR), is the replacement of P-waves by rapid oscillations or fibrillatory waves (f-waves) that can vary in size, shape and frequency throughout the AF episode.

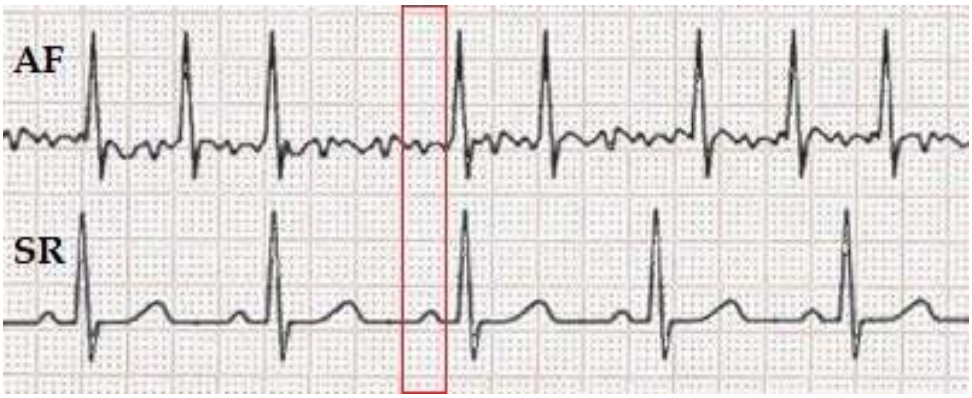

Fig. 3-12 ECG in AF (Upper) and in SR (Lower) conditions. Modified from [6].

3.9.2 AF Mechanisms

Atrial fibrillation's pathology is complex and not entirely understood, with different mechanisms influencing the start, duration and finish of AF episodes. These mechanisms include structural changes or fibrosis such as heart diseases, hypertension or diabetes, electrophysiological mechanisms such as a shortening in the refractory period, in the AF cycle length or abnormalities in pulmonary vein sleeves, and genetic factors.

Regarding the generation of atrial arrhythmias, three main hypotheses are postulated:

- multiple wavelet hypothesis, which states that AF is generated by various wavefronts propagated in a chaotic manner through the atria [11];
- focal hypothesis, where a focal source in the pulmonary veins lead to fibrillatory conduction and localized reentry [12];
- the presence of a mother rotor defined as a stable, high-frequency rotating pattern that drives AF [13].

3.9.3 Types of AF

Although there is no common agreement today on the best AF classification, current clinical guidelines advocate differentiating between paroxysmal, persistent and permanent AF [14].

4. Paroxysmal AF: AF with spontaneous interruption generally within 7 days but mostly in 24-48 h,
5. Persistent: AF that does not interrupt spontaneously but with therapeutic interventions (pharmacological or electrical), and

6. Permanent or chronic AF: AF in which interruption attempts have not been made or, if made, have not been successful.

One of the objectives of this thesis is to try to discriminate between the 3 types of AF.

3.9.4 Atrioventricular nodal function during AF

There are many ways of studying the effect of AF but this thesis will focus on the assessment of spatial heterogeneity of ventricular repolarization i.e. characterization of T-waves. The atrioventricular (AV) node plays a critical role in patients with AF as it acts as a filter to the irregular impact of atrial impulses that bombard the node. The AV node is a natural barrier and restricts the conduction of this impulses into the His-Purkinje system during AF. The atrial impulses lead to summation and/or cancellation of wavefronts in the AV node, creating a high level of disorganization [15]. Hence, the ventricular activity during AF is irregular and its study could lead to the discrimination between different types of AF episodes. There have been several studies aimed on characterizing the atrioventricular conduction using a mathematical model [16, 17]. However, the assessment in this thesis will be done using the $\mathcal{V}$-index.

3.10 $\mathcal{V}$-index

The $\mathcal{V}$-index is an electrocadiogram (ECG)-based estimator of the standard deviation of ventricular myocytes' repolarization times s_ϑ. The spatial dispersion of ventricular repolarization is responsible for the genesis of the T-wave on the ECG as can be seen in Fig. 3-13.

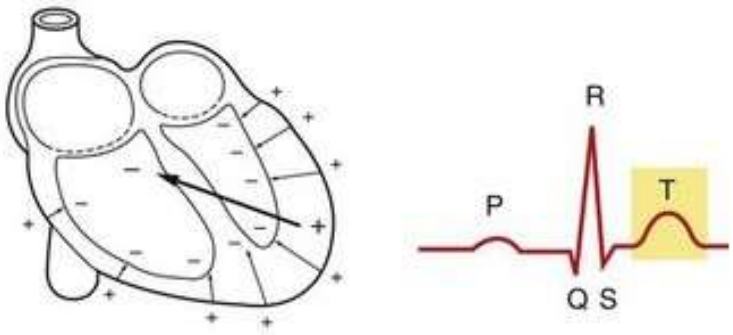

Fig. 3-13 Genesis of the T-wave.

However, an amplification of the repolarization favours the development of ventricular tachycardia/fibrillation as it creates suitable conditions for reentry mechanisms [18, 19]. Therefore, the assessment of the heterogeneity of the repolarization form the ECG would have great clinical value for the identification of life-threatening arrhythmias.

Several parameters related to T-wave morphology (width [20], amplitude) and duration ($T_{apex} - T_{end}$ [21, 22] and QT dispersion [23]) have been proposed to quantify the heterogeneity. However, when applied, they showed limitations [24, 25], have been questioned [26] or provided controversial interpretations [25, 27, 28]. Having this in mind, a novel method to quantify the dispersion of myocytes' repolarization times, rooted on a biophysical model of the ECG was derived. This method was based on van Oosterom's take on Dominant T-wave formalism (DTW) [29]. Sassi and Mainardi show that the variability of lead factors, which are the weights which modulate the DTW to generate the T-wave of each lead, across successive beats is related to the standard deviation of the repolarization times [30].

The DTW formalism is done by first, subdividing the heart's surface in M contiguous regions (nodes) where the sources are lumped together. Then, for each instant t, the equation of the surface vector potentials is considered:

$$\begin{bmatrix} \psi_1(t) \\ \cdots \\ \psi_L(t) \end{bmatrix} = \psi(t) = \mathrm{A} \begin{bmatrix} D_1(t) \\ \cdots \\ D_M(t) \end{bmatrix} \qquad (3\text{-}5)$$

where $\psi(t)$ is the vector of potentials (one for each of the L leads considered) and $\mathrm{A}_{L\times M}$ is a transfer matrix and is fixed for a given patient and lead configuration. Matrix A accounts for the volume of the conductor (conductivity and geometry) and the solid angle under which the single source contributes to the potentials in ψ. The functions $D_m(t)$ describe the repolarization phase of the transmembrane potentials (TMP) of the myocytes for a given subdivision. It has been shown that it is possible to link the shape of the T-wave in each lead to the TMP [29]. Therefore, making the approximation that the only difference across different $D_m(t)$ functions is the repolarization time (RT) ρ_m, that is $D_m(t) = D_m(t - \rho_m)$, then:

$$\psi(t) = \mathrm{A} \begin{bmatrix} D_m(t - \rho_1) \\ \cdots \\ D_m(t - \rho_M) \end{bmatrix} \qquad (3\text{-}6)$$

In turn, the RT of each node may be expressed as $\rho_m = \overline{\rho} + \Delta\rho_m$ where $\overline{\rho} = \sum_{m=1}^{M} \rho_m / M$ is the average repolarization time. After a series of approximations described in [30], the following equation is reached:

$$\psi(t) \approx -\boldsymbol{A}\Delta\rho\dot{D}(t-\overline{\rho}) + \frac{1}{2}\boldsymbol{A}\Delta\rho^2\ddot{D}(t-\overline{\rho}) \quad (3\text{-}7)$$

$$\Psi \approx w_1 T_d + w_2 \dot{T}_d \quad (3\text{-}8)$$

where $\Psi_{L\times N}$ is a matrix containing N ECG samples recorded from L leads, w_1 and w_2 are 2 sets of L x 1 vectors of leads factors, T_d is a 1 x N vector obtained after sampling $\dot{D}(t)$ and $\dot{T}_d$ its derivative. The dominant T-wave is a term set by van Oosterom for the quantity $-T_d$.

Finally, an approximate measure of the dispersion of the average deviations $\Delta\rho_m$ across the ventricles is described by the following equation:

$$\mathcal{V}_i = \frac{std[w_2(i)]}{std[w_1(i)]} \approx s_\vartheta \quad (3\text{-}9)$$

It has been shown that the quantity $\mathcal{V}_i$ for each lead L is independent from the transfer matrix A [30] therefore it depends neither on the column conductor nor the lead considered and it will be referred to as the $\mathcal{V}$-index. Chauan et al. [31] showed that in a healthy human $s_\vartheta \approx 20\,ms$ across the ventricles.

The diagnostic and prognostic abilities of the $\mathcal{V}$-index have been thoroughly tested by Abächerli et al. in [32], in which the $\mathcal{V}$-index was computed in patients with symptoms suggestive of non-ST-elevation myocardial infarction. They concluded that the $\mathcal{V}$-index significantly improved the diagnostic accuracy of the ECG for the diagnosis of Acute Myocardium Infarction (AMI) and increased the ECG sensitivity from 41% to 86%. Furthermore, the index helped with the prediction of all-cause mortality during follow-up.

The $\mathcal{V}$-index was also used to assess the effect of drugs such as moxifloxacin or sotalol which provide different alteration of the QT interval length ranging from subtle (moxifloxacin) to evident (sotalol) [33]. The study showed that the $\mathcal{V}$-index had the capability of assessing drug-induced pro-arrhythmic effects as well as having the advantage of being (i) a direct estimator of spatial heterogeneity of ventricular

repolarization and (ii) only marginally affected by misdetection of T-waves fiduciary points.

3.11 Objectives and Outline

The objective of this thesis is the assessment of spatial heterogeneity of ventricular repolarization in patients with atrial fibrillation which includes:

- Simulation: use physiological T-waves to study the differences that arise in the $\mathcal{V}$-index in 3 cases:
    - Theoretical case
    - Sinus Rhythm condition
    - Atrial Fibrillation condition

  The AF condition was achieved by adding simulated f-waves to the physiological T-waves using the method described in [34].

- Study of Swiss AF database: compute and compare the $\mathcal{V}$-indexes of 2013 patients in paroxysmal and persistent SR and paroxysmal, persistent and permanent AF, in the 3 main $\mathcal{V}$-index computation methodologies.

Chapter 4. MATERIALS

For this thesis, Swiss Atrial Fibrillation (Swiss-AF) cohort carried out a study of 2400 patients across 13 sites in Switzerland. Out of the ECG signals of the 2400 patients, 2013 had signals clear enough to conduct the computation of the $\mathcal{V}$-index, out of which 902 patients present paroxysmal, 608 persistent and 503 permanent AF. The patients were then divided into 5 groups: AF (Paroxysmal, Persistent and Permanent) and SR (Paroxysmal and Persistent). The SR patients were patients with AF for which the ECG was recorded during SR. It is worth mentioning that Swiss-AF does not have a control group with patients without AF.

Eligible patients had to be ≥65 years old and had to have one of the 3 AF patterns studied. They were chosen by a comprehensive screening of in- and outpatients in participating hospitals and by contacting general practitioners in the area. Main exclusion criteria included inability to provide informed consent, the presence of exclusively nonsustained episodes of secondary form of AF (e.g. after cardiac surgery or severe sepsis) or any acute illness within the last 4 weeks. The latter group of patients were eligible for enrolment after stabilization of their acute episode.

The local ethics committees approved the study protocol, and informed written consent was obtained from each participant. All data was collected in a standardized manner by trained study personnel and an overview of the study procedures for the baseline and follow-ups can be seen in Table 4-1.

Table 4-1 Overview of the study procedures. Procedures for baseline have been highlighted. From [31].

Procedure	Baseline	Year 1	Year 2	Year 3	Year 4+*
Written informed consent	X				
Study case report form	X	X	X	X	(X)
Clinical measures	X	X	X	X	(X)
Resting electrocardiogram	X	X	X	X	(X)
Outcomes		X	X	X	(X)
Cerebral MRI	X		X		
Cognitive assessment	X	X	X	X	(X)
Blood sampling	X		X		
Disability, quality of life	X	X	X	X	(X)
Health economics	X	X	X	X	(X)

MRI = magnetic resonance imaging * Long term perspective, no funding obtained yet

This thesis is going to focus in the baseline resting electrocardiogram of the patients enrolled.

The electrocardiogram consisted in 16-lead ECG recordings of 5 minutes duration that were obtained using the same ECG acquisition technology at all centres (CS-200 Excellence and CS-200 Touch, Schiller AG, Baar, Switzerland). As mentioned previously, this thesis is only going to use the 12 Standard Lead ECG as it is commonly used in clinics. The digital ECGs were then stored with a sampling frequency of 1 kHz (signal bandwidth 0.04-387Hz) and a resolution of 1 µV/bit. The sampling frequency is twice as high as that of standard ECG devices so it allows advanced signal processing analyses [35].

Chapter 5. METHODS

The methodology of this thesis is divided in two distinct stages: AF simulation and Study of Swiss-AF database.

AF simulation's main processes are add AF, calculate w_1 and $w_2$and calculate the $\mathcal{V}$-index of the theoretical values and the experimental values with and without f-waves.

Swiss-AF database's main processes include Elimination of f-waves if necessary for AF patients, and then for all the patients: a Pre-processing stage which includes filtering and Baseline Alignment, the T-wave detection stage which includes the use of Pan Tompkins algorithm to determine the position of the QRS, Rough Beat Alignment, T-Wave Delineation, Beat Re-Alignment and cross correlation to identify the good leads. Finally, as in the AF simulation, the stages of w_1 and $w_2$and $\mathcal{V}$-index calculation.

5.1 AF Simulation

The purpose of the AF simulation is to determine if the f-waves affect the computation of the $\mathcal{V}$-index and if it is better to cancel them before doing the comparison with the SR patients.

For this stage, T-waves from the 12 Standard Leads and theoretical w_1, $w_2$and $\mathcal{V}$-index values for seven patients were used.

An example of the T-waves provided for one of the patients are shown in Fig. 5-1.

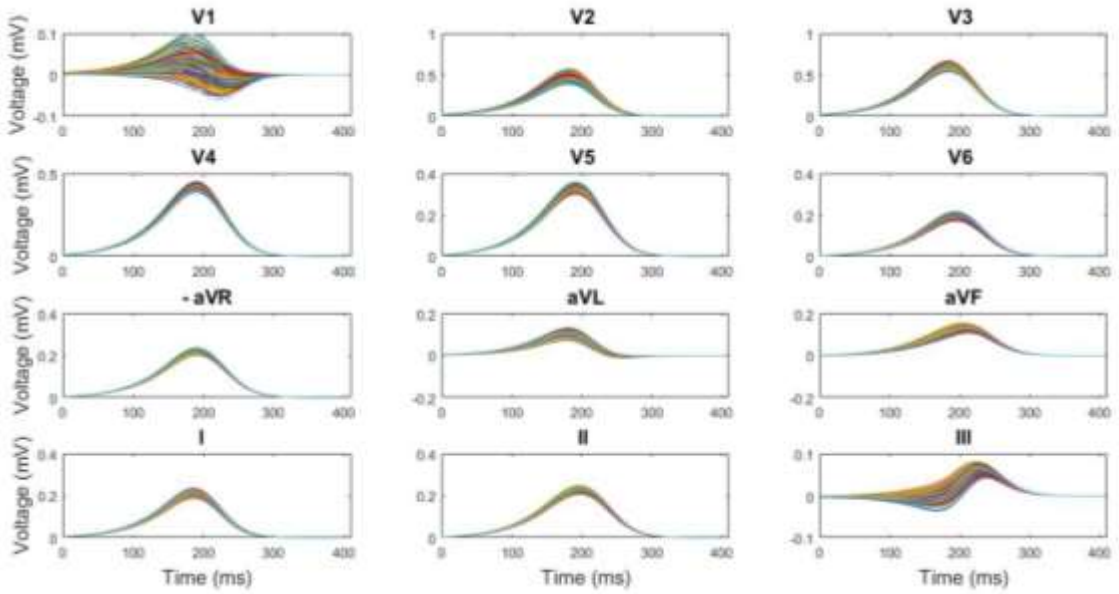

Fig. 5-1 T-waves for 12 Standard Leads.

The overall processes followed during AF simulation are shown in Fig. 5-2.

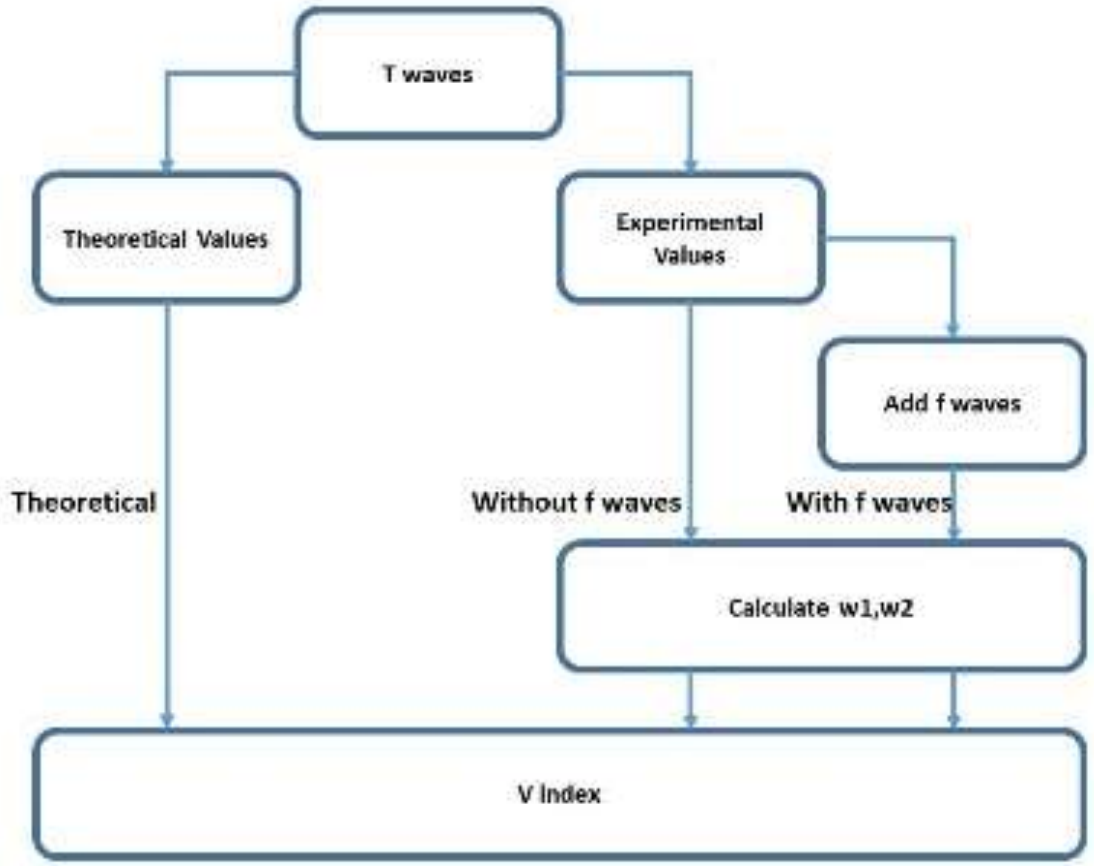

Fig. 5-2 Block Diagram of Processes in AF Simulation.

5.1.1 Add f-waves

To see the effect the f-waves had in the computation of the $\mathcal{V}$-index, fibrillatory waves were simulated and added to the T-waves following the steps described in [34].

A sawtooth model for simulating f-waves was proposed in Stridh and Sörnmo (2001) and recently the model was extended to include a stochastic signal component so that more complex f-wave patterns could be generated. This method consisted in adding the sawtooth model component $d_l(t)$ and a white noise component $s_l(t)$ so that:

$$f_l(t) = d_l(t) + s_l(t), \quad l \in \{X, Y, Z\} \tag{5-1}$$

where $\{X, Y, Z\}$ represent the 3 orthogonal leads.

Component $d_l(t)$ is described by the following equations:

$$d_l(t) = \sum_{i=1}^{l} a_{l,i}(t)\sin(2\pi i F_{l,0} t + i\frac{\Delta F}{F_m}\sin(2\pi F_m t) \tag{5-2}$$

$$a_{l,i}(t) = \frac{2}{i\pi}(a_l + \Delta a_l \sin(2\pi F_a t), i = 1, \ldots, l, \tag{5-3}$$

the values of the parameters used are summarised in Table 5-1.

Table 5-1 Parameter values for simulating f-waves. From [34].

Parameter	Value
Harmonics number, I	3
Maximum frequency deviation, ΔF	0.25 Hz
Modulation frequency, F_m	0.2 Hz
Amplitude modulation frequency, F_a	0.2 Hz
Sawtooth amplitude, a_X	[15, 45] μV
Sawtooth amplitude, a_Y	[15, 40] μV
Sawtooth amplitude, a_Z	[25, 70] μV
Modulation amplitude, Δa_l	$\Delta a_l = \frac{1}{3} a_l$
AF frequency, $F_{l,0}$	[3, 7] Hz
White noise variance, $\sigma^2_{l,s}$	$\sigma^2_{l,s} = \frac{1}{2} a_l$

The Sawtooth amplitude a_X, a_Y, a_Z was chosen randomly within the range given and the study was done for AF frequency [3,12] Hz as [34] states that even though the AF frequency typically found is in the interval 3-7 Hz, in persistent and permanent AF, the AF frequency is usually higher and found in the interval 5-12 Hz .

The stochastic component $s_l(t)$ results from bandpass filtering of a white noise with variance $\sigma_{l,s}^2$ as a fraction of the sawtooth amplitude a_l. The filter chosen was a third order Butterworth and had two passbands symmetrically related to the AF frequency $F_{l,0}$ by $[0.65F_{l,0}$, $0.95F_{l,0}$ and $[1.05F_{l,0}$, $1.35F_{l,0}]$.

Fig. 5-3 shows $d_l(t), s_l(t)$ and $f_l(t)$ for the 3 orthogonal leads and AF frequency 5 Hz.

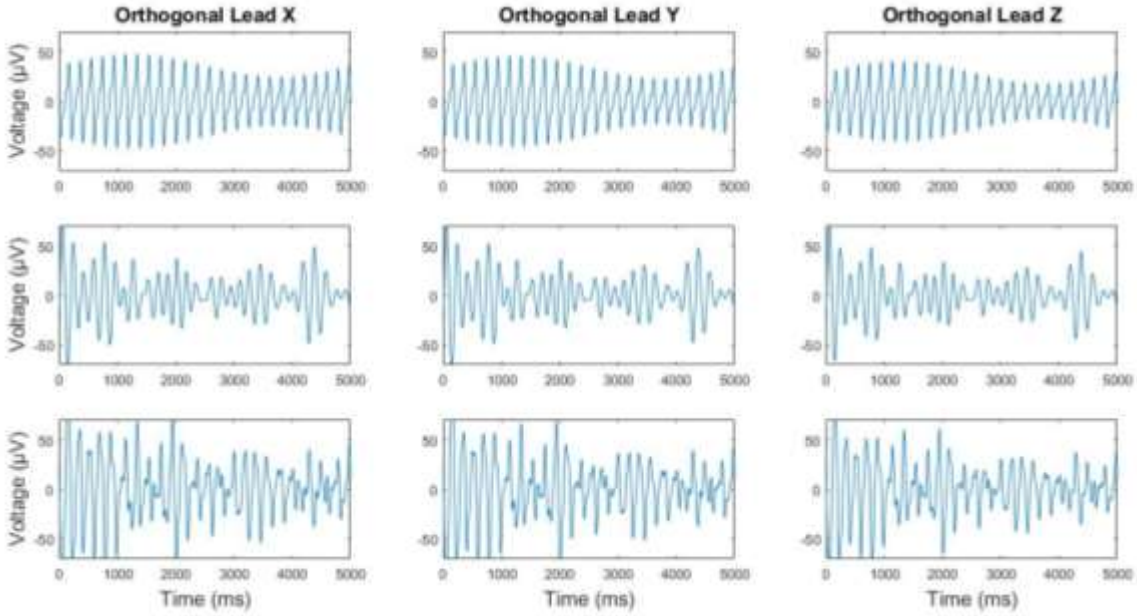

Fig. 5-3 $d_l(t)$,$s_l(t)$ and $f_l(t)$ for the 3 Orthogonal Leads and AF simulation frequency of 5 Hz.

Once $f_l(t)$ was computed for the 3 Orthogonal Leads, using the $Dower\ Matrix_{8\times3}$ and the relationship between the leads, $f_l(t)_{3\times N}$ was transformed to the 12 Standard Leads and added to the T-waves. The process was:

$$f_{8leads_l}(t)_{8\times N} = Dower\ Matrix * f_l(t) \tag{5-4}$$

Being $f_{8leads_l}(t)$ the simulated f-waves in 8 of the leads (V1, V2, V3, V4, V5, V6, I, II) and N the number of samples.

The rest of the leads were calculated using the relationship between leads:

$$III = II - I \tag{5-5}$$

$$aVF = II - \frac{1}{2} * I \tag{5-6}$$

$$aVL = I - \frac{1}{2} * II \tag{5-7}$$

$$aVR = -\frac{1}{2} * (I + II) \tag{5-8}$$

Fig. 5-4 shows the T-waves once the f-waves were added.

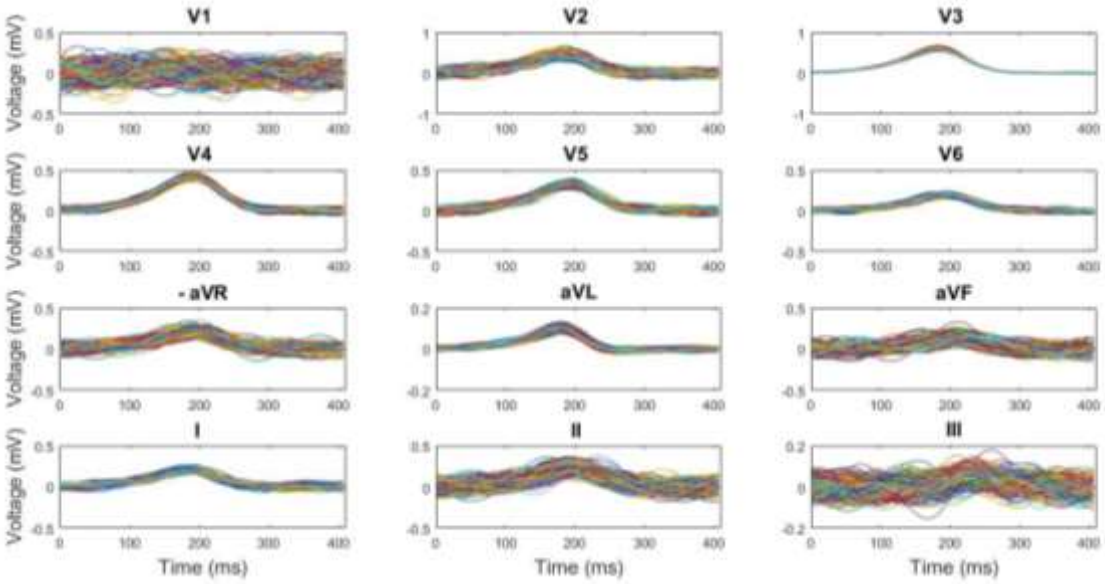

Fig. 5-4 T-waves for 12 Standard Leads with f-waves.

5.1.2 Calculate w_1 and w_2

For the experimental values both with and without f-waves, w_1 and w_2 must be calculated in order to calculate the $\mathcal{V}$-index. To do so, this thesis describes 3 different methods hereinafter Method 1, Method 2 and Method 3.

5.1.2.1 Method 1

Method 1 consisted in estimating the dominant T-wave (DTW) and the lead factors for each beat by minimizing the Frobenious norm [30]:

$$\epsilon = \left\| \Psi - w_1 T_d - w_2 \dot{T}_d \right\|_F \quad (5\text{-}9)$$

where Ψ is the vector of potentials, w_1 and w_2 are the lead factors and T_d and $\dot{T}_d$, the dominant T-wave and its derivative. Keeping this in mind, [30] alternatively minimizes the function:

$$\hat{\epsilon}^2 = \sum_{i=1}^{L} \int_{\mathrm{JT}} \left[\Psi_i(t) - w_1(i) T_d(t) - w_2(i) \dot{T}_d(t) \right]^2 dt \quad (5\text{-}10)$$

which is a continuous-time extension of Eqn. (5-9).

First, 'basic' estimates were obtained as initial values for the iteration process. T_d and w_1 were obtained from:

$$T_d = c_2 \lambda_1 v_1^T \quad (5\text{-}11)$$

$$w_1 = \frac{u_1}{c_2} \quad (5\text{-}12)$$

where c_2 is set so that the integral of $T_d(t)$

$$-\int_{t_{de}}^{t_{re}} T_d(\tau)\, d\tau \approx 100 \quad (5\text{-}13)$$

Evaluates the average difference in the intracellular potential before (t_{de}) and after repolarization (t_{re}). The rest of the parameters (u_1, λ_1, v_1^T) are obtained from the singular value decomposition (SVD) of Ψ:

$$\Psi = \mathrm{U}\Lambda\mathrm{V}^T = \sum_{i=1}^{L} u_i \lambda_i v_i^T. \quad (5\text{-}14)$$

$\dot{T}_d(j)$ is then defined as:

$$\dot{T}_d(j) = \frac{[\dot{T}_d(j+1) - \dot{T}_d(j-1)]}{2\Delta} \quad (5\text{-}15)$$

and w_2 is forced to minimize the residual:

$$\epsilon = \left\| \Upsilon - w_2 \dot{T}_d \right\|_F \quad (5\text{-}16)$$

where $\Upsilon = \Psi - w_1 T_d$. That is:

$$w_2 = \frac{\Upsilon \dot{T}_d}{\left\| \dot{T}_d \right\|^2} \quad (5\text{-}17)$$

When the initial values are calculated, a new value of T_d is obtained from:

$$T_d(j)\left[\|w_1\|^2 + \frac{2\|w_2\|^2}{(\Delta t)^2}\right] - \frac{[T_d(j+1) + T_d(j-1)]\|w_2\|^2}{(\Delta t)^2} = \sum_{i=1}^{L}\left\{\Psi_{i,j} \mathrm{w}_1(i) - \frac{\left[\Psi_{i,j+1} - \Psi_{i,j-1}\right]\mathrm{w}_2(i)}{2\Delta t}\right\} \quad (5\text{-}18)$$

where Δt is the inverse of the sampling rate, with

$$\dot{T}_d(j) = -\frac{\sum_{i=1}^{L}\left[T_d(j)\mathrm{w}_1(i)\mathrm{w}_2(i) - \mathrm{w}_2(i)\Psi_{i,k}\right]}{\sum_{i=1}^{L} \mathrm{w}_2{}^2(i)} \quad (5\text{-}19)$$

Finally, values w_1 and w_2 are computed by solving:

$$\begin{cases} \mathrm{w}_1\|T_d\|^2 + \mathrm{w}_2 \dot{T}_d T_d{}^T = \Psi T_d{}^T \\ \mathrm{w}_1 \dot{T}_d T_d{}^T + \mathrm{w}_2\left\|\dot{T}_d\right\|^2 = \Psi \dot{T}_d{}^T \end{cases} \quad (5\text{-}20)$$

T_d is newly obtained from Eqn. (5-18)(5-19) and the two steps are iterated. Sassi and Mainardi verify that 3 iterations grant an error on the estimates smaller than 1% [30].

The DTWs estimated with this method for one of the patients is shown in Fig. 5-5.

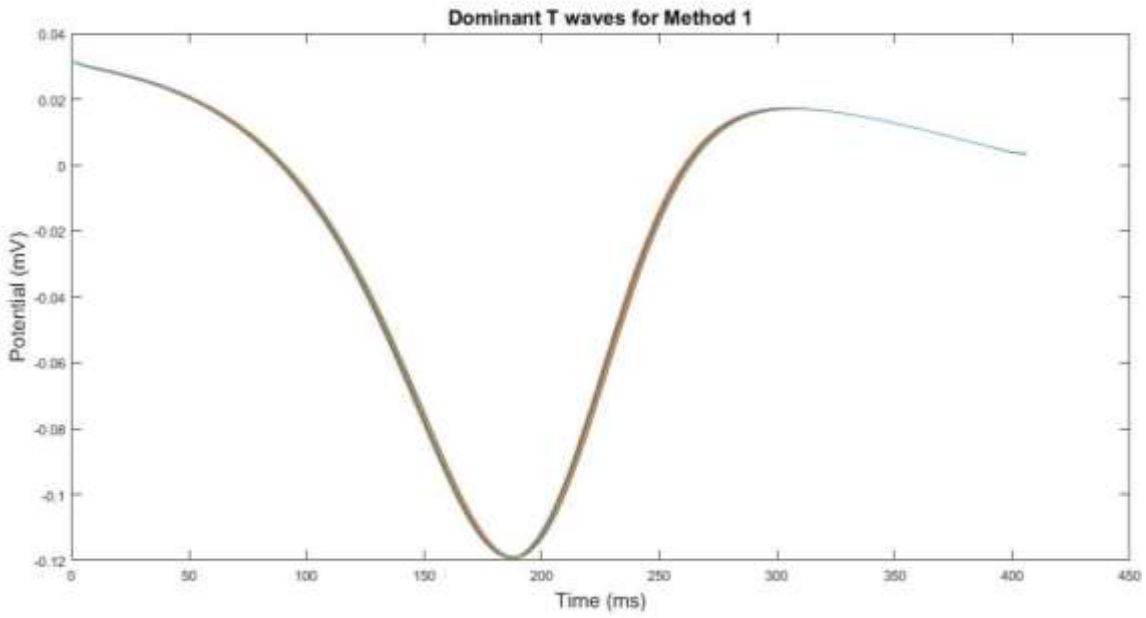

Fig. 5-5 Dominant T-waves estimated with Method 1.

5.1.2.2 Method 2

This method assumes that the average shape of the repolarization phase of transmembrane potentials does not change significantly between nearby beats [36] and uses a single DWT, shared across beats instead of calculating a DTW for each beat as seen in Method 1. This enables the method to reduce the impact of noise.

The method is similar to method 1, but in this case, the function to minimize is:

$$\hat{\epsilon}^2 = \sum_{l=1}^{L} \sum_{b=1}^{B} \int_{\mathrm{JT}} \left[\Psi_{l,b}(t) - w_{1,l,b}(i) T_d(t) - w_{2,l,b}(i) \dot{T}_d(t)\right]^2 dt \qquad (5\text{-}21)$$

where b is the beat index and B the total number of beats.

Differently to Method 1, the iterative algorithm stopping criteria was chosen when the estimate of $\mathcal{V}$-index varied less than a certain threshold between successive iterations (0.01 ms was used).

The DTWs estimated with this method for one of the patients is shown in Fig. 5-6.

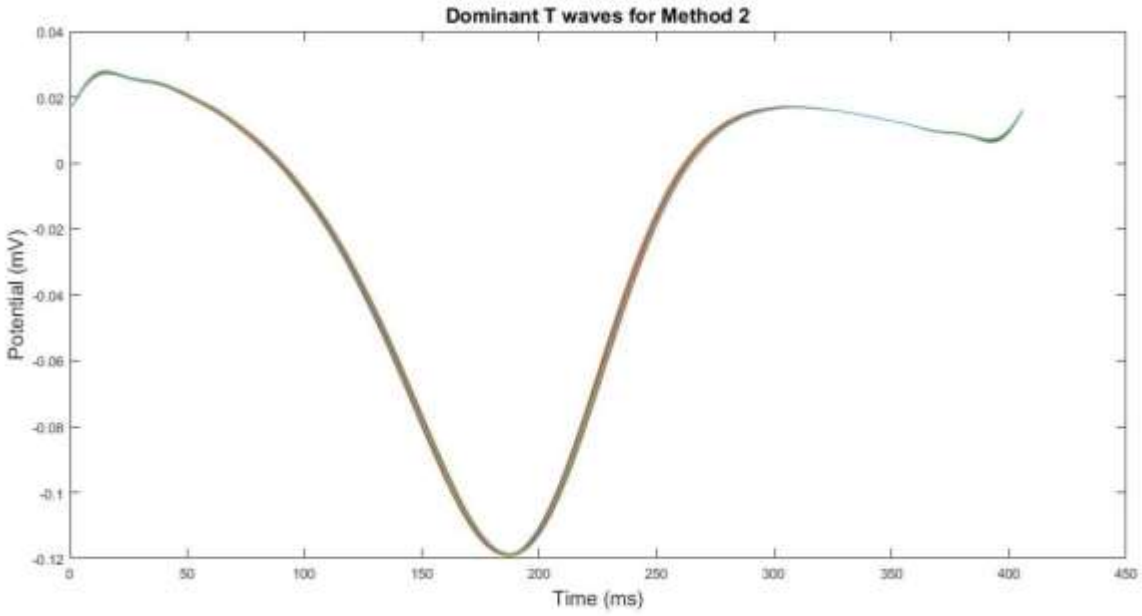

Fig. 5-6 Dominant T-waves estimated with Method 2.

5.1.2.3 Method 3

To overcome the impact of noise, Method 3 was based on an analytical model based on a trigonometric expansion of T_d. Roonizi et al. describe in detail the method in [37].

Bringing back equation (3-7) from the Introduction of the $\boldsymbol{\mathcal{V}}$-index

$$\Psi(t) \approx -\boldsymbol{A}\Delta\rho\dot{D}(t-\overline{\rho}) + \frac{1}{2}\boldsymbol{A}\Delta\rho^2\ddot{D}(t-\overline{\rho}) \qquad (3\text{-}7)$$

where $\Psi_{L\times N}$ is a matrix containing N ECG samples recorded from L leads, w_1 and w_2 are 2 sets of L x 1 vectors of leads factors, $\mathrm{T_d}$ is a 1 x N vector obtained after sampling $\dot{\mathrm{D}}(\mathrm{t})$ and $\dot{\mathrm{T}}_\mathrm{d}$ its derivative can more commonly be expressed as:

$$\Psi = \sum_{k=1}^{N} w_k \frac{d^{k-1}}{dt^{k-1}} T_d(t_i) \qquad (5\text{-}22)$$

where $T_d = d/dt\, D(t_i - \rho_r)$, $w_k = (-1)^k A(\Delta\rho)^k/k!$ Is the lead factors and N is the number of terms T_d and its derivatives contribute to model the potentials. In Method 1 and Method 2 N = 2. However, in theory for having a better approximation of the potentials and lead factors, more terms in the Taylor Expansion (5-22) are needed. This method uses N = 5.

This method is based on defining the following 2B-dimensional vector as sinusoidal basis waveforms:

$$\Phi(t_i) = [\phi_{c,0}(t_i), \dots, \phi_{c,B-1}(t_i), \phi_{s,0}(t_i), \dots, \phi_{s,B-1}(t_i)]^T \quad (5\text{-}23)$$

where

$$\phi_{c,n}(t_i) = \cos(\lambda_n t_i) \ and \ \phi_{s,n}(t_i) = \sin(\lambda_n t_i), \quad (5\text{-}24)$$

$\lambda_n = 2\pi f_n$ and f_n is the frequency of the sinusoidal waves.

Then the observation samples $x(t_i)$ collected in the vector $x_{1\times T}$ can be approximated as:

$$\hat{x}(t_i) = \sum_{n=0}^{B-1} \alpha_{c,n}\phi_{c,n}(t_i) + \alpha_{s,n}\phi_{s,n}(t_i) \quad (5\text{-}25)$$

$$\text{or } \hat{x} = \alpha_c^T \Phi_c + \alpha_s^T \Phi_s,$$

The main reason for choosing sinusoidal waveforms as bases functions for T_d is that these waveforms have two interesting properties: i) orthogonality; ii) they are a functional set closed under the operation of differentiation. In fact:

$$\frac{d^k}{dt^k}\phi_{c,n}(t_i) = \begin{cases} (-1)^{\frac{k}{2}}\lambda_n^k \phi_{c,n}(t_i) & \text{k is even} \\ (-1)^{\frac{k+1}{2}}\lambda_n^k \phi_{s,n}(t_i) & \text{k is odd} \end{cases} \quad (5\text{-}26)$$

and

$$\frac{d^k}{dt^k}\phi_{s,n}(t_i) = \begin{cases} (-1)^{\frac{k}{2}}\lambda_n^k \phi_{s,n}(t_i) & \text{k is even} \\ (-1)^{\frac{k+1}{2}}\lambda_n^k \phi_{c,n}(t_i) & \text{k is odd} \end{cases} \quad (5\text{-}27)$$

Using Eqn. (5-25) the potentials Ψ can be represented as:

$$\Psi = Q_c\Phi_c + Q_s\Phi_s \quad (5\text{-}28)$$

where Φ_c and Φ_s are previously defined in (5-25) and Q_c and Q_s are L x B matrices that represent the complete set of transform coefficients.

The initial estimate of T_d is using SVD and can be further represented as:

$$T_d = p_c^T \Phi_c + p_s^T \Phi_s \quad (5\text{-}29)$$

where p_c and p_s are coefficients related to T_d. As the bases waveforms for this method are sinusoids, then p_c and p_s are the vector of Fourier coefficients.

By substituting (5-29) in (5-22), the potentials can be approximated as:

$$\Psi = W(H_c \Phi_c + H_s \Phi_s) \quad (5\text{-}30)$$

where $W_{L\times N}$ is the complete set of lead factors, H_c and H_s are the N x B dimension matrices whose elements are:

$$h_c(k,n) = \begin{cases} (-1)^{\frac{k}{2}} \lambda_n^k p_{c,n} & \text{k is even} \\ (-1)^{\frac{k+1}{2}} \lambda_n^k p_{s,n} & \text{k is odd} \end{cases} \quad (5\text{-}31)$$

and

$$h_s(k,n) = \begin{cases} (-1)^{\frac{k}{2}} \lambda_n^k p_{s,n} & \text{k is even} \\ (-1)^{\frac{k+1}{2}} \lambda_n^k p_{s,n} & \text{k is odd} \end{cases} \quad (5\text{-}32)$$

Now from (5-28) and (5-30) we have

$$Q = WH \quad (5\text{-}33)$$

where $Q = [Q_c\ Q_s]$ and $H = [H_c\ H_s]$. Now, the problem changes to find W and H, so that the error function $e = |Q - WH|_F$ is minimized.

To do so, an iterative procedure is followed. As with the previous methods, T_d is initially estimated using SVD and represented as (Td = pc). Having p_c and p_s, the initial values of H can be computed using Eqn. (5-31) and (5-32). Then the only unknown left would be W which can be computed as $W = (H^T H)^{-1} H Q^T$. The next step would be to update

T_d and the coefficient vector p_c and p_s are used. Roonizi et al. [37] show that p_c and p_s can be obtained as:

$$p_{c,n} = \frac{1}{2}\frac{\sum_{m=1}^{L}[q_c(m,n)z_1 + q_s(m,n)z_2]}{\sum_{m=1}^{L}[z_1 z_1 + z_2 z_2]},$$
$$p_{s,n} = \frac{1}{2}\frac{\sum_{m=1}^{L}[q_s(m,n)z_1 - q_s(m,n)z_2]}{\sum_{m=1}^{L}[z_1 z_1 + z_2 z_2]} \quad (5\text{-}34)$$

where $q_c(m,n)$ and $q_s(m,n)$ are each of the elements of Q_c and Q_s and z_1 and z_2 are obtained from:

$$z_1 = \sum_{k=1}^{N} W_{m,k}(-1)^{\frac{k}{2}}\lambda_n^k,$$
$$z_2 = \sum_{k=1}^{N} W_{m,k}(-1)^{\frac{k+1}{2}}\lambda_n^k. \quad (5\text{-}35)$$

Having the new estimated values of coefficients p, T_d can be updated and the algorithm is repeated until an acceptable error is reached.

The DTW estimated with this method for one of the patients is shown Fig. 5-7.

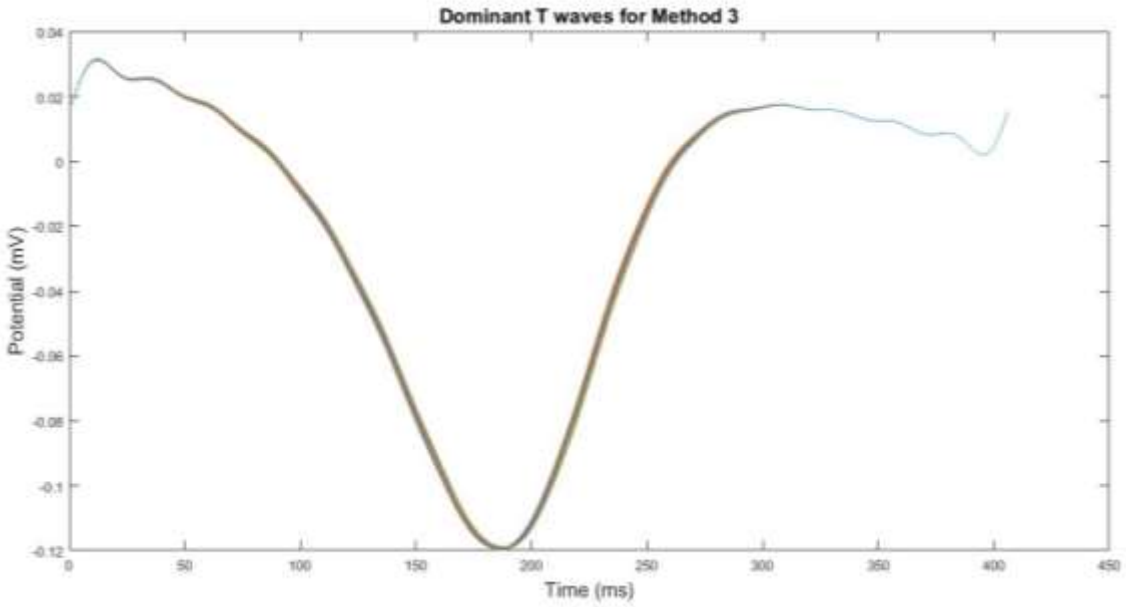

Fig. 5-7 Dominant T-waves estimated with Method 3.

Roonizi et al. compare the 3 methods used and conclude that all three methods were able to estimate the $\mathcal{V}$-index. However, Method 3 seemed to provide more reliable estimates as being an analytical scheme, allows to consider more lead factors than Method 1 and Method 2 [36].

5.1.3 Calculate $\mathcal{V}$-index

Once the Tdoms, w_1 and w_2 are calculated the $\mathcal{V}$-index is computed as described in the Introduction:

$$\mathcal{V}\text{-}index = \frac{std[w_2(i)]}{std[w_1(i)]} \quad (5\text{-}36)$$

5.2 Study of Swiss AF database

The main part of this thesis was the study of the Swiss AF database which as mentioned before, divided the patients into 5 groups: AF (Paroxysmal, Persistent and Permanent) and SR (Paroxysmal and Persistent) in order to later do some comparisons between the $\mathcal{V}$-index results obtained from each of the subgroups.

The processes followed in this stage include: Elimination of f-waves in AF patients if necessary and then in all the patients: Pre-processing, T-wave detection, w_1 and w_2 calculation and $\mathcal{V}$-index calculation. The processes w_1 and w_2 calculation and $\mathcal{V}$-index calculation are analogous to the processes described in the AF Simulation stage.

In order to determine the necessity of eliminating the f-waves of the AF patients before computing the $\mathcal{V}$-index, the study of Swiss AF database was divided into 2 sub-stages:

- Comparison between AF patients with and without f-waves
- Comparison between AF and SR patients.

The AF patients of the second comparison will or will not have f-waves depending on the results obtained in the first comparison.

AF Patient Id 01_2062 (Permanent) will be used as example for all the figures.

The overall processes followed during the study of the Swiss-AF database are shown in Fig. 5-8.

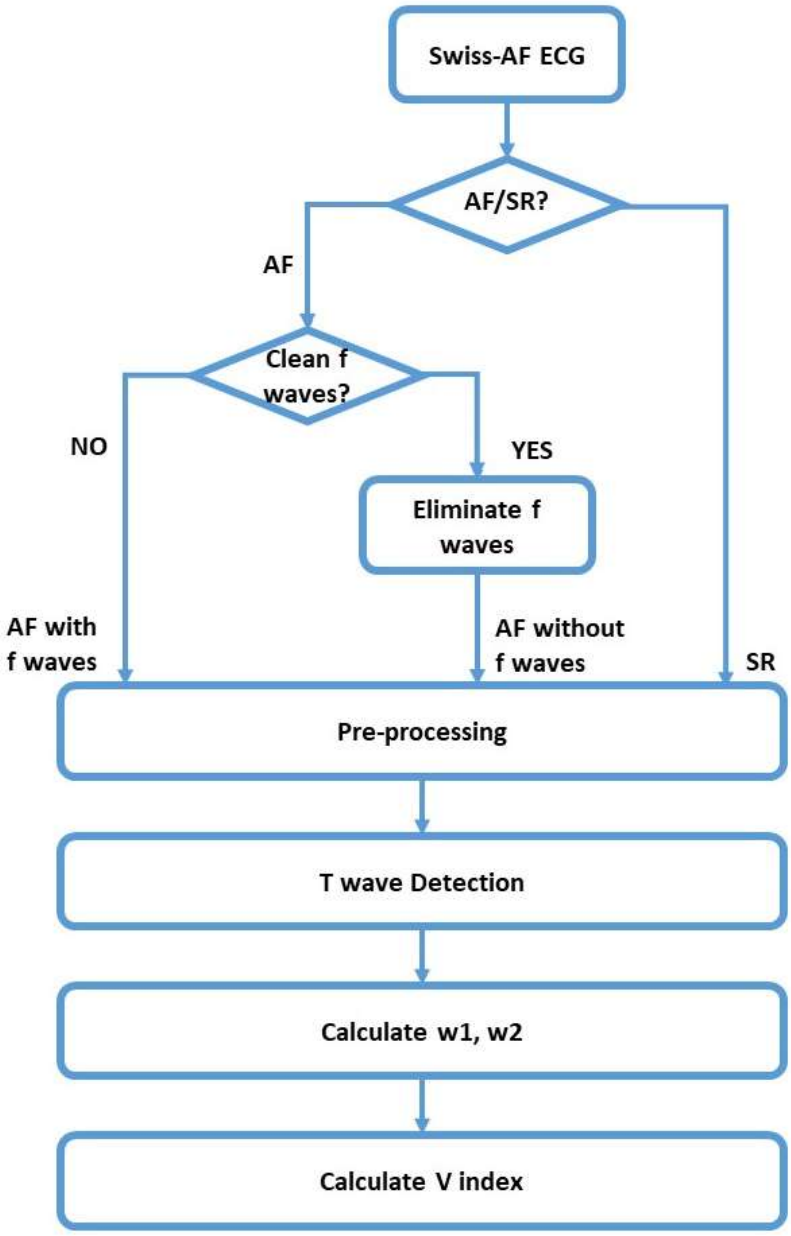

Fig. 5-8 Block Diagram of Processes in Swiss-AF Study.

5.2.1 Elimination of f-waves

The first process that is going to be described is the Elimination of f-waves. A new technique for vectorcardiographic loop alignment was recently introduced in the paper "Spatiotemporal QRST cancellation techniques for analysis of atrial fibrillation" [38] for the purpose of separating morphologic beat-to-beat variability from respiratory-induced variations. The method consisted on the pre-processing of the signal, T-wave detection, Atrial Fibrillation Reduction, Beat Averaging, Estimation of QRST Cancellation Parameters, QRST Cancellation and f-waves elimination.

5.2.1.1 Pre-Processing

First, the ECG signal was filtered with a pass-band third order Butterworth filter which had 0.5 Hz and 40 Hz as the pass-band cut-off frequency. These frequencies were chosen to filter the signal offset and the influence the 50 Hz electric grid had on the signal. The next step was to compute the Pan Tompkins algorithm using lead 12 (Lead III) as the reference lead. QRS amplitude and location of QRS peak where the output variables. This enabled the computation of the number of beats (nBeats) which were used throughout the cancellation method.

5.2.1.2 Atrial Fibrillation Reduction

The goal of this stage was to compute an estimated atrial fibrillation (yest) which was used to reduce the atrial fibrillation component of the signal and obtain Zglob = y-yest. The method to compute the estimated atrial fibrillation is described in [38]. An approach is used in which the fibrillation cycle prior and after the QRST complex is replicated and summed during the QRST interval but linearly weighted such that the weights decrease from one at the onset of the interval to zero at the end. The estimated fibrillation was set to zero whenever both the adjacent RR intervals were too short.

The QRST complex was determined by first creating a window from the beginning of the QRS Interval to the end of the T-wave. The beginning of the QRST interval was determined by simply subtracting 50 samples from the position of the QRS peak. However, the end of the QRST interval was computed by determining the end of the T-wave, calculated with the T-wave delineator, and adding 150 samples of margin. Fig. 5-9 shows an example of one of the beats where the beginning of the QRST, peak of QRS and end of QRST can be seen.

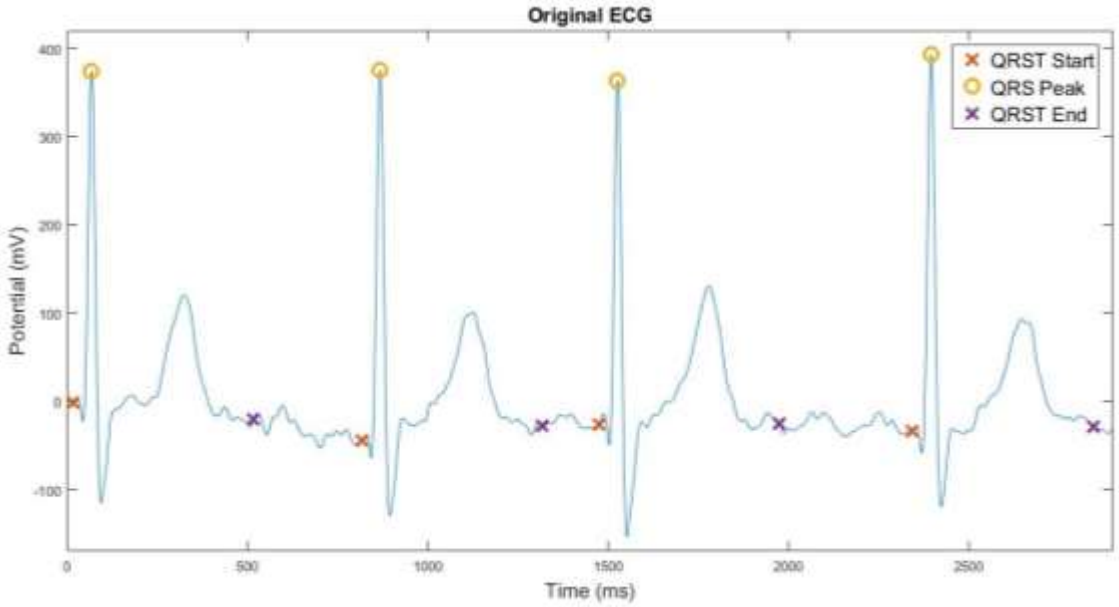

Fig. 5-9 Original ECG signal with QRST start (red), QRS Peak (yellow) and QRST end (purple) marked.

Fig. 5-10 shows the original ECG signal and Zglob obtained.

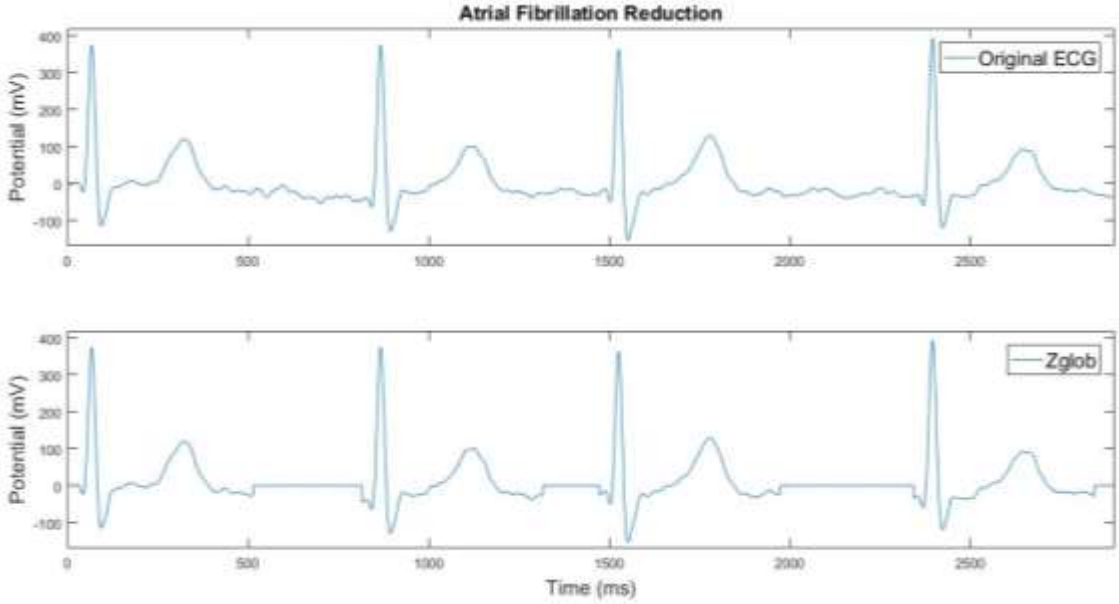

Fig. 5-10 Original Signal and Zglob obtained from Atrial Fibrillation Reduction.

5.2.1.3 T-wave delineator

The T-wave delineator is a process used to determine the beginning and ending of the T-waves and will be used in the following stages.

This process has as input all the T-waves of each lead so it has the disadvantage that a rough estimation of the T-wave window has to be made. In this case, it was made by

choosing the beginning of the T-wave 150 samples after the QRS peak and the end of the T-wave 450 samples after as shown in Fig. 5-11.

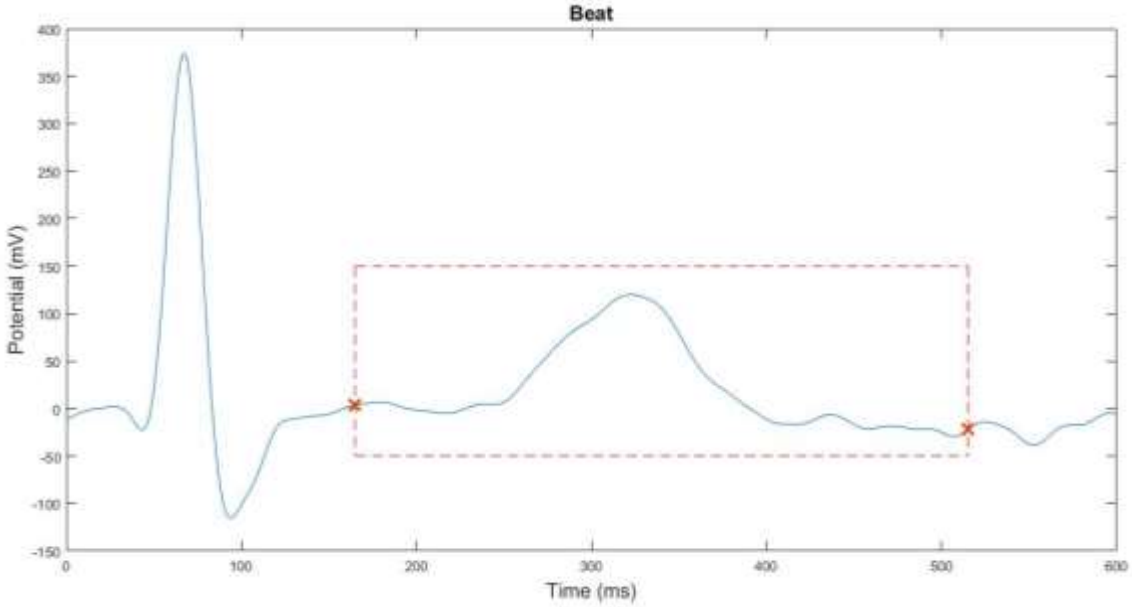

Fig. 5-11 Sample Beat with Rough T-wave Window used to compute T-wave delineator.

For each T-wave, the maximum derivative is computed. From that point, the Reference Line, a straight line that passes through the maximum derivative point and has a gradient equal to a fourth of the maximum derivative, is defined. The end of the T-wave is then determined by the point of the T-wave which has the maximum distance from the Reference Line.

Fig. 5-12 shows a summary of the process:

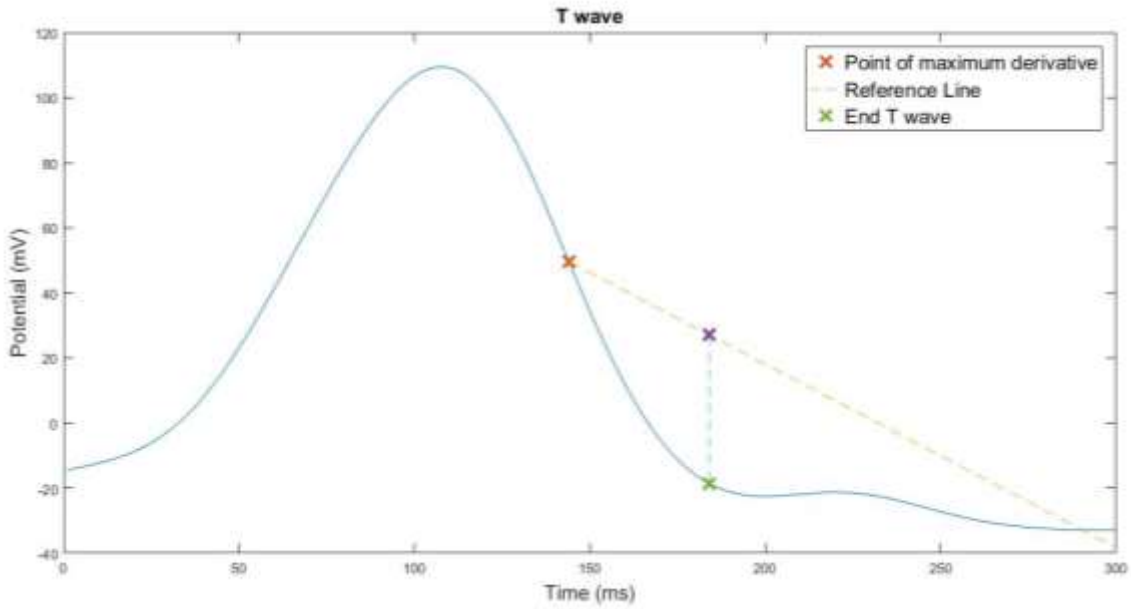

Fig. 5-12 Summary of T-wave delineator (Toff) on sample T-wave.

Once all the T-wave endings were found, the maximum was chosen and a 150 sample margin was added in order to ensure the whole of the T-wave was considered.

5.2.1.4 Beat Averaging

From the previous stage we obtained the intermediate signal (Zglob) for each lead but for this stage we need a signal Z for each cycle and lead to obtain the average beat $X_{(\mathrm{N}+2\Delta)\times \mathrm{L}}$ where N is the samples of each beat. The maximum time synchronization error (Δ) was defined by default as 5 ms (5 samples) and L is the number of leads.

5.2.1.5 Estimation QRST Cancellation Parameters

In this stage the QRST cancellation parameters Q (rotation matrix), D (scaling matrix) and τ (taw) are estimated by solving the following minimization problem:

$$\epsilon^2_{min} = \min_{\mathrm{D,Q,\tau}} \|Z - J_\tau XDQ\|^2_F \qquad (5\text{-}37)$$

An alternative iterative approach is described in [38] where the error is:

$$\epsilon^2 = tr(ZZ^T) + tr(J_\tau XDD^T X^T J_\tau^T) - 2tr(D^T X^T J_\tau^T ZQ^T) \qquad (5\text{-}38)$$

and can be minimized with respect to Q by maximizing the last term under the assumption that D is known. The maximization is performed by using singular value decomposition

(SVD) of the matrix $T = D^T X^T J_\tau^T Z$ where D X and Z have already been defined and J_τ is the time shift matrix, defined as:

$$J_\tau = [0_{N\times(\Delta+\tau)} \quad I_{N\times N} \quad 0_{N\times(\Delta-\tau)}] \tag{5-39}$$

which corrects the misalignment in time between the observed and the averaged beat.

The SVD of matrix T leads to:

$$T = U\Sigma V^T \text{ and } \hat{Q} = UV^T \tag{5-40}$$

A new parameter $Z' = ZQ^{-1}$ is introduced and for a given Q, the diagonals entries in D can be estimated by:

$$\hat{d}_l = ([J_\tau X]_l^T [J_\tau X]_l)^{-1}([J_\tau X]_l^T [Z']_l), \; l = 1, \ldots, L \quad , \tag{5-41}$$

Finally, for each τ, in the Interval [-Δ, Δ], Q and D were iteratively estimated to minimize the overall error. Typically, a solution close to $Q = D = I$ (I being the identity matrix) is desirable and, therefore, the algorithm is initialized with $D_0 = I$. The rotation at step k, Q_k , is then calculated from D_{k-1} .

The iteration stops when it reaches the maximum number of iterations (maxQDiter) which in this case was set to 10 as suggested by [38]. Then, the τ that minimizes the vector of errors was chosen as the optimum τ (tawop).

5.2.1.6 QRST Cancellation and f-wave elimination

With the optimum τ, the ventricular activity Yv was modelled and subtracted from the original signal to compute the atrial activity, yAF.

Finally, the atrial activity is subtracted from the original ECG signal. Fig. 5-13 shows the Original ECG signal and que signal without f-waves.

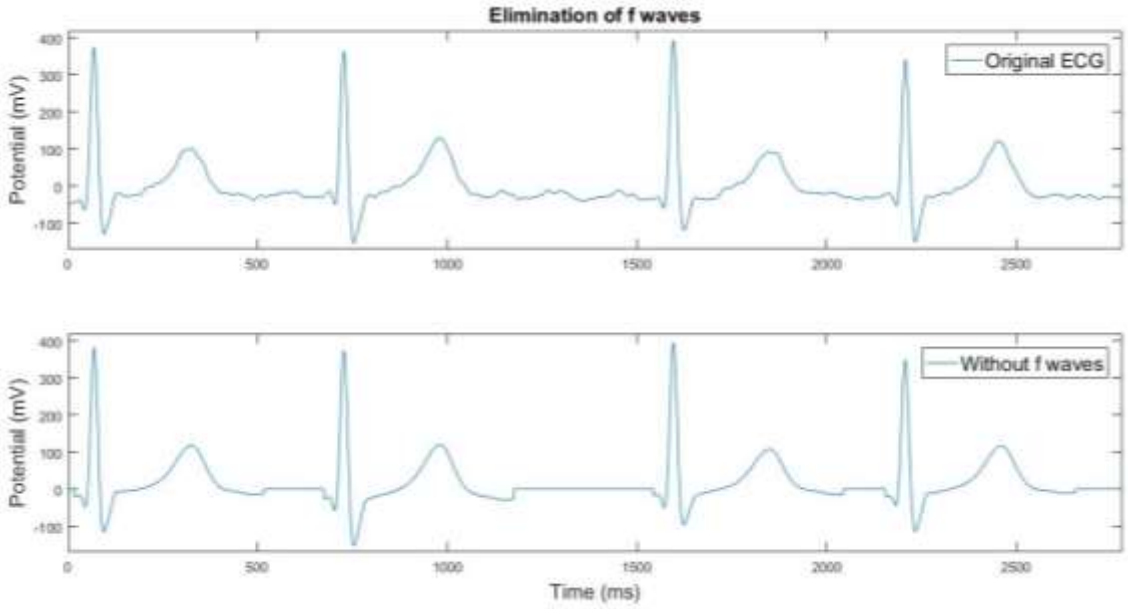

Fig. 5-13 Original ECG and ECG output without f-waves.

As it can be seen, the T-waves are now free from f-waves and the baseline which also presented f-waves, after the elimination, is zero.

5.2.2 Pre-processing

Independently if the f-waves were or not cleaned, all the patients went through the pre-processing stage which consisted in filtering, Baseline Alignment and QRS peak identification with Pan Tompkins Algorithm. The pre-processing stage is analogous to the pre-processing stage described in the Elimination of f-waves with the particularity that this stage also contains a Baseline Alignment process.

The Base Alignment process estimates the baseline offset using the linear regression computed on the TP track which is defined checking the most frequent value on the ECG.

5.2.3 T-wave detection

In order to study the $\mathcal{V}$-index, the T-waves have to be properly detected. This is done by roughly selecting a window, which contains the T-waves, then use the T-wave delineator previously described to compute the beginning and end of the T-wave and re-select the window.

The window is selected by first aligning the beats using the QRS peak calculated with Pan Tompkins Algorithm and selecting the upper and lower sides of the window by adding a certain number of samples to the position of the QRS peak. 150-samples was selected to place the lower side of the window and 500 samples to place the upper side.

The results of aligning the beats and using the rough windows to select the T-waves are shown in Fig. 5-14.

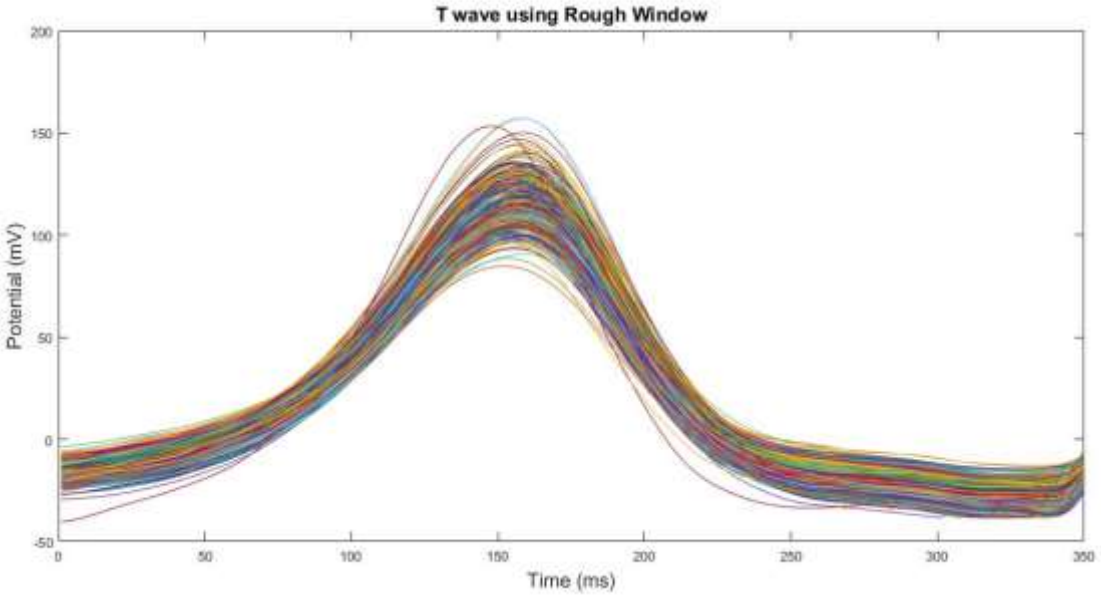

Fig. 5-14 Aligned T-waves using a Rough T-wave Window.

Inside this window, the T-wave delineator determined the beginning and ending of the T-wave by calculating the point with maximum derivative and determining the maximum distance between the T-waves and a Reference Line created from the point with gradient equal to one fourth of the maximum derivative. Fig. 5-15 shows the window derived from the T-wave delineator.

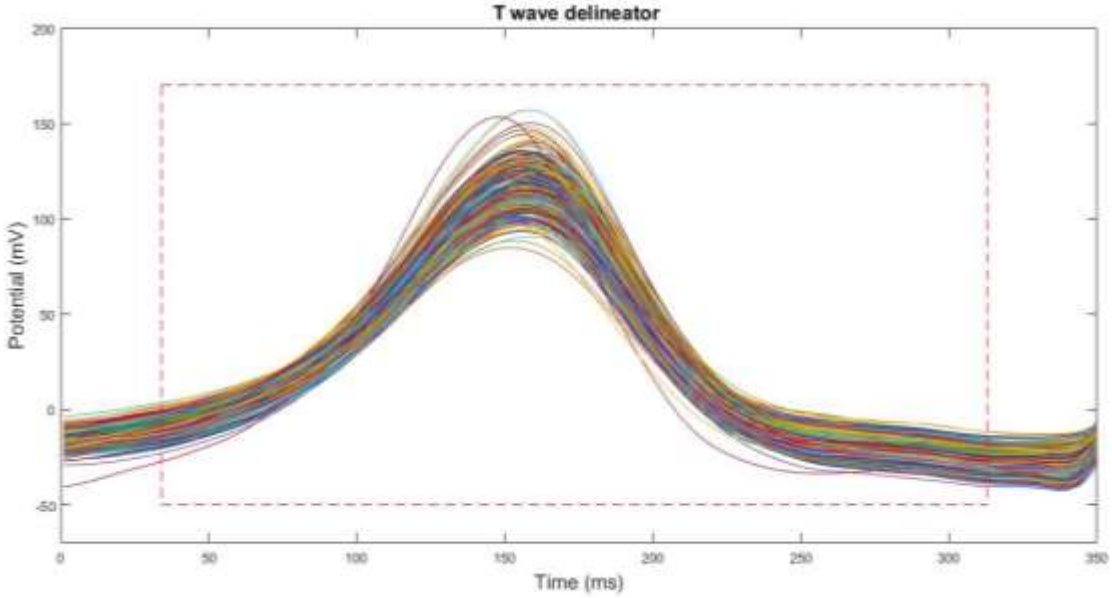

Fig. 5-15 Aligned T-wave with the new Ton and Toff from the T-wave delineator.

With the new window, the Beat alignment was carried out again and the T-waves obtained were averaged by lead to create a template. Finally, the leads which presented clear enough T-waves were selected if the mean of the cross-correlation between the T-waves of each beat and the T-wave template of the beat was higher than 0.8. The calculation of w_1, w_2 and subsequently of the V index were done only if more than 3 leads complied with the cross-correlation requirements.

The final 2 stages: w_1 and w_2 calcualtion and $\mathcal{V}$-index calculation are anomalous to the stages already defined in section 5.1.2 and 5.1.3.

Chapter 6. RESULTS

This section will describe the results obtained in the stages of this thesis: Simulation and Swiss-AF study.

6.1 AF Simulation

As mentioned, the AF simulation study was done in order to determine if it was necessary to eliminate the f-waves from the AF patients before calculating the $\mathcal{V}$-index. To do so, 7 sets of T-waves were analysed and the theoretical $\mathcal{V}$-index values were compared against the $\mathcal{V}$-index of the T-waves with and without simulated f-waves.

The f-waves were simulated for different frequencies as specified in the Methods and the results can be seen in the following figures:

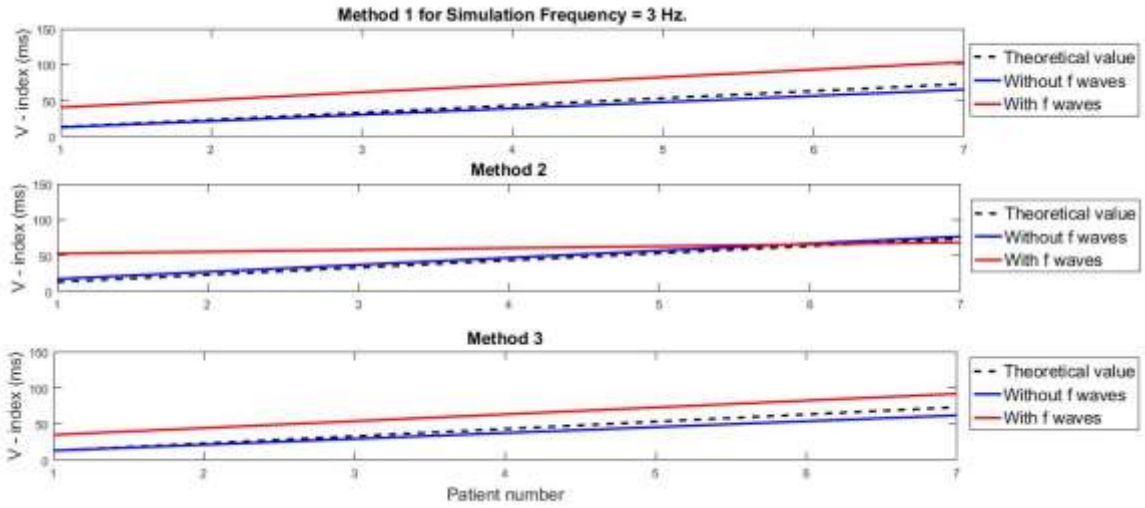

Fig. 6-1 AF Simulation Comparisons for simulation frequency = 3Hz.

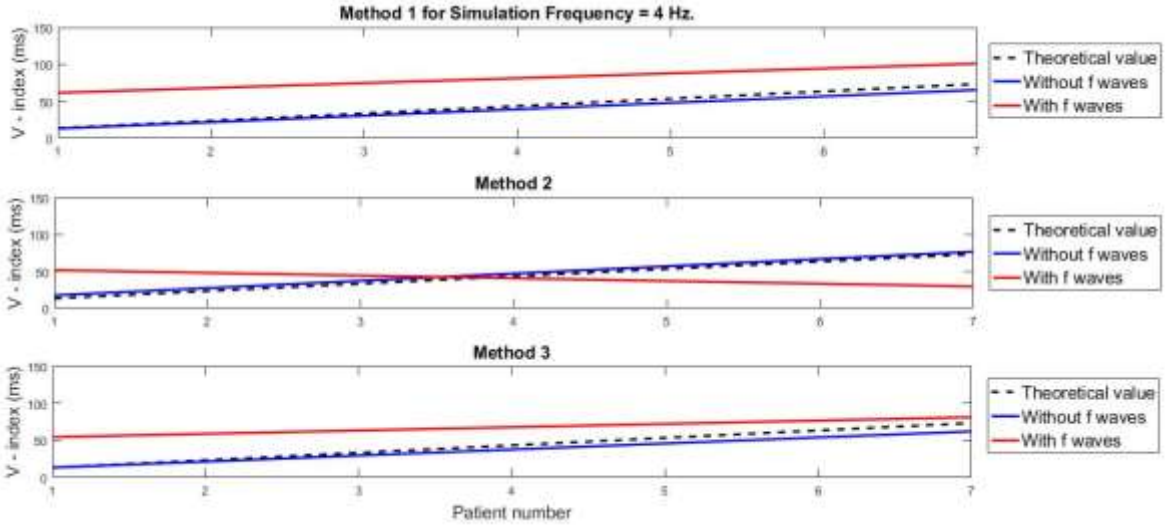

Fig. 6-2 AF Simulation Comparisons for simulation frequency = 4Hz.

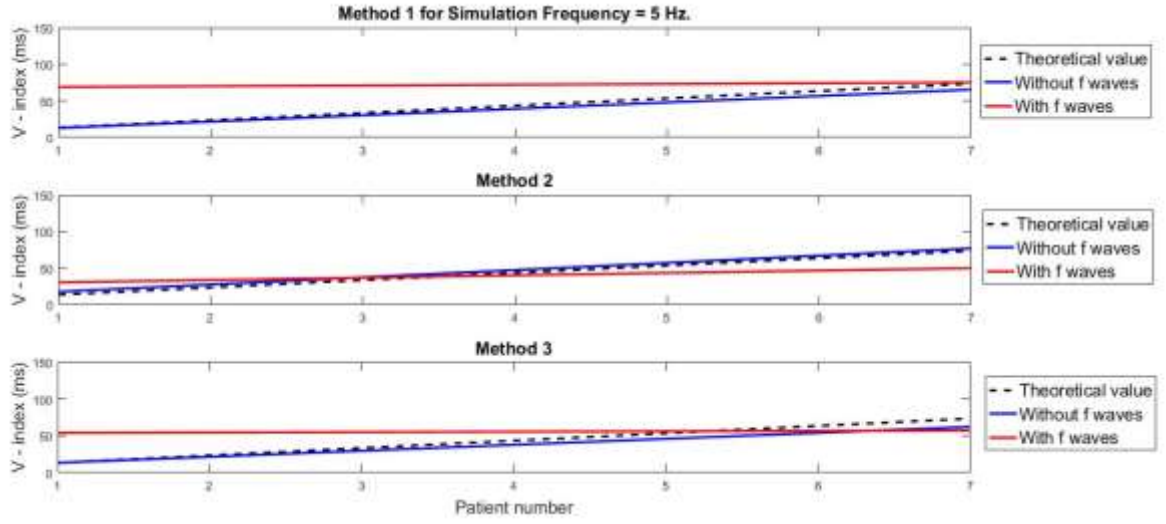

Fig. 6-3 AF Simulation Comparisons for simulation frequency = 5Hz.

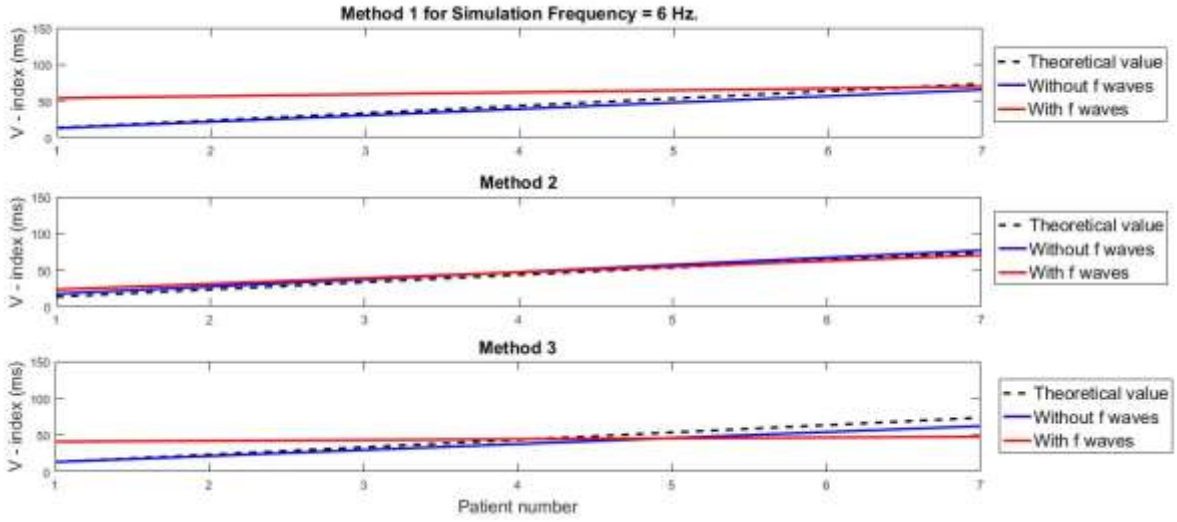

Fig. 6-4 AF Simulation Comparisons for simulation frequency = 6Hz.

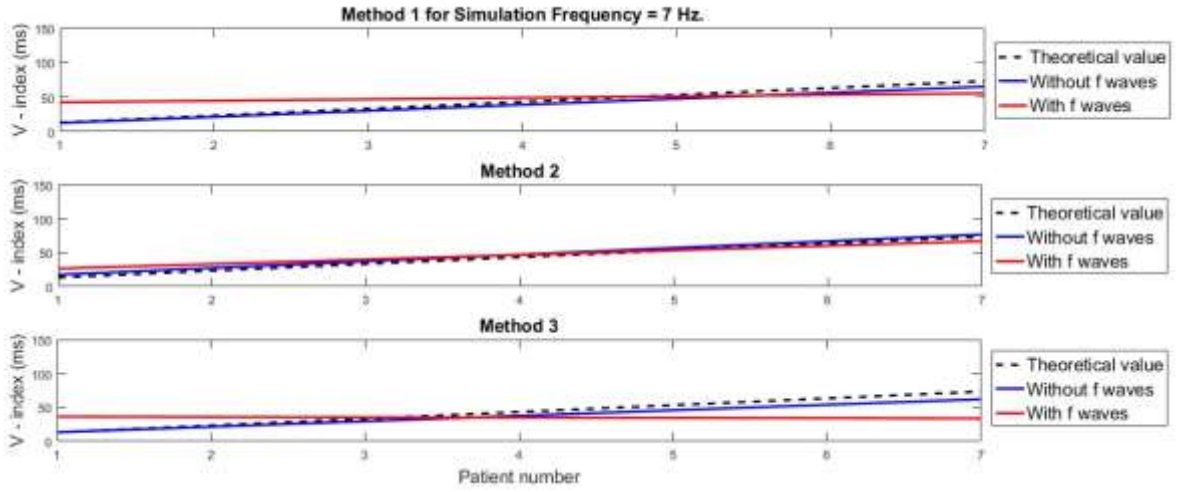

Fig. 6-5 AF Simulation Comparisons for simulation frequency = 7Hz.

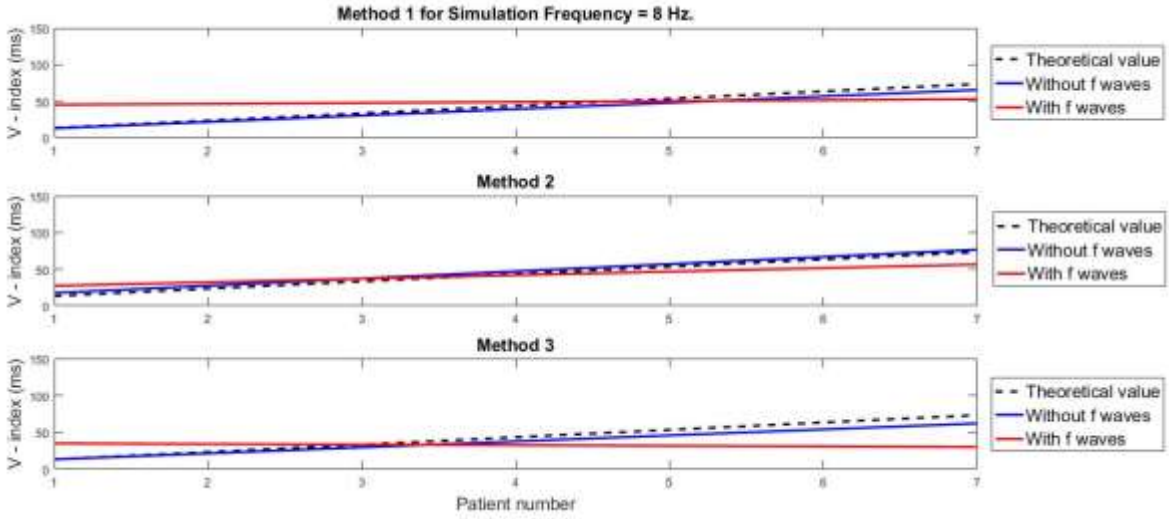

Fig. 6-6 AF Simulation Comparisons for simulation frequency = 8Hz.

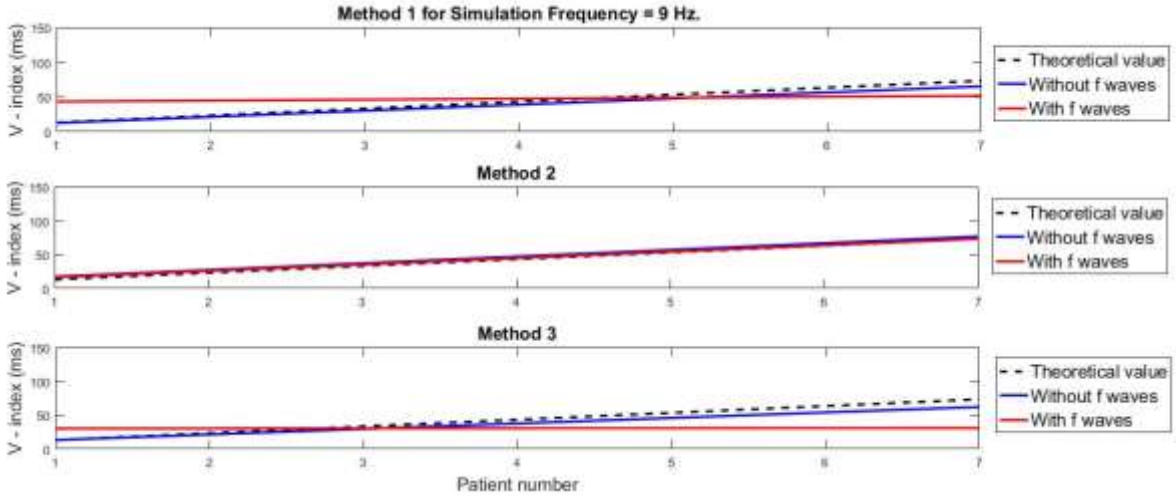

Fig. 6-7 AF Simulation Comparisons for simulation frequency = 9Hz.

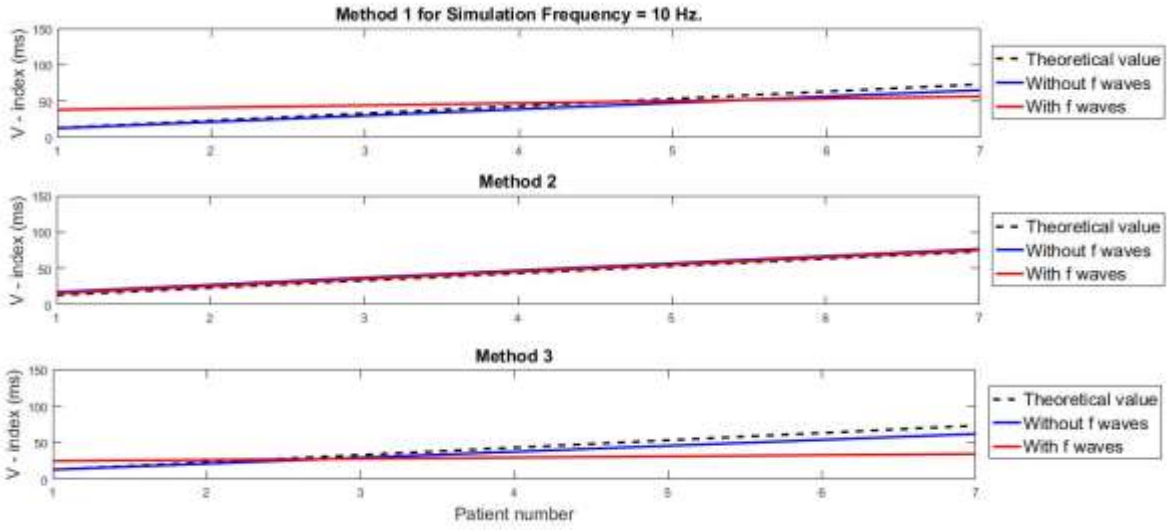

Fig. 6-8 AF Simulation Comparisons for simulation frequency = 10Hz.

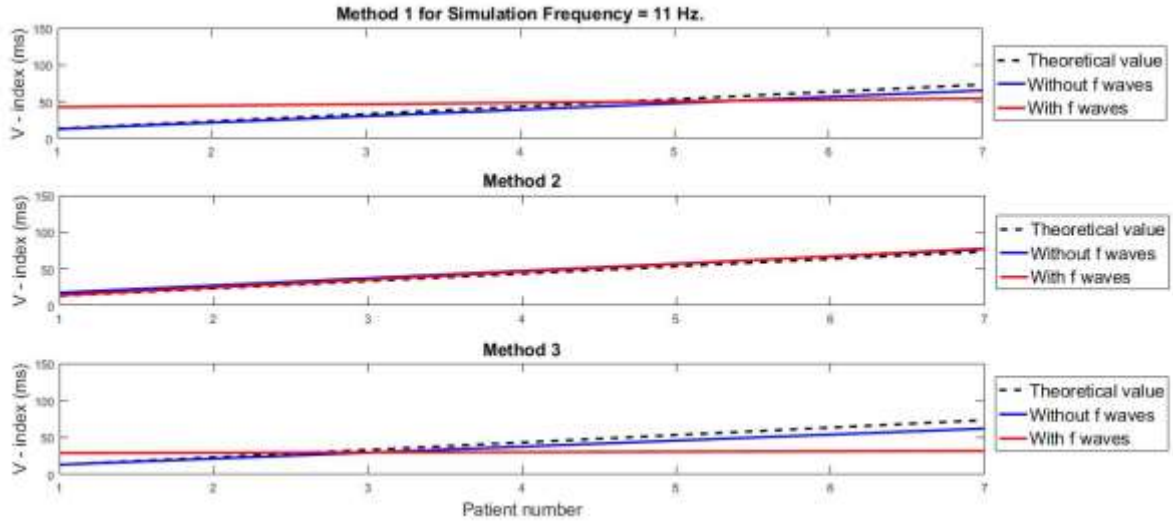

Fig. 6-9 AF Simulation Comparisons for simulation frequency = 11Hz.

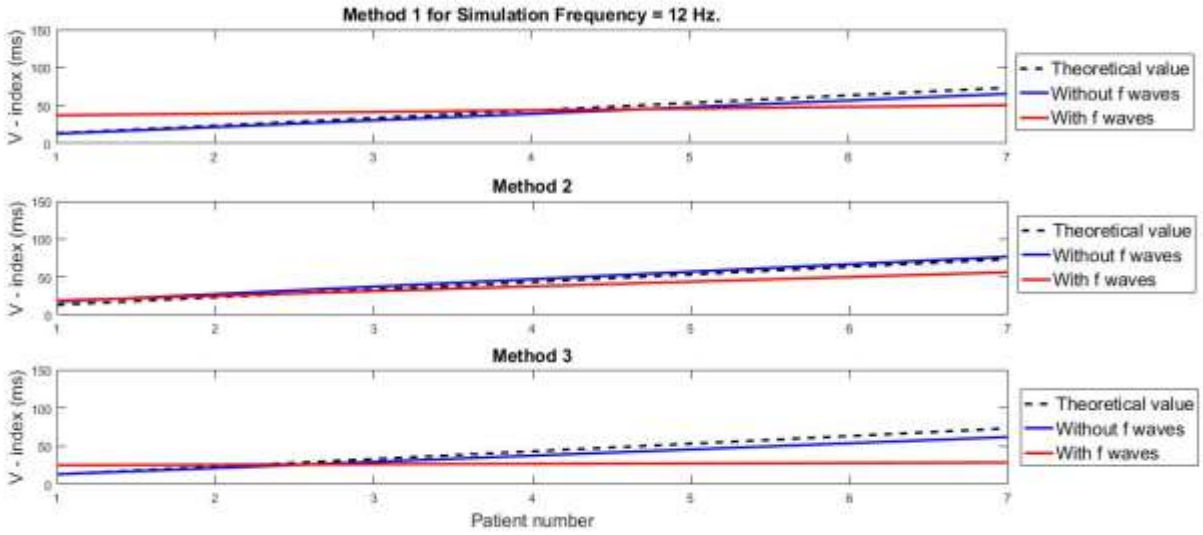

Fig. 6-10 AF Simulation Comparisons for simulation frequency = 12Hz.

For each simulation frequency [3-12Hz] the figures show the Theoretical $\mathcal{V}$-index for the 7 patients with increasing s_ϑ as a dashed black line. The comparison is then made between the Theoretical values and the $\mathcal{V}$-index obtained from the T-waves with (red) and without (blue) f-waves. It can be already observed that the results obtained from the T-waves without f-waves has less deviation compared to the theoretical values.

Table 6-1 shows for each of the simulation frequencies and each of the 3 methods used to compute the $\mathcal{V}$-index, the Mean Absolute Percentage Error (MAPE) between the theoretical values of $\mathcal{V}$-index against those with and without f-waves.

Table 6-1 Mean Absolute Percentage Error between theoretical V-index values and V-index values for T-waves with and without f-waves.

Simulation Frequency (Hz)	Method	Theoretical vs Signal without f-waves MAPE (%)	Theoretical vs Signal with f-waves MAPE (%)
3	1	9.03	92.80
	2	11.73	85.14
	3	11.60	67.40
4	1	9.03	123.15
	2	11.73	87.38
	3	11.60	90.78

5	1	9.03	116.72
	2	11.73	50.15
	3	11.60	81.18
6	1	9.03	89.64
	2	11.73	33.04
	3	11.60	65.91
7	1	9.03	60.24
	2	11.73	42.07
	3	11.60	65.70
8	1	9.03	69.05
	2	11.73	36.18
	3	11.60	62.10
9	1	9.03	65.26
	2	11.73	30.77
	3	11.60	53.78
10	1	9.03	52.36
	2	11.73	30.96
	3	11.60	43.18
11	1	9.03	59.32
	2	11.73	36.92
	3	11.60	46.60
12	1	9.03	49.74
	2	11.73	31.93
	3	11.60	51.15

The MAPE was calculated using the following formulas:

$$delta\_signal = |test\_signal - reference\_signal| \quad (6\text{-}1)$$

$$percentage\_difference = \frac{delta\_signal}{reference\_signal} \quad (6\text{-}2)$$

$$mean\_percentage\_difference = \frac{1}{M}\sum percentage\_difference * 100 \quad (6\text{-}3)$$

The reference signal was considered to be the theoretical $\mathcal{V}$-index values, the test signal was the $\mathcal{V}$-index for the T-waves with and without f-waves and M was the number of $\mathcal{V}$-index considered, in this case 7.

As could be deduced, the MAPE for theoretical $\mathcal{V}$-Index values against $\mathcal{V}$-index values for T-waves without f-waves remain independent with changes in the simulation frequency as the simulation frequency affects the simulated f-waves which are not present. The maximum error between the theoretical $\mathcal{V}$-index and $\mathcal{V}$-index computed from the T-waves without f-waves is 11.73% for Method 2 and the lowest 9.03% for Method 3. However, the results for MAPE for theoretical $\mathcal{V}$-index values against $\mathcal{V}$-index values for T-waves with f-waves are very different. The maximum error is 123.15% for Method 1 and simulation frequency 4 Hz and the minimum error is 30.77% for Method 2 and simulation frequency 9Hz which are both much higher than the errors found in the previous case.

Following these results, the assumption that the f-waves affect the computation of the $\mathcal{V}$-index is proven and justifies the decision to make a previous Swiss-AF study in order to confirm the effect of f-waves in the computation of the $\mathcal{V}$-index in real ECG signals.

6.2 Swiss-AF Study

6.2.1 AF patients with and without f-waves

Based on the results of the previous stage, a study to confirm the affect the f-waves have in the computation of the $\mathcal{V}$-index was made. Out of the 879 AF patients, 736 provided usable $\mathcal{V}$-index values for both cases (with and without f-waves). Out of those, 125 presented paroxysmal AF, 205 persistent AF and 406 permanent AF episodes. The following figures show the results of the comparison: Fig. 6-11 shows the comparison between all the AF patients while Fig. 6-12, Fig. 6-13 and Fig. 6-14 show the comparison for Paroxysmal, Persistent and Permanent AF.

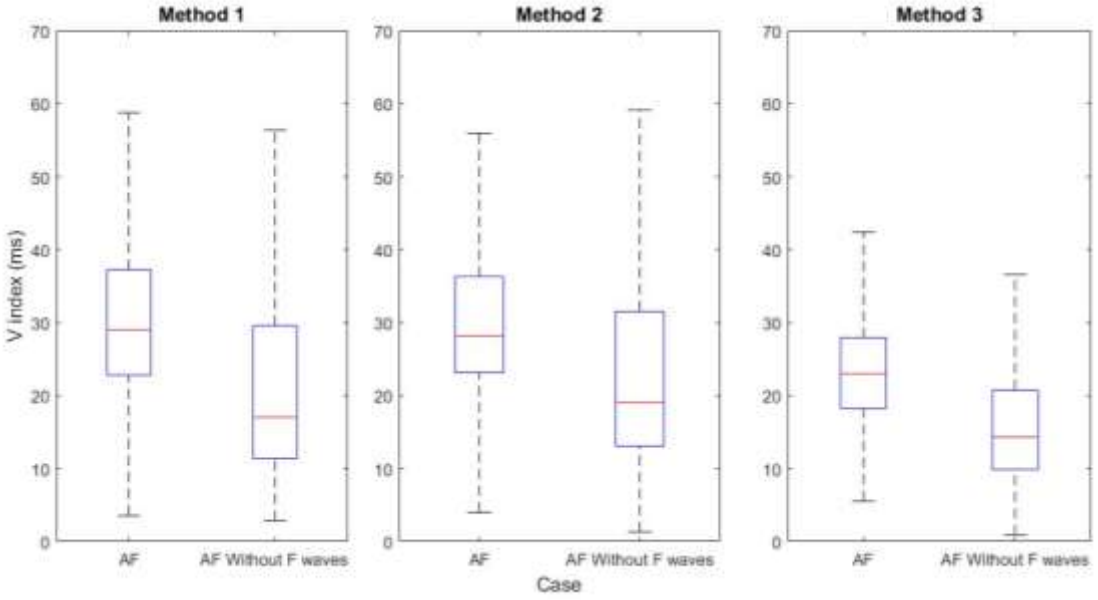

Fig. 6-11 Comparison between All AF patients with and without f-waves.

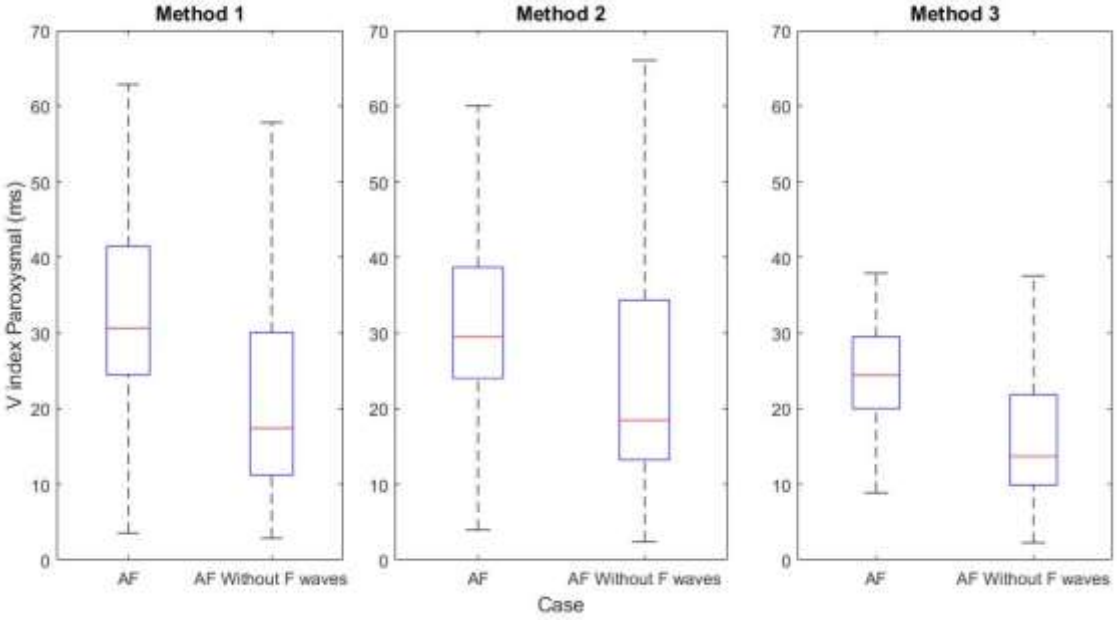

Fig. 6-12 Comparison between Paroxysmal AF patients with and without f-waves.

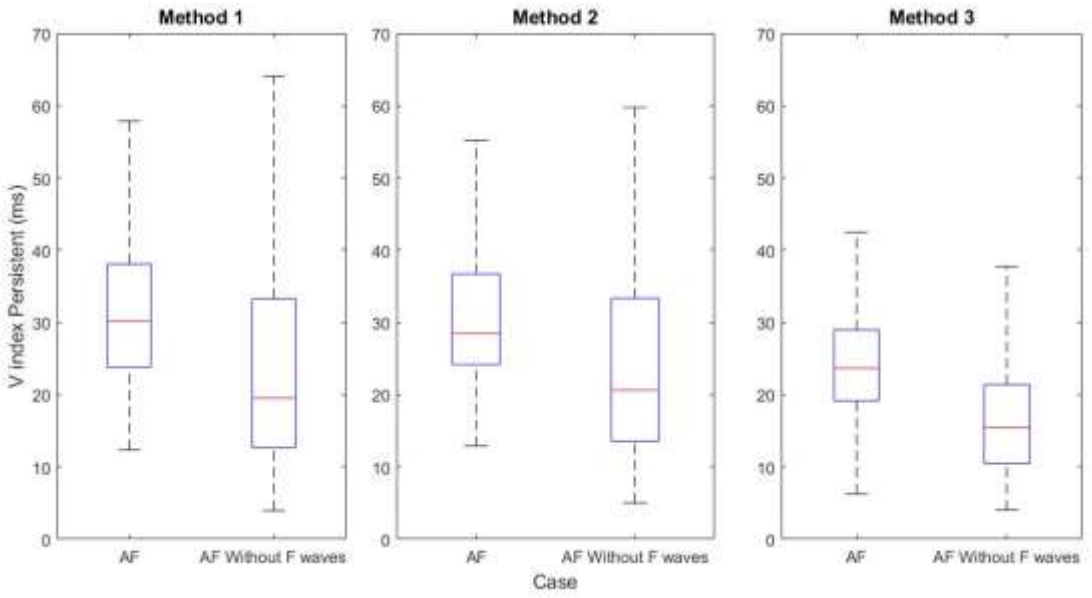

Fig. 6-13 Comparison between Persistent AF patients with and without f-waves.

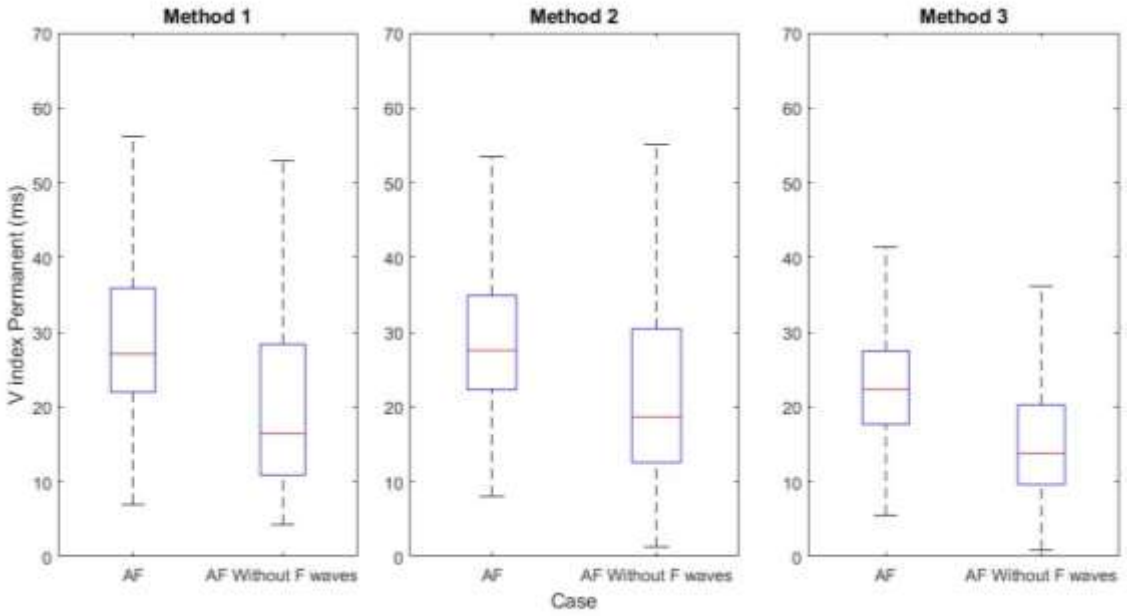

Fig. 6-14 Comparison between Permanent AF patients with and without f-waves.

It can be seen from the figures that there is a clear decrease in the median of the $\mathcal{V}$-index when the f-waves are removed. Table 6-2 collects the values for the median and standard deviation in milliseconds (*ms*) of the $\mathcal{V}$-index for the different AF episodes and methods obtained when comparing AF with and without f-waves.

Table 6-2 Median and Standard Deviation for the V-index values of the different comparisons and the Increase in Median between the values with and without f-waves.

AF Episode	Method	$\mathcal{V}$-index		Δ Median
		AF (ms)	AF without f-waves (ms)	(%)
All	1	28.99 ± 13.23	17.03 ± 18.32	41.25
	2	28.13 ± 12.54	13.05 ± 19.76	32.14
	3	23.01 ± 8.44	14.30 ± 9.89	37.84
Paroxysmal	1	30.66 ± 12.61	17.43 ± 19.12	43.16
	2	29.49 ± 12.98	18.47 ± 20.79	37.36
	3	24.38 ± 9.20	13.69 ± 10.76	43.86
Persistent	1	30.17 ± 14.81	19.50 ± 19.91	35.36
	2	28.49 ± 13.26	20.63 ± 23.43	27.57
	3	23.65 ± 8.60	15.44 ± 10.48	34.73
Permanent	1	27.10 ± 12.41	16.42 ± 17.14	39.41
	2	27.58 ± 11.92	18.68 ± 17.17	32.27
	3	22.37 ± 8.05	13.79 ± 9.27	38.33

Δ Median (%) was computed as:

$$\Delta \text{ Median } (\%) = \frac{Median\_AF \; - Median\_AF\_without\_f\_waves}{Median\_AF} * 100 \qquad (6\text{-}4)$$

Seeing that the Δ Median (%) of all the comparisons are positive, the median of the $\mathcal{V}$-index of AF patients without f-waves is lower than in patients with the f-waves. Furthermore, for these comparisons, the null hypothesis was rejected when the P value ≤ α, with α = 0.05. The null hypothesis were rejected in all the comparisons and were deemed statistically significant as the P values of all the comparisons were ≤ 0.05. Therefore, the premise that the f-waves influenced the computation of the $\mathcal{V}$-index has been proven and subsequently, the final results to be shown are a comparison between the Sinus Rhythm (SR) patients and the Atrial Fibrillation (AF) patients without f-waves.

6.2.2 SR patients and AF patients without f-waves

Finally, the results obtained in the comparisons for SR patients and AF patients without f-waves are going to be presented.

Out of the 879 AF patients and 1134 SR patients, 772 AF and 1092 SR patients gave usable $\mathcal{V}$-index results. The 772 AF patients include 135 with Paroxysmal, 217 with Persistent and 420 with Permanent fibrillatory episodes and the 1092 SR patients include 747 with Paroxysmal and 345 with Permanent episodes. These results are summarised in Table 6-3.

Table 6-3 Summary of Patients.

Patient Type	Original Number	Study Number	Paroxysmal	Persistent	Permanent
AF	879	772	135	217	420
SR	1134	1092	747	345	-
Total	2013	1864	882	562	420

A comparison between SR patients and AF patients without f-waves was made for Paroxysmal and Persistent episodes. Fig. 6-15 and Fig. 6-16 show the box plots obtained:

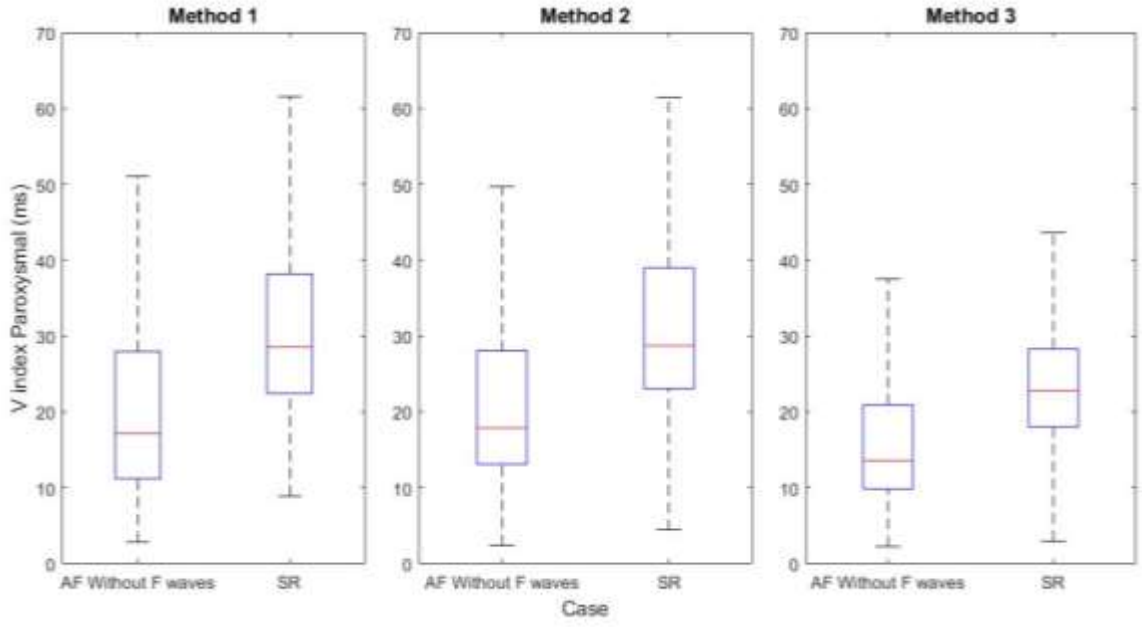

Fig. 6-15 Comparison between Paroxysmal patients in AF without f-waves and SR conditions.

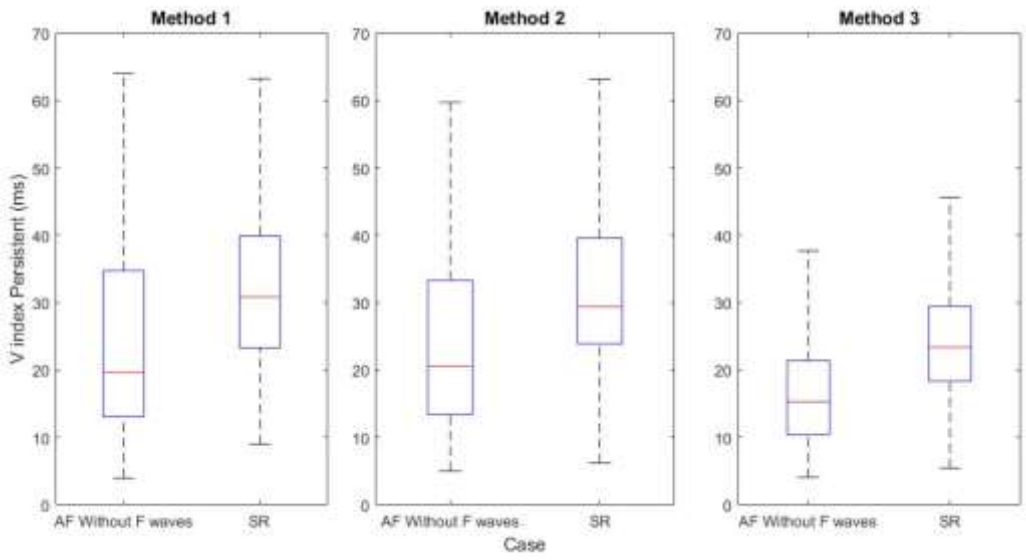

Fig. 6-16 Comparison between Persistent patients in AF without f-waves and SR conditions.

Table 6-4 summarises the results:

Table 6-4 Median and Standard Deviation for the V-index values of the different comparisons and the Increase in Median between the values of the patients in AF without f-waves and SR conditions.

Episode	Method	$\mathcal{V}$-index		Δ Median (%)
		AF without f-waves (ms)	SR (ms)	
Paroxysmal	1	17.16 ± 18.56	28.57 ± 16.34	66.52
	2	17.90 ± 20.34	28.75 ± 14.84	60.59
	3	13.60 ± 10.51	22.86 ± 9.38	68.06
Persistent	1	19.65 ± 20.31	30.86 ± 17.65	57.05
	2	20.57 ± 23.71	29.40 ± 14.39	42.90
	3	15.30 ± 11.16	23.36 ± 9.39	52.69

Δ Median (%) was computed as:

$$\Delta \text{ Median } (\%) = \frac{Median\_SR - Median\_AF\_without\_f\_waves}{Median\_AF\_without\_f\_waves} * 100 \qquad (6\text{-}5)$$

Both Fig. 6-15 and Fig. 6-16, and Table 6-4 show that there is an increase in the median of the $\mathcal{V}$-index for patients during SR than for patients during AF without f-waves. This may be due to the fact that during fibrillation the ventricular myocytes' repolarization

times decreases. The null hypothesis is rejected when the P value ≤ α, with α = 0.05 and in this case, the null hypotheses were rejected in all the comparisons and were deemed statistically significant as the P values of all the comparisons was ≤ 0.05.

Fig. 6-16 shows the comparison made for SR patients for Paroxysmal and Persistent episodes and Table 6-5 summarises the statistical parameters.

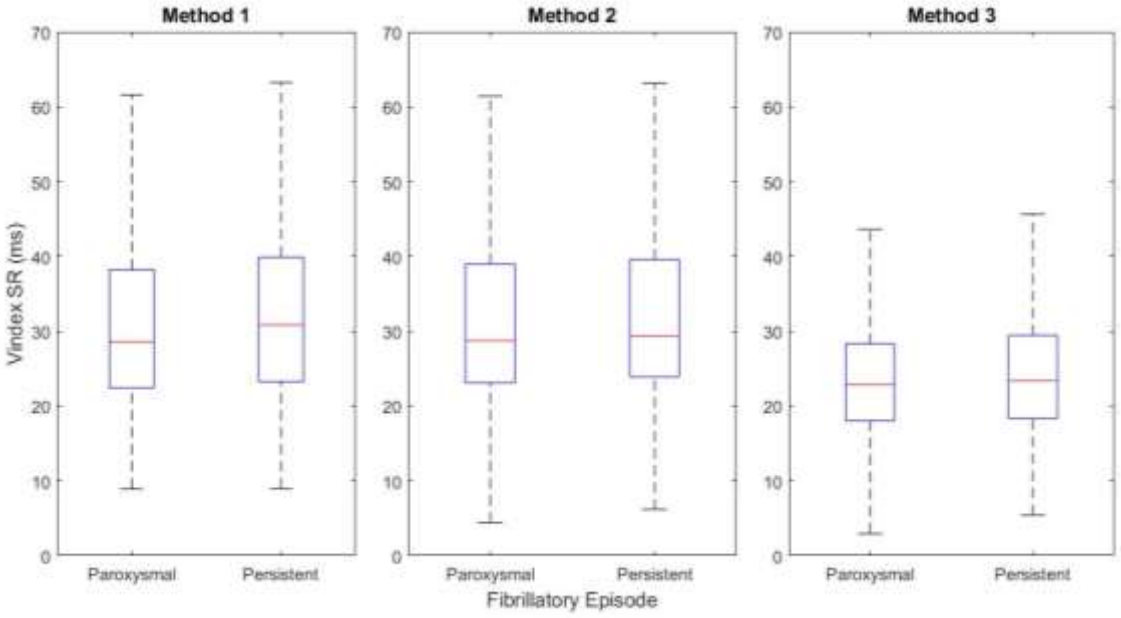

Fig. 6-17 Comparison between Paroxysmal and Persistent patients in SR conditions.

The statistical values of the $\mathcal{V}$-index are presented in Table 6-5 as median ± standard deviation in milliseconds (*ms*).

Table 6-5 Median and Standard Deviation for the V-index values of the different comparisons, the Increase in Median between the values of the Paroxysmal and Persistent patients in SR and the P value of those comparisons.

Method	$\mathcal{V}$-index		Δ Median (%)	P value ≤ 0.05
	Paroxysmal (ms)	Persistent (ms)		
1	28.57 ± 16.34	30.86 ± 17.65	8.03	0.0355
2	28.75 ± 14.84	29.40 ± 14.39	2.27	0.2482
3	22.86 ± 9.38	23.36 ± 9.39	2.20	0.279

Δ Median (%) was computed as:

$$\Delta \text{ Median } (\%) = \frac{Median\_Persistent - Median\_Paroxysmal}{Median\_Paroxysmal} * 100 \qquad (6\text{-}6)$$

As it can be seen from the boxplots and Table 6-5, even though the median of the $\mathcal{V}$-index is higher in patients with Persistent AF than in patients with Paroxysmal AF, the difference is very low (maximum 8%). In addition, for Method 2 and 3 the P values are not ≤ 0.05 so the null hypothesis cannot be rejected which means that the results are not statistically significant.

Fig. 6-18 shows the comparison made for AF patients without f-waves of the $\mathcal{V}$-index results for Paroxysmal, Persistent and Permanent AF.

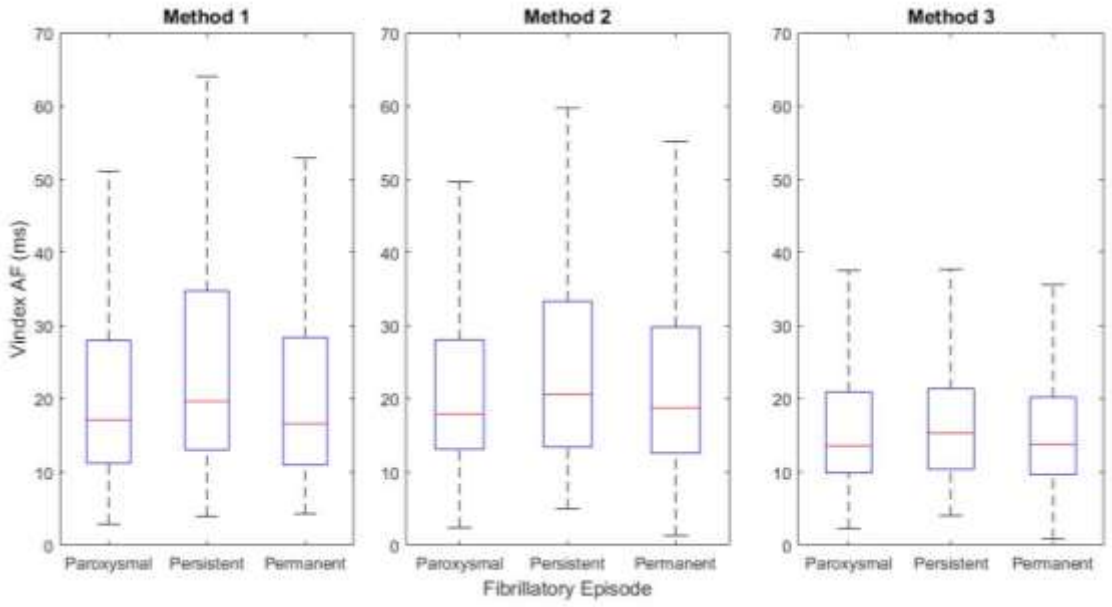

Fig. 6-18 Comparison between Paroxysmal, Persistent and Permanent patients in AF conditions.

The statistical values of the $\mathcal{V}$-index are presented in Table 6-6 as median ± standard deviation in milliseconds (*ms*).

Table 6-6 Median and Standard Deviation for the V-index values of the Paroxysmal, Persistent and Permanent patients in AF conditions.

Method	$\mathcal{V}$-index		
	Paroxysmal (ms)	Persistent (ms)	Permanent (ms)
1	17.16 ± 18.56	19.65 ± 20.31	16.62 ± 17.03
2	17.90 ± 20.34	20.57 ± 23.71	18.76 ± 16.99
3	13.60 ± 10.51	15.30 ± 11.16	13.77 ± 9.31

In this case after the general Anova P value ≤ 0.05, being a case of multiple comparison, the corrected significance levels, αc, were defined as αc = [α/N α/N-1 α/N-2] for P values = [p1 p2 p3] being the P values sorted lowest to highest and with N = the total number of comparisons. Therefore [p1 p2 p3] ≤ [0.01667 0.025 0.05] for the null hypothesis to be rejected.

As one of the objectives was to be able to discriminate between Persistent and Permanent AF episodes, Fig. 6-19 shows a zoomed in version of Fig. 6-18.

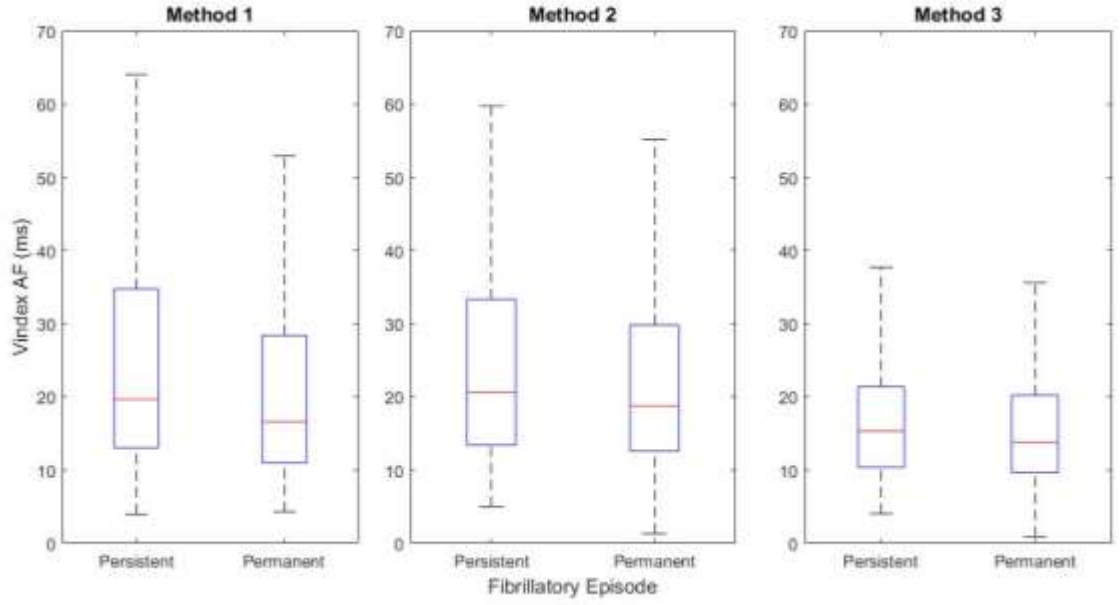

Fig. 6-19 Comparison between Persistent and Permanent patients in AF conditions.

A study was made on the statistical values of the $\mathcal{V}$-index and its results are shown in Table 6-7.

Table 6-7 Median and Standard Deviation for the V-index values of the different comparisons, the Increase in Median between the values of the Persistent and Permanent patients in AF and the P value of those comparisons.

Method	$\mathcal{V}$-index		Δ Median (%)	P value ≤ 0.05
	Persistent (ms)	Permanent (ms)		
1	19.65 ± 20.31	16.62 ± 17.03	18.23	0.01
2	20.57 ± 23.71	18.76 ± 16.99	9.69	0.02
3	15.30 ± 11.16	13.77 ± 9.31	11.08	0.03

Δ Median (%) was computed as:

$$\Delta \text{ Median } (\%) = \frac{Median\_Persistent - Median\_Permanent}{Median\_Permanent} * 100 \qquad (6\text{-}7)$$

Seeing that the Δ Median (%) of the comparisons are positive, the median of the $\mathcal{V}$-index for patients with Persistent episodes is higher than for patients with Permanent episodes. Furthermore, for these comparisons, the null hypothesis was rejected when the P value ≤ α, with α = 0.05. The null hypotheses were rejected in all the comparisons and were deemed statistically significant as the P values of all the comparisons was ≤ 0.05.

From these values, one could argue that it is possible to discriminate between Persistent and Permanent episodes in patients with AF.

Chapter 7. DISCUSSION

Non-invasive assessment of ventricular repolarization heterogeneities during atrial fibrillation is not a straightforward task, consequence of the irregular ventricular activity present under this particular condition. There have been many ECG-derived markers proposed for the assessment of the heterogeneities of ventricular repolarization such as the QT interval, QT dispersion or T-wave alternans to mention a few. However, these markers require the patient to be in SR to be properly assessed [39] which makes them less appropriate for studying AF as the properties of the AV node and atrial electrophysiology influence the highly irregular ventricular response.

In respect to QT measurements for instance, $\mathcal{V}$-index has the advantages of being:

i. a direct estimator of SHRV, and
ii. robust against noise and artefacts as it is only marginally affected by misdetection of T-waves fiduciary points (as for instance the T-peak or T-end).

However, it must be considered that the computational cost of the $\mathcal{V}$-index is fairly higher than for algorithms available for the QT interval computation [33]. This was proven by evaluating the $\mathcal{V}\text{-}index$ after different concentrations of moxifloxacin, which alters subtly the QT interval length, and after sotalol, which alters evidently the QT interval length, were administered.

To assess the standard deviation of the repolarization times s_ϑ many studies of the T-waves have been made. Huysduynen et al. [40] uses T-wave symmetry, T-wave amplitude and T-wave area as indexes which scaled linearly with s_ϑ. However, the $\mathcal{V}$-index represents a direct measurement of s_ϑ, while the Huysdynen's indexes only provided an indirect assessment [30].

Sassi et al. demonstrated theoretically and using numerical values (Finite Elements 2D simulations) that a tight relationship between $\mathcal{V}$-index and the dispersion of repolarization existed [41]. This study showed that:

i. numerical estimates of $\tilde{\mathcal{V}}_i$, from synthetic ECG, independently from the numerical scheme employed to simulate them, were substantially coherent with theoretical values $\mathcal{V}_i$.
ii. when analysing real ECG recordings, only stationary beats should be considered.

Furthermore, promising results for the $\mathcal{V}\text{-}index$ being an ECG-derived marker of SHVR have been shown [33, 42, 43].

In particular, [43] compares estimates from the $\mathcal{V}\text{-}index$ with direct measures of SHVR derived from unipolar electrograms recorded simultaneously in the left and right ventricular endocardium and in the left ventricular epicardium. The study was limited by the relatively small number of patients sampled (14) but it showed that the $\mathcal{V}\text{-}index$ had higher significant correlation with with direct measures of SHVR (r = 0.80), whereas other estimates based on T-peak and T-peak to T-end measures showed lower correlations ($r \leq 0.41$ and $r \leq 0.36$). This adds further evidence regarding the reliability of the $\mathcal{V}\text{-}index$ as a non-invasive estimator of SHVR.

One of the main problems encountered when studying ventricular repolarization heterogeneities is deciding the beginning Ton and the ending Toff of the T-wave. Different cardiologists could assign different position for Toff as shown in Fig. 7-1 obtained from [44].

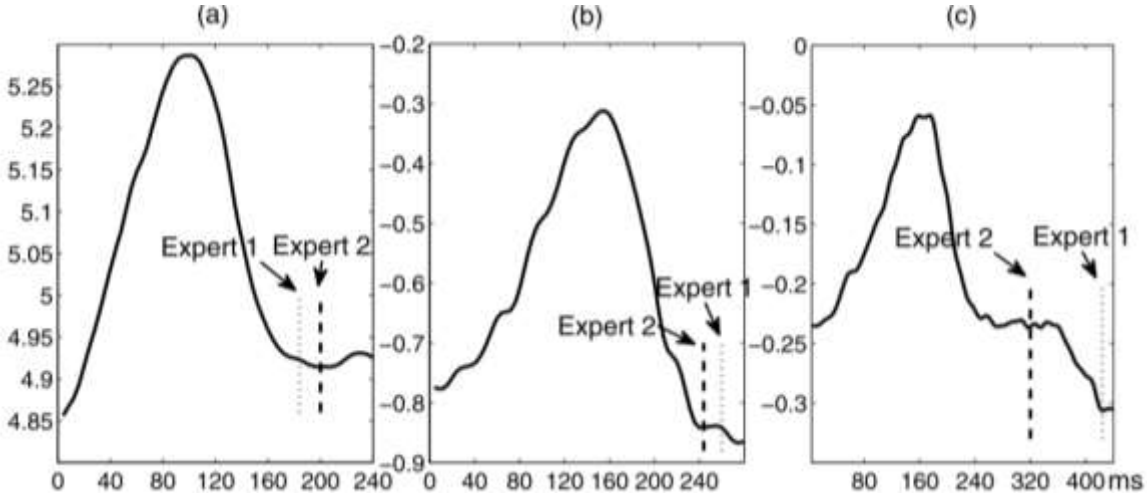

Fig. 7-1 Two cardiologists' marks of T-wave ends for 3 beats in a QT Dataset. The differences are 17ms (a), 15ms (b) and 104ms (c). From [45].

This is due to the varying morphology of the T-wave and the possible presence of noise, physiological artefacts and fibrillatory waves during AF. To surpass this problem, the T-wave delineator was introduced in this study. However, the delineator had the drawback that a rough preliminary window had to be chosen in order to correctly determine Ton and Toff.

The diagnostic value of the $\mathcal{V}$-index has been proven in various studies such as [32] and [33] and proposed the $\mathcal{V}$-index to be a fully automated ECG marker which is to be reported by the ECG machine as an easily interpretable number, similar to the results of a blood test.

To my knowledge, there have been no studies where the $\mathcal{V}$-index was used to characterize supraventricular arrhythmias and this study has succesfully proven that the $\mathcal{V}$-index can be used to discriminate between Persistent and Permanent AF.

Chapter 8. CONCLUSION AND FURTHER WORK

Non-invasive assessment of the SHVR is gaining acceptance as a tool for characterizing the heterogeneity of the ventricular repolarization [45-47] as its diagnostic value has been proven by several studies. The validity of the $\mathcal{V}$-index has been thoroughly proven and the problem related to the estimate of the lead factors w_1 and w_2 have been addressed and a solution has been found.

The aim of this thesis was the assessment of spatial heterogeneity of ventricular repolarization in patients with atrial fibrillation, which included:

- Simulation: use physiological T-waves to study the differences that arise in the $\mathcal{V}$-index in 3 cases:
    - Theoretical case
    - Sinus Rhythm condition
    - Atrial Fibrillation condition

  The AF condition was achieved by adding simulated f-waves to the physiological T-waves using the method described in [34].

- Study of Swiss AF database: compute and compare the $\mathcal{V}$-indexes of 2013 patients in Paroxysmal and Persistent SR and Paroxysmal, Persistent and Permanent AF, in the 3 main $\mathcal{V}$-index computation methodologies.

The aim was met and the results have shown that:

- the method used to estimate the lead factors w_1 and w_2 from the ECG introduce bias in the $\mathcal{V}$-index. However, throughout the comparisons, the standard deviation of the $\mathcal{V}$-index for Method 3 was the lowest. This proves that the analytical form (with 5 being the number of Taylor terms) has a more reliable estimate [36].

- there is a significant effect of the presence of f-waves when computing the $\mathcal{V}$-index and thus, the fibrillatory component should be removed from the AF signals before the computation.
- with some limitations, the methods developed for eliminating the f-waves and delineating the T-wave generally worked.
- no statistically significant results were provided when trying to discriminate paroxysmal from persistent patterns in SR patients
- in AF patients, the comparison between Persistent and Permanent patterns gave significant results as s_ϑ was higher for Persistent than for Permanent AF patients.

Further work could include using higher number of Taylor terms to improve the Method 3 as the error of approximation for potentials, lead factors and standard deviation of the lead factors decreased when the number of Taylor terms increased [36].

The signals provided by the Swiss-AF databank were all baseline ECGs. Another possible further work would be to analyse also the follow-up ECGs in order to compare the same patient at different points in time. The Swiss-AF cohort has funding for up to 3 years after the baseline [35] results so this is a feasible further development.

Moreover, the investigation of another parametric model of the DTW that could more precisely model the T-waves and the lead factors even if it meant a probable increase of computational cost

The development and use of neural networks to do an automatic discrimination of Persistent and Permanent AF patients could also be an interesting further development as it would provide the clinician not only the $\mathcal{V}$-index values but also a preliminary diagnosis of the fibrillatory episode which could aid the clinician in deciding the correct procedure to be taken. This studies could also focus on determining the Specificity and Sensitivity of the $\mathcal{V}$-index as a diagnostic tool.

Chapter 9. REFERENCES

1 *GBD 2015 Mortality and Causes of Death, Collaborators. "Global, regional, and national life expectancy, all-cause mortality, and cause-specific mortality for 249 causes of death, 1980-2015: a systematic analysis for the Global Burden of Disease Study 2015". Lancet. 388 (10053): 1459–1544, 2016.*

2 *AD Elliot, R Mahajan, RK Pathak, DH Lau and P Sanders. "Exercise Training and Atrial Fibrillation Further Evidence for the Importance of Lifestyle Change". Circulation. 133: 457–459, 2016.*

3 *AC Guyton and JE Hall. "Text book of medical physiology." W. B. Saunders Co., 2006.*

4 *KE Barret, SM Barman, S Boitano and HL Brooks. "Ganong's Review of Medical Physiology". 23rd ed. McGraw Hill Professional, 2009.*

5 *JG Betts, P Desaix, JE Johnson, O Korol, D Kruse, B Poe et al. "Anatomy & physiology." OpenStax College, Rice University pp. 787–846. ISBN 1938168135, 2014*

6 *GA Stouffer, SR Marschall, C Patterson, JS Rossi and FH Netter. "Netter's Cardiology." 2nd ed. Elsevier Health Sciences, 2010.*

7 *JG Webster and JW Clark. "Medical Instrumentation: Application and Design". New York: Wiley, 1998.*

8 *SS Chgh, JL Blackshear, WK Shen, SC Hammill and BJ Gersh, "Epidemiology and natural history of atrial fibrillation: Clinical implications" J. Am. Coll. Cardiol., vol 37, pp. 371-378, 2001.*

9 *J Heeringa, DA van der Kuip, A Hofman, JA Kors, G van Herpen, BH Stricker et al. "Prevalence, incidence and lifetime risk of atrial fibrillation: The Rotterdam study," Eur. Heart J. col. 27, pp. 949-953, 2006.*

10 *L. Mainardi, L. Sörnmo, S. Cerutti, "Understanding Atrial Fibrillation: The Signal Processing Contribution" Synthesis Lectures on Biomedical Engineering Vol. 3, No. 1 , pp. 1-129, 2008*

11 *GK Moe and JA Abildskov. "Atrial fibrillation as a self-sustaining arrhythmia independent of focal discharge". American Heart Journal, 58(1):59–70, 1959.*

12 *M Haissaguerre, P Jais, DC Shah, A Takahashi, M Hocini, G Quiniou et al. "Spontaneous initiation of atrial fibrillation by ectopic beats originating in the pulmonary veins." The New England Journal of Medicine, 339:659–666, 1998.*

13 *M Haissaguerre, M Hocini, A Denis, et al. "Driver domains in persistent atrial fibrillation". Circulation, 130:530–538, 2014.*

14 *S. Mittal, "Differentiating Paroxysmal from persistent atrial fibrillation" J. Am. Coll. Cardiol, Vol. 63, No. 25, 2014*

15 *VDA Corino, F Sandberg, LT Mainardi and L Sörnmo. "An Atrioventricular Node Model for Analysis of the Ventricular Response During Atrial Fibrillation." IEEE Trans Biomed Eng, 58:3386–95, 2011.*

16 *VDA Corino, F Sandberg, F Lombardi, LT Mainardi and L Sörnmo, "Atrioventricular nodal function during atrial fibrillation: Model building and robust estimation." Biomedical Signal Processing and Control,Vol. 8, Issue 6, pp. 1017-1025, 2013.*

17 *VDA Corino, F Sandberg, LT Mainardi, PG Platonov and L Sörnmo. "Noninvasive characterization of atrioventricular conduction in patients with atrial fibrillation" Journal of Electrocardiology 48, pp. 938 – 942, 2015.*

18 *CS Kuo, K Munakata, CP Reddy and B Surawicz. "Characteristics and possible mechanism of ventricular arrhythmia dependent on the dispersion of action potential durations," Circulation, vol. 67, no. 6, pp. 1356–1367, 1983.*

19 *JA Vassallo, DM Cassidy, KE Kindwall, FE Marchlinski and ME Josephson. "Nonuniform recovery of excitability in the left ventricle," Circulation, vol. 78, no. 6, pp. 1365–1372, 1988.*

20 *PD Arini, GC Bertrán, ER Valverde and P Laguna. "T-wave width as an index for quantification of ventricular repolarization dispersion: Evaluation in an isolated rabbit heart model," Biomed. Signal Process. Control, vol. 3, pp. 67–77, 2008.*

21 *GX Yan and C Antzelevitch, "Cellular basis for the normal T-wave and the electrocardiographic manifestations of the long-QT syndrome," Circulation, vol. 98, no. 18, pp. 1928–1936, 1998.*

22 *A Mincholé, E Pueyo, JF Rodríguez, E Zacur, M Doblaré and P Laguna. "Quantification of restitution dispersion from the dynamic changes of the T-wave peak to end, measured at the surface ECG," IEEE Trans. Biomed. Eng., vol. 58, no. 5, pp. 1172–1182, 2011.*

23 *CP Day, JM McComb and RW Campbell. "QT dispersion: An indication of arrhythmia risk in patients with long QT intervals," Br. Heart J., vol. 63, no. 6, pp. 342–344, 1990.*

24 *W Zareba, "Dispersion of repolarization: Time to move beyond QT dispersion," Ann. Noninvasive Electrocardiol., vol. 5, pp. 373–381, 2000.*

25 *Y Xia, Y Liang, O Kongstad, Q Liao, M Holm, B Olsson et al. "In vivo validation of the coincidence of the peak and end of the T-wave with full repolarization of the epicardium and endocardium in swine," Heart Rhythm, vol. 2, no. 2, pp. 162–169, 2005.*

26 *AJ Moss, "What resides in T-wave residuum?" J. Cardiovasc. Electrophysiol., vol. 16, no. 9, pp. 952–953, 2005*

27 *C Antzelevitch, S Sicouri, JMD Diego, A Burashnikov, S Viskin, W Shimizu et al. "Does Tpeak –Tend provide an index of transmural dispersion of repolarization?" Heart Rhythm,vol. 4, no. 8, pp. 1114–1116 (Author's reply pp. 1116–1119), 2007.*

28 *T Opthof, R Coronel, FJG Wilms-Schopman, AN Plotnikov, IN Shlapakova, P Danilo et al. "Dispersion of repolarization in canine ventricle and the electrocardiographic T-wave: Tp-e interval does not reflect transmural dispersion," Heart Rhythm,vol.4, no. 3, pp. 341–348, 2007.*

29 *A van Oosterom, "Genesis of the T-wave as based on an equivalent surface source model," J. Electrocardiol., vol. 34 (suppl.), pp. 217–227, 2001.*

30 *R Sassi and LT Mainardi. "An estimate of the dispersion of repolarization times based on a biophysical model of the ECG". IEEE Trans Biomed Eng 2011;58:3396–3405*

31 *VS Chauhan, E Downar, K Nanthakumar, JD Parker, HJ Ross, W Chan et al. "Increased ventricular repolarization heterogeneity in patients with ventricular arrhythmia vulnerability and cardiomyopathy: A human in vivo study," Am. J. Physiol. Heart Circ. Physiol., vol. 290, pp. 79–86, 2006.*

32 *R Abächerli, R Twerenbold, J Boeddinghaus, T Nestelberger, P Mächler, R Sassi, MW Rivolta et al. "Diagnostic and prognostic values of the V-index, a novel ECG marker quantifying spatial heterogeneity of ventricular repolarization, in patients with symptoms suggestive of non-ST-elevation myocardial infarction." Int J Cardiol, 2017.*

33 *MW Rivolta, LT Mainardi and R Sassi, "Quantification of ventricular repolarization* heterogeneity during moxifloxacin or sotalol administration using V index" Physiological Measurement 36(4):803-811, 2015.

34 *A Petrėnas, V Marozas, A Sološenko, R Kubilius, J Skibarkienė, J Oster et al. "Electrocardiogram modeling during paroxysmal atrial fibrillation: application to the detection of brief episodes" Physiological Measurement 38(11):2058-2080, 2017.*

35 *D Conen, N Rodondi, A Müller, JH Beer, A Auricchio, P Ammann et al. "Design of the Swiss Atrial Fibrillation Cohort Study (Swiss-AF): structural brain damage and cognitive decline among patients with atrial fibrillation" Swiss Med Wkly., 147:w14467, 2017.*

36 *EK Roonizi, MW Rivolta, LT Mainardi and R Sassi, "A comparison of three methodologies for the computation of V-index," Computing in Cardiology Conference (CinC), Nice, pp. 593-596, 2015.*

37 *EK Roonizi, LT Mainardi and R Sassi, "A new algorithm for estimating the v-index using sinusoidal basis functions," 37th Annual International Conference of the IEEE Engineering in Medicine and Biology Society (EMBC), Milan, pp. 386-389, 2015.*

38 *M Stridh and L Sörnmo. "Spatiotemporal QRST cancellation techniques for analysis of atrial fibrillation." IEEE Trans Biomed Eng., 48(1):105-11, 2001.*

39 *HJJ Wellens, PJ Schwartz, FW Lindemans et al. "Risk stratification for sudden cardiac death: current status and challenges for the future." European Heart Journal, 35(25):1642–1651, 2014.*

40 *BHV Huysduynen, CA Swenne, HHM Draisma, ML Antoni, HVD Vooren, EEVD Wall et al. "Validation of ECG indices of ventricular repolarization heterogeneity: A computer simulation study," J. Cardiovasc. Electrophysiol., vol. 16, no. 10, pp. 1097–1103, 2005.*

41 *R Sassi, L Mainardi, P Laguna and JF Rodríguez. "Validation of the Vindex through finite element 2D simulations"* Comput. Cardiol., vol. 40, pp. 337–340, 2013.

42 *R Sassi, MW Rivolta, LT Mainardi, RC Reis, MOC Rocha, ALP Ribeiro et al. "Spatial repolarization heterogeneity and survival in chagas disease." Methods Inf Med., 53(6):464–468, 2014.*

43 *M Orini, C Blasi, M Finlay, B Hanson, P Lambiase, R Sassi et al. "Validation of the V-index as a metric of ventricular repolarization dispersion using intracardiac recordings." In Computing in Cardiology Conference (CinC), pp. 673-676, IEEE, 2015.*

44 *Y Zhou and N Sedransk. "Functional data analytic approach of modeling ECG − T-wave shape to measure cardiovascular behaviour." The Annals of Applied Statistics, Vol. 3(N. 4):1382 − 1402, 2009.*

45 *JM Cao, Z Qu, YH Kim, TJ Wu, A Garfinkel, JN Weiss et al. "Spatiotemporal heterogeneity in the induction of ventricular fibrillation by rapid pacing importance of cardiac restitution properties." Circulation 84:1318–1331, 1999.*

46 *BH van Huysduynen, CA Swenne, HH Draisma, ML Antoni, H van De Vooren, EE van Der Wall et al. "Validation of ECG Indices of Ventricular Repolarization Het-erogeneity: A Computer Simulation Study." J Cardiovasc Electrophysiol 16:1097–1103, 2005.*

47 *VS Chauhan, E Downar, K Nanthakumar, JD Parker, HJ Ross, W Chan et al. "Increased ventricular repolarization heterogeneity in patients with ventricular arrhythmia vul-nerability and cardiomyopathy: a human in vivo study." Am J Physiol Circ Physiol, 290:H79–H86, 2005.*